Journal of the
OPTICAL SOCIETY *of* AMERICA

VOLUME 32 FEBRUARY, 1942 NUMBER 2

The Optical Properties of Diffusing Materials

SEIBERT Q. DUNTLEY
Massachusetts Institute of Technology, Cambridge, Massachusetts
(Received October 25, 1941)

1. INTRODUCTION

FROM a color standpoint, the optical properties of an optically homogeneous, isotropic material may be considered known when the absorption coefficient and the Fresnel coefficient of surface reflectance have been determined at each wave-length throughout the visible spectrum. Such a material represents a highly special case. In the general case, radiation is redirected again and again as it passes through the material. Examples of the general case include pigmented films, such as paint, lacquers, printing inks, and other industrial finishes, as well as plastics, paper, rubber, and textiles. All these materials contain particles or fibers which are responsible for the diffusion of light within the substance. With few exceptions, the index of refraction of these particles differs from that of the vehicle, or continuous phase. When this occurs, the simple absorption mechanism which suffices for optically homogeneous, isotropic materials is vastly complicated by the scattering and re-scattering of the permeating radiation. Also, because the flux is diffused within the film, the Fresnel reflections at the surfaces assume greatly increased importance. It is the purpose of this paper to develop laws which govern the behavior of diffusing materials.

Modern plastics provide an excellent illustration of an instance where these new principles are needed. Ordinarily the plastics manufacturer supplies to his customers a molding powder which they use to produce a variety of articles having various shapes and sizes. The manufacturer of the powder finds himself faced with the problem of insuring that duplicate articles made from successive shipments of the powder will be a match in color regardless of their shape or thickness. This condition imposes truly stringent requirements upon the match, for it is a matter of industrial experience that even though two samples of plastic are a spectrophotometric match both in reflectance and in transmittance at some particular thickness, they are not necessarily a match at some other thickness. It is customary for the manufacturer of the powder to test his product by making from it a step wedge, and requiring that each new lot match the original shipment at each step along the wedge. One of the purposes of this paper will be to establish a set of optical constants such that if two plastics have like values of these constants at all wave-lengths they will constitute a spectrophotometric match both in reflectance and in transmittance in any and all thicknesses.

The theory to be discussed describes the optical properties of a diffusing material in terms of eight constants similar to the coefficient of absorption and the surface-reflection factor needed for the special non-scattering case previously mentioned. The theory treats the most general possible case which is represented by colored particles dispersed in a colored vehicle of

BOSTON UNIVERSITY
COLLEGE OF LIBERAL ARTS
LIBRARY

different refractive index and bounded by reflecting surfaces.

2. HISTORICAL

The optical properties of some types of non-isotropic non-homogeneous media have been discussed in the literature by several authors. The interest of these authors was stimulated by the needs of the particular problems with which they were faced. For this reason their treatments are

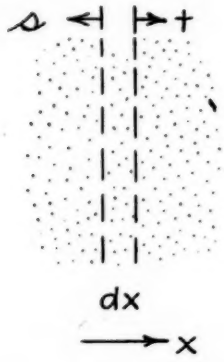

FIG. 1.

either empirical or, if theoretical, are limited to special cases. The empirical approach to the problem has found many adherents in industry, and this method is typified by the equation of Hanstock,[1] and by the equation of Sawyer.[2] Although such equations are useful in the problem for which they are set up, they contain only the information built into them. A theory based upon fundamental physical principles offers the possibility of predicting useful information, and affords an opportunity to connect the optical properties of a pigmented material with the optical properties of its components. For these reasons this paper describes a fundamental theory having its root in the principle of conservation of energy.

The concepts embodied in the general theory of the optical properties of diffusing materials were not conceived at any one time or by any one investigator. In fact, contributions to the problem have been rather evenly spaced throughout the years from 1905 to the present.

The first fundamental approach to this type of problem was made by the astronomer, Arthur Schuster.[3] In 1905 he published a theory describing the escape of radiation from the self-luminous, foggy atmosphere of a star. He conceived the idea of two diffuse fluxes moving in opposite directions through the gas, each contributing back-scattered flux to the other. Since the scattering particles are gas molecules, Schuster rightly considered half the scattered flux to go forward and half to go backward. Because some of the particles are self-luminous, his equations contain terms representing the emission of light by the gas. The symbol E was used to denote the total energy radiated per second in a wave-length range between λ and $\lambda+d\lambda$ by a completely black surface. Schuster considered a thin, parallel-sided slab within the star atmosphere, so chosen that the boundary surfaces were normal to the direction in which the escaping radiation is to be viewed. This is illustrated in Fig. 1. Let* t be the diffuse flux incident on the layer dx in the forward direction and let s be that impinging on dx in the opposite direction. Schuster assumed that in passing through the layer dx, diffuse flux would be increased by emitted light, decreased by absorption, diminished by that part of itself scattered to the rear, and augmented by the back-scattered flux from the oppositely-moving flux body. This situation is represented by the following simultaneous differential equations. Here S represents the total scattering coefficient, and μ represents the over-all absorption coefficient.

$$dt/dx=\mu E-\mu t-\tfrac{1}{2}St+\tfrac{1}{2}Ss,$$
$$-ds/dx=\mu E-\mu s-\tfrac{1}{2}Ss+\tfrac{1}{2}St.$$

It will be remembered that these equations involve the assumption that half the scattered flux is directed forward and half backward. As shown by the late Lord Rayleigh,[5] this is true only for particles very small compared with the wave-length of light. The size of particles in diffusing materials is seldom small enough to fall in this category. It is well known that maximum optical effects are encountered when the effective pigment particle diameter is approximately one-half the wave-length of visible light. In most diffusing materials, the particle size ranges from

* For the purposes of this paper all equations have been written to conform with the terminology of Ryde (reference 8) which has been officially adopted by the International Commission on Illumination (reference 4) for the specification of opal glass.

this value upward, and in the case of paper and textiles, the particles (fibers) are many times larger. It will be seen, therefore, that the differential equations proposed by Schuster cannot be used directly to describe a diffusing material. Nevertheless, in 1918, Channon, Renwick, and Storr[6] applied the Schuster equations to opal glass by assuming the emission of the particles to be zero. This procedure failed to take into account that flux is not generated within the glass but rather enters it from without. Although the effect of the air-glass surfaces was not properly allowed for, Channon was able to secure some encouraging experimental agreement with his formulas based upon the Schuster equations.

Silberstein[7] was the first to point out that when non-radiating turbid media are permeated by light from an external source, the residue of the unscattered beam obeys a different law from the scattered flux. If I_x is used to represent unscattered flux incident upon a layer dx at any point x within the medium, then Silberstein considered that, in passing through layer dx, it was diminished by absorption and by scattering, as indicated in the following equation:

$$dI_x/dx = -\mu I_x - SI_x.$$

TABLE I.

I'_x	The unscattered residue of the primary beam at any depth x within the medium
μ	The absorption coefficient for internal diffused flux
μ'	The absorption coefficient for incident flux
S	The total scattering coefficient for internal diffused flux
B	The portion of S scattered backward
F	The portion of S scattered forward
S'	The total scattering coefficient for incident light
B'	The portion of S' scattered backward
F'	The portion of S' scattered forward
i	The quantity of diffused flux moving in the forward direction
s	The quantity of diffused flux moving in the backward direction

He further removed the restriction that half the scattered flux go forward and half go backward, and his equation for the diminution of I_x is properly written:

$$dI_x/dx = -(\mu+B+F)I_x,$$

where B represents that portion of the total scattering coefficient S which is directed backward, and F represents that portion of S directed forward. In the differential equations for i and s Silberstein inserted terms FI_x, and BI_x, to allow for the fact that two bodies of diffuse flux were, respectively, augmented by light scattered from the incoming primary beam.

In 1931,* the differential equations for i and s were further improved by J. W. Ryde.[8] He recognized that the scattering coefficients B and F are, in general, not the same for the incoming light as for the internal diffuse light. Although, by definition, $B+F=S$, in general, $B \neq F$. The

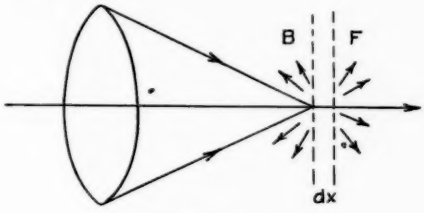

FIG. 2.

division of scattering power between B and F will generally depend upon the angular opening of the cone through which radiation converges on the layers. This is illustrated in Fig. 2. Fortunately, only two cases are encountered. First, when the cone angle is that of the incident light; and second, when the cone angle is 180°, i.e., completely diffused internal flux. For clarity, the scattering coefficient will bear a prime whenever incident light is referred to. When the prime is missing, diffuse light is to be understood.†

When radiation falls on a layer of particles having completely random orientations and positions, the total amount of scattering is independent of the angular opening of the cone of incidence, for each element of the cone will be

* Kubelka and Munk (see reference 9) published a paper in 1931 deriving the same differential equations given by Schuster (except for the emission terms). Their solutions, however, were of a form different from those obtained by Channon, Renwick, and Storr. In 1935 Steele (see reference 10) applied the Kubelka and Munk results to white paper. Reasonable success has attended their application and they are widely known throughout the paper industry.

† Ryde also inserted into the differential equations the assumption that the scattering coefficients for the medium are proportional to the number of particles per unit volume. This was done by writing the scattering coefficients as products, NB, NF, etc. Although there seems to be some experimental justification for this assumption in the case of opal glass in which Ryde was interested, there exists no verification that the assumption is valid in all cases. It is unnecessary to insert this assumption into the differential equations.

scattered like a parallel bundle. Accordingly, it is true that $B+F=B'+F'$. However, in a system in which the particles do not possess random orientations or positions $B+F$ may differ from $B'+F'$.

3. EXTENSION OF THE THEORY

In the interest of generality it must be recognized that the absorption coefficient for incident light need not be the same as the absorption

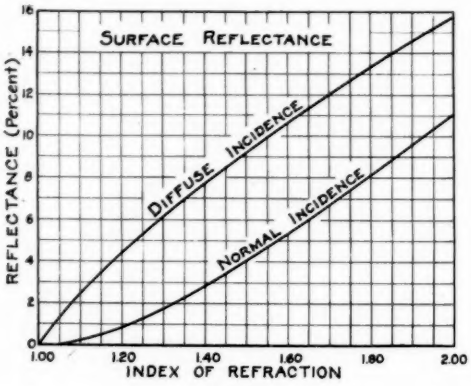

FIG. 3.

coefficient for the internal diffused light. Not only is a different path length involved, but in a system not possessing completely random orientation and position of the particles, a greater portion of the light may traverse the layer dx, without striking a particle in the case of the incident light, than in the case of the diffuse light. Thus, μ' may differ from μ for the same reason that $B+F$ may differ from $B'+F'$. It seems necessary, therefore, to use μ', the absorption coefficient for incident light, rather than μ, the absorption coefficient for diffuse light, in the differential equation for I_x' which describes the disappearance of the unscattered residue of the primary beam. With this extension, the differential equations describing the internal optical properties of diffusing materials are as follows:

$$dI'_x/dx=-(\mu'+B'+F')I'_x,$$
$$dt/dx=F'I'_x-\mu t-Bt+Bs,$$
$$-ds/dx=B'I'_x-\mu s-Bs+Bt.$$

For convenience, Table I reviews the symbols* and their meanings.

* See footnote on p. 62.

It will be noted that the above differential equations may be thought of as a steady state equation of continuity for the flux permeating the interior of the diffusing material. They are not concerned with reflection effects at the boundaries of the vehicle. They involve the assumption that the radiation is monochromatic, and the assumption that the medium may be divided laminarwise without destroying its overall homogeneity. It must be remembered that the treatment is thermodynamic in nature, and attempts no description of the behavior of light in passing over the particles. For this reason, such effects as those explained by Rayleigh, and phenomena like those reported by Keen and Porter[11] will appear as variations in the size of the two absorption coefficients and four scattering coefficients, and in their wave-length dependence. For the purposes of this paper it is agreed that the values of these six constants are to be experimentally determined.

The solution of the differential equations may be expressed in a variety of forms. Experience has shown the use of hyperbolic functions to be desirable. The following solutions have been patterned after those of Ryde,[8] but do not contain the restrictions he imposed.* If the diffusing material exists in the form of a parallel-sided sheet of thickness X, and if the vehicle, or continuous phase, experiences no discontinuity of index of refraction at the surfaces of the sheet, then the values of diffuse reflectance (R') and of the diffuse transmittance (T') are given by the following equations in which the value of T'

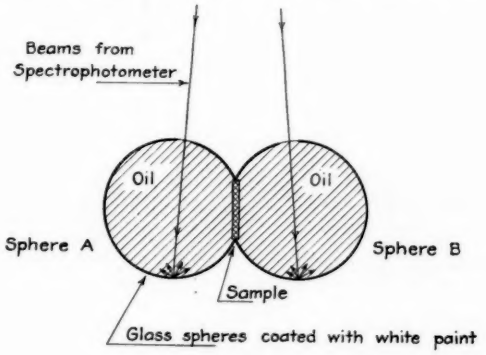

FIG. 4.

* Ryde's solutions impose the following restrictions: (1) $\mu'=\mu$; (2) $B+F=B'+F'$.

contains the residue of the unscattered flux.

$$T'=\frac{Q'K+P'\epsilon^{-(\mu'+B'+F')X}B\sinh KX}{(\mu+B)\sinh KX+K\cosh KX}$$
$$-(Q'-1)\epsilon^{-(\mu'+B'+F')X},$$
$$R'=\frac{P'K\epsilon^{-(\mu'+B'+F')X}+Q'B\sinh KX}{(\mu+B)\sinh KX+K\cosh KX}-P',$$
$$K=[\mu(\mu+2B)]^{\frac{1}{2}}$$
$$P'=\frac{(\mu-\mu')B'+(B-B')(B'+F')}{(\mu'^2-\mu^2)+2\mu'(F'+B')-2\mu B+(F'+B')^2},$$
$$Q'=\frac{(\mu+\mu')F'+(B+F')(B'+F')}{(\mu'^2-\mu^2)+2\mu'(F'+B')-2\mu B+(F'+B')^2}.$$

It will be noted that when scattering is absent ($B=B'=F=F'=0$) the solutions reduce to $R'=0$ and $T'=\epsilon^{-\mu'X}$. When the thickness (X) is infinite the solutions become $T'=0$ and

$$R'_\infty=Q'B/(\mu+B+K)-P'.$$

In retrospect it will be noted that treatments based upon the Schuster differential equations describe the internal optical properties of diffusing materials in terms of two constants—an absorption coefficient and a scattering coefficient. As the theory has been improved, the number of constants has been increased to three by Silberstein, to four by Ryde, and to six by the present paper. In recent years equations of the two-constant type have been derived by several authors. Such treatments include those of Kubelka and Munk,[9] Gurevich,[12] Smith,[13] Neugebauer,[14] and Amy.[15]

Although the present differential equations involving six constants lead to more complicated solutions than those obtained from the two-constant theory, it seems preferable to make the differential equations as rigorous and as complete a description of the physical facts as possible, so that the resulting solution is a complete description of the most general case possible. The solution can then be simplified in any permissible manner contingent on the character of the medium being investigated.

4. BOUNDARY REFLECTIONS

In the discussion thus far it has been assumed that the continuous medium had no boundaries. However, the most common form of a diffusing material is a parallel-sided flat sheet surrounded by air. If light falls on the surface of such a material, the portion reflected (r'_1) will be governed by the familiar Fresnel equation which, for normal incidence, reduces to $r'_1=(n-1/n+1)^2$ where n is the refractive index of the continuous medium. If the incident light is diffuse, the corresponding reflection factor has been shown by

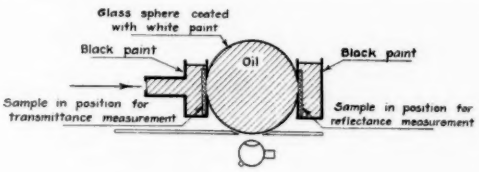

FIG. 5.

Walsh[16] to be

$$r_1=\frac{1}{2}+\frac{(n-1)(3n+1)}{6(n+1)^2}+\left\{\frac{n^2(n^2-1)^2}{(n^2+1)^3}\right\}\log\left(\frac{n-1}{n+1}\right)$$
$$-\frac{2n^3(n^2+2n-1)}{(n^2+1)(n^4-1)}+\left\{\frac{8n^4(n^4+1)}{(n^2+1)(n^4-1)^2}\right\}\log n.$$

Figure 3 shows r'_1 for normal incidence and for diffuse incidence for various values of n.

When the flux within the pigmented material seeks to escape through either surface it encounters a greater reflection factor than when it entered. If no diffusion took place within the film, the outgoing factor would be identical with value for incident flux. However, due to scattering within the film, part of the flux approaches the boundary at greater than the critical angle, so that total internal reflection takes place. Experiments have shown that this effect frequently makes the surface reflectance for emergent flux take on values as high as 40 percent. At first glance, it would seem that this reflectance could be calculated by applying the Fresnel equation for the range within which total reflection does not occur and then adding the fraction totally reflected. However, this operation is impossible because total reflection occurs at high angles of incidence, so that slight departures from uniformity of diffusion have a pronounced effect. For the purposes of this investigation the emergent reflection factor r_2 will be added to the list

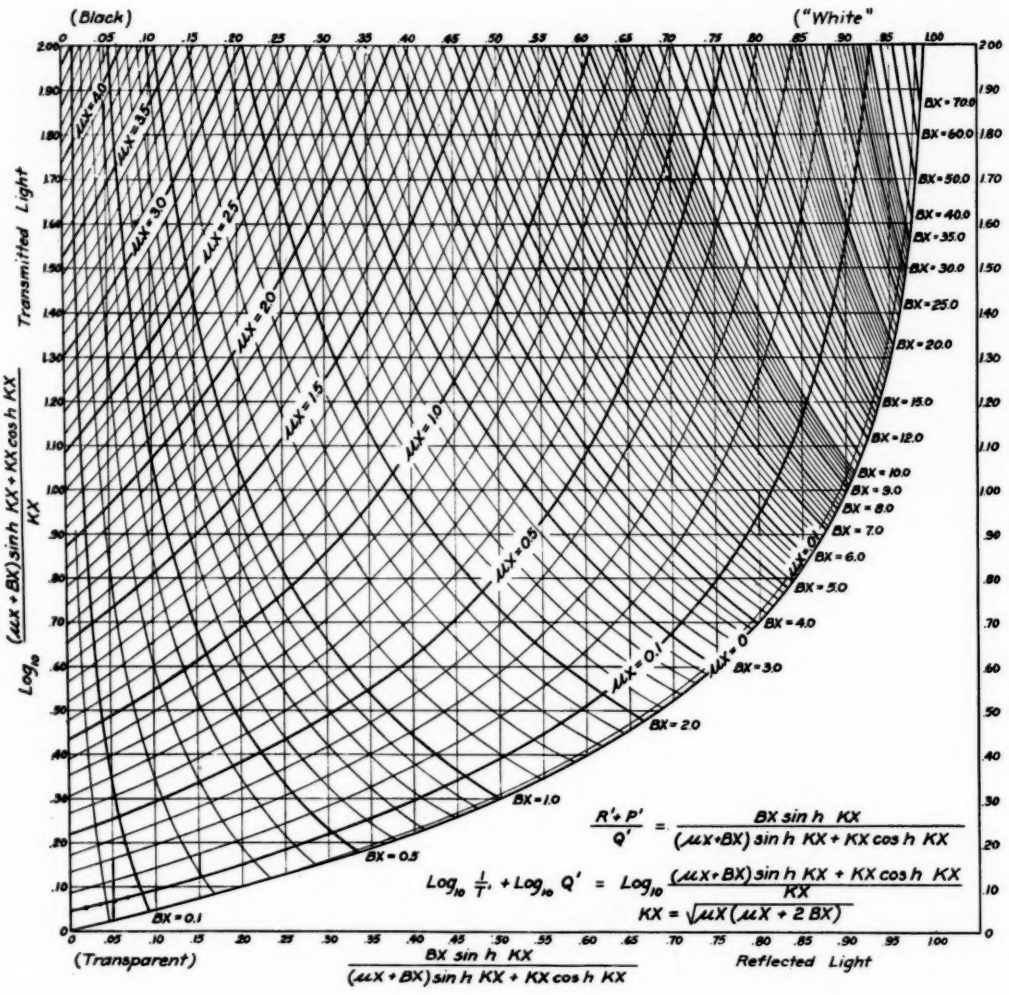

FIG. 6.

of optical constants of a diffusing material which must be experimentally determined.

5. DETERMINATION OF THE OPTICAL CONSTANTS

The foregoing theory has shown that the optical properties of a pigmented material are determined by eight constants. All eight of these constants must be evaluated experimentally if the theory is to be fully used. It is necessary, in general, to know the result of eight measurements to evaluate these eight constants. This requirement is complicated by the transcendental nature of the equations and by the occurrence of most of the parameters in powers higher than the second. The situation has been importantly simplified and two of the constants eliminated by measuring the sample in such a manner that no surface reflections occur.

A technique of photometry has been devised employing a sphere or spheres filled with transparent oil, the refractive index of which was chosen to match that of the vehicle of the diffusing material. The diffusing material itself is

immersed in the oil. These spheres were built as attachments for the recording photoelectric spectrophotometer described by Hardy.[17]

The first attachment was designed to afford values of diffuse reflectance and diffuse transmittance under conditions of diffused illumination. The sample was placed between two optically identical integrating spheres and the two beams from the spectrophotometer were allowed to enter the respective spheres as shown in Fig. 4. The photoelectric cell was arranged to view the sphere wall illumination of either sphere at the will of the operator. Provision was also made for replacing the right-hand sphere by a completely absorbing blackened box. When this was done the comparison beam of the photometer was brought to the photo-cell by an auxiliary optical path, so arranged that the flux entered neither of the spheres. With the photo-cell adjusted to look into the sphere B, readings were taken both with and without the sample in place. These values were denoted by t and t_0. The photo-cell was then moved to sphere A, where a reading was taken with the sample in place. This value was noted as r. Sphere B was then replaced by the blackened box, and the auxiliary optical path. A reading was taken and denoted by r_b. Finally the sample was removed, and a reading taken and denoted by r_0. If these photometric procedures are analyzed by the method described by Hardy and Pineo,[18] it can be shown that the values of diffuse reflectance and diffuse transmission, R and T, are related to the measured quantities by the equations:

$$T=\frac{r_0 t}{r t_0}(1+t_0^2), \quad R=\left(1-\frac{r_0}{r_b}\right)\left(\frac{1+t_0^2}{t_0}\right).$$

This method yields numerous advantages, for the optical constants B' and F' are not encountered. Furthermore, the values of R are absolute since no standard of reflectance is employed. However, the method places a premium on photometric precision, and the writer feels that for routine work the second type of photometric attachment is to be preferred.

The second type of photometric attachment is shown in Fig. 5. This consists of an 8-inch glass sphere covered with white paint and filled with oil. Attached to the front and back of the sphere are oil reservoirs in which the sample can be immersed. The walls of these reservoirs are painted black in order to absorb those components of the radiation not a part of the photometric quantity being measured. A block of magnesium carbonate sealed into a glass cell is immersed in the second chamber to serve as a reflectance standard. When transmittance measurements are made, a duplicated magnesium carbonate block, sealed in a glass cell, is placed in the reflectance position. Thus the method of measurement in every way corresponds to the usual procedure with a Hardy spectrophotometer. With this photometric system the values of R' and T' may be measured directly. It must be remembered, however, that the reflectance value is relative and it should be multiplied by the absolute reflectance of magnesium carbonate before being used as a value of R'.

The determination of the optical constants may be still further simplified if measurements of R' and T' are made with a sample of sufficient thickness that no flux is transmitted unscattered. This can easily be determined by holding the sample a few inches from the eye and attempting to see objects through it. When there is no residue from the unscattered beam, then the equations for R' and T' can be conveniently written:

$$\frac{R'+P'}{Q'}=\frac{BX\sinh KX}{(\mu X+BX)\sinh KX+KX\cosh KX},$$

$$\log_{10}\frac{1}{T'}+\log_{10}Q'=\log_{10}\frac{(\mu X+BX)\sinh KX+KX\cosh KX}{KX}.$$

It will be noted that only the constants μ and B occur explicitly in these equations, the other four constants being contained only in the values P' and Q'.

Even with these several simplifications, the above solutions cannot be solved directly for μ and B because of the transcendental nature of the equations. In order to surmount this difficulty a diagram was constructed (Fig. 6)* having as its axis of abscissa values of the right-hand side of

* A limited number of planographed reproductions of the original diagram are available for distribution by the author.

the reflectance equation, and along its axis of ordinate values of the right-hand side of the transmittance equation. It will be noted that the right-hand side of these equations contain only BX and μX. Therefore, it is possible to construct a family of curves which show at any point the corresponding values of BX and μX.

In almost all cases it will be found that the constant P' is small compared with R', and that the constant Q' differs but little from unity. Therefore, as a rough first approximation the values of R' determined by the photometer may be thought of as applying directly to the scale of numbers along the axis of abscissa. Similarly, the experimentally measured values of optical density ($D'=\log_{10} 1/T'$), may be thought of as corresponding directly to the numbers along the axis of ordinates. If it is true that $P'=0$, and $Q'=1$, then the values of BX and μX thus determined will be true values, and from them the points representing multiple unit thicknesses of the material can be predicted. If the photometer is used to measure a multiple thickness, and a point is plotted to represent it, the measured point and the predicted point should coincide. Ordinarily, however, they will not do so for $P'\neq 0$ and $Q'\neq 1$. It will be noted, however, that the vertical displacement between the two plotted points is a direct measure of $\log_{10} Q'$. The horizontal distance between the two points is a measure of P' after the value of Q' has been allowed for. After determining values of P' and Q' they should be inserted in the equation and a revised value of BX and μX determined. A typical calculation of this type is shown below:

Data:	Thickness	R'	D'
	1	51.8%	0.331
	3	63.8%	0.988
From Fig. 6:	$\mu X=0.02$	and	$BX=1.13$
Then:	$3\mu X=0.06$	and	$3BX=3.39$
From Fig. 6:	$D'_3=0.690$		
From the data:	$D'_3=0.988$		
Subtracting:	$\Delta D'=0.298$		
Then:	$\log Q'=\frac{1}{3}\Delta D'=0.149$;		$Q'=1.41$
From Fig. 6:	$R'_3=73.5$		
From the data:	$R'_3=63.8$		
Subtracting:	$\Delta R'=9.7$		
Then:	$P'=\frac{1}{2}(\Delta R')(Q')=\frac{1}{2}\times 9.7\times 1.41=6.9$		
Substituting:	$(R'+P')(1/Q')=(51.8+6.9)(0.710)=41.7$		
	$D'+\log Q'=0.331+0.149=0.480$		

Corrected values of μX and BX are determined from Fig. 6:
$\mu X=0.30$; $BX=1.15$.

A typical test of this method is illustrated by Fig. 7, which represents spectrophotometric reflectance and transmittance curves of a double thickness of a yellow plastic as determined by the oil-filled photometer. This sample showed prominently the effects of fine particle scattering, and it was chosen as one to which the two-constant theory could not properly be applied. The points marked by crosses represent values of reflectance and transmittance as predicted from experimental data on one thickness and on three thicknesses of the same plastic. The points marked by circles represent values of reflectance and transmittance as predicted by the two-constant theory using the same original data.

With some types of samples,[10,19,20] the values predicted by the two-constant theories are in much better agreement with experiments than in the case of the yellow plastic just described. This is indicated by the fact that often P' is very nearly zero and Q' is very nearly one. In fact, when the assumption is made that $P'=0$, $Q'=1$, the diagram represents a two-constant theory, and may be used as such whenever this procedure will suffice.

6. THE PREDICTION OF PHOTOMETRIC APPEARANCE

When a diffusing material is to be presented to a photometer there are four important ways in which it might be measured. These are the diffuse reflectance ρ', the diffuse transmittance τ', the diffuse reflectance with a backing of reflectance R_b in optical contact (ρ'_b), and the diffuse reflectance of an infinite thickness (ρ'_∞). The interreflections between the surfaces and between surfaces and the medium itself can be expressed in series form and these series summed. The result of such procedures is given below.*

$$\rho'=r_1'+(1-r_1')(1-r_2)\frac{R'(1-r_2R)+r_2TT'}{(1-r_2R)^2-r_2^2T^2},$$

$$\tau'=(1-r_1')(1-r_2)\frac{T'(1-r_2R)+r_2R'T}{(1-r_2R)^2-r_2^2T^2},$$

* The expressions for ρ' and τ' are taken from Ryde (see reference 8).

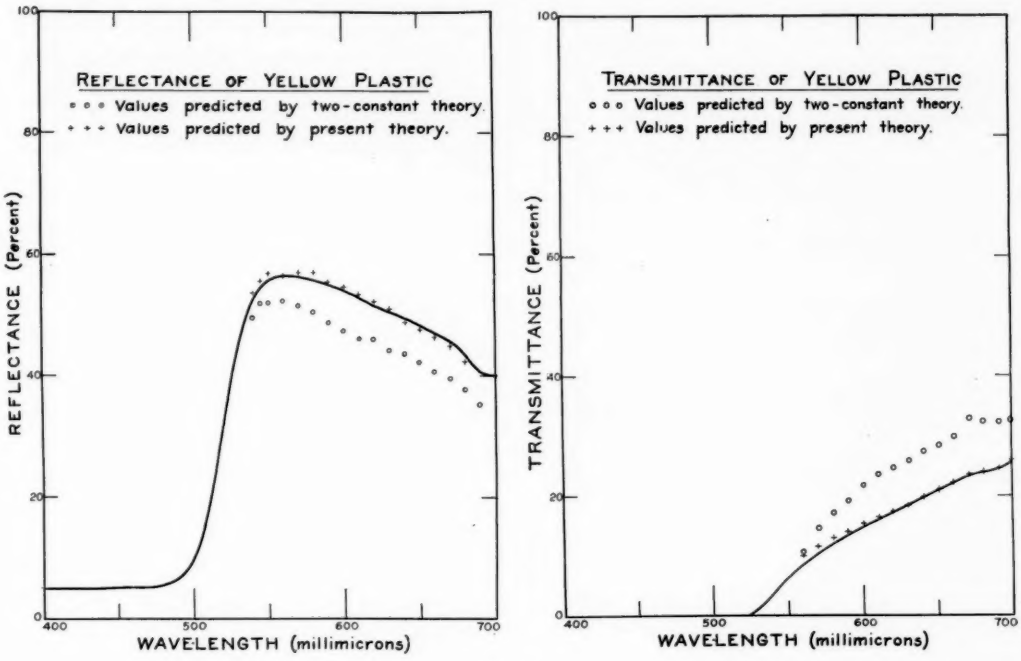
REFLECTANCE OF YELLOW PLASTIC
o o o Values predicted by two-constant theory.
+ + + Values predicted by present theory.
REFLECTANCE (Percent)
WAVELENGTH (millimicrons)
TRANSMITTANCE OF YELLOW PLASTIC
o o o Values predicted by two-constant theory.
+ + + Values predicted by present theory.
TRANSMITTANCE (Percent)
WAVELENGTH (millimicrons)

FIG. 7.

$$\rho_b' = r_1' + (1-r_1')(1-r_2) \times \frac{R'(1-R_bR)+R_bTT'}{(1-R_bR)(1-r_2R)-r_2R_bT^2},$$

$$\rho_\infty' = r_1' + (1-r_1')(1-r_2)\frac{R_\infty'}{1-r_2R_\infty}.$$

Inspection of the above equations shows that the presence of the vehicle surfaces imposes a great handicap on the determination of the internal optical constants of the diffusing material. No reliable values of these constants can be obtained if the distinction between ρ' and R', and between τ' and T' is not recognized. In all ordinary photometers it is ρ' and τ' that are determined. The determination of R and R', T and T' is ordinarily impossible from conventional photometric measurements. As previously stated, it was found necessary to measure these values directly in the manner described earlier in this paper.

7. SUMMARY

The optical properties of diffusing materials have been described in terms of eight constants consisting of two surface reflection factors, two absorption coefficients, and four scattering coefficients. These coefficients are capable of describing the optical properties of the most general type of diffusing material which consists of a system of colored particles dispersed in a colored vehicle and bounded by reflecting surfaces. A practical photometric system for measuring the samples is described, together with an easy method for determining the optical constants. This method has the advantage that in the case of a problem not requiring the specification of all eight constants, the necessary ones are determined first in such a manner that the lack of need for the rest is immediately apparent.

BIBLIOGRAPHY

(1) R. F. Hanstock, Trans. Opt. Soc. **33**, 137 (1932).
(2) R. H. Sawyer, Am. Soc. Test. Mat. Bull. **108**, 12A (1941).
(3) A. Schuster, Astrophys. J. **21**, 1, (1905).
(4) *International Commission on Illumination Neuvième Session* (1937), p. 3.
(5) Lord Rayleigh, Proc. Roy. Soc. **A90**, 219 (1914).

(6) Channon, Renwick, and Storr, Proc. Roy. Soc. **A94**, 222 (1918).
(7) L. Silberstein, Phil. Mag. **4**, 129 (1927).
(8) J. W. Ryde, Proc. Roy. Soc. **A90**, 219 (1931); J. Soc. Glass Tech. **16**, 408 (1932).
(9) Kubelka and Munk, Zeits. f. tech. Physik **12**, 593 (1931).
(10) F. A. Steele, Paper Trade Journal **100**, no. 12 (1937).
(11) Keen and Porter, Proc. Roy. Soc. **A89**, 370 (1914).
(12) M. Gurevich, Physik. Zeits. **31**, 753 (1930).
(13) T. Smith, Trans. Opt. Soc. **33**, 150 (1932).
(14) H. E. I. Neugebauer, Zeits. f. tech. Physik **18**, 137 (1937).
(15) L. Amy, Rev. d'optique **16**, 81 (1938). Sannie, Amy, Sarraf Rev. d'optique **16**, 86 (1938).
(16) Walsh, Dept. Sci. Ind. Res. Illumination Research Tech. Papers **2**, 10 (1926).
(17) A. C. Hardy, J. Opt. Soc. Am. **25**, 305 (1935).
(18) Hardy and Pineo, J. Opt. Soc. Am. **21**, 502 (1931).
(19) D. B. Judd, Nat. Bur. Stand. J. Research **19**, 287 (1937).
(20) D. R. Duncan, Proc. Phys. Soc. **52**, 380 (1940).

FEBRUARY, 1942 J. O. S. A. VOLUME 32

The Dispersion of Optical Glass*

M. HERZBERGER
Kodak Research Laboratories, Eastman Kodak Company, Rochester, New York

(Received November 1, 1941)

THIS investigation was initiated by the question whether the focal length of a photographic objective for different wave-lengths in the infra-red could be calculated if the focal length for some part of the visible spectrum were known.

Before this work was begun, Kingslake and Conrady[1] had published a series of measurements of glass indices in the infra-red, and our first investigations showed that there exists a function $S(\lambda)$ such that the power of a lens system follows the equation

$$\phi_\lambda = S(\lambda)\phi, \tag{1}$$

with good approximation, where $S(\lambda)$ is a universal function, not depending on the glasses chosen, but varying with the type of chromatic correction (i.e., photographic, visual, or other type). This equation is a mathematical statement of the well-known fact that, for ordinary glasses, the secondary spectrum in the visible region cannot be corrected.[2] We have found that the equation is valid for wave-lengths as far as 1.0μ, and holds for even greater wave-lengths, with reservations which will be discussed later.

Our next problem was to find for $S(\lambda)$ an analytical expression which would have some connections with a reasonable dispersion formula.

Formula (1) is valid because of the fact that we can calculate μ (which we shall use in this paper as an abbreviation for $n-1$) for any wave-length as soon as we know the values for any two particular wave-lengths:

$$\mu(\lambda) = S(\lambda)\mu_1 + T(\lambda)\mu_2. \tag{2}$$

This equation holds true for almost all glasses with an accuracy of a few units in the fifth decimal throughout the visible spectrum. However, there are some glasses for which the deviation is larger than one unit in the fourth decimal, namely, the very dense flints, the KzF and KzFS series of the Schott Company, and the so-called "telescope flints" of other manufacturers. For these glasses, formula (2) gives only a rough approximation, which certainly does not permit extrapolation into the infra-red or ultraviolet. Two data are not sufficient to characterize these glasses, nor are three, but it seems that four data are enough.

Let $R(\lambda)$ be the remainder which we find in applying formula (2) to one of these special glasses:

$$\mu(\lambda) = S(\lambda)\mu_1 + T(\lambda)\mu_2 + R(\lambda). \tag{3}$$

In particular, R_A represents the numerical value of the remainder for the red line $A'(0.7682\mu)$, and

* Communication No. 829 from the Kodak Research Laboratories.

[1] R. Kingslake and H. Conrady, "A refractometer for the near infra-red," J. Opt. Soc. Am. **27**, 257 (1937).

[2] See for instance, F. H. Perrin, "A study of Harting's criterion for complete achromatism," J. Opt. Soc. Am. **28**, 86 (1938).

R_h the remainder for the violet line $h(0.4047\mu)$. We shall then show the existence of two more universal functions $C(\lambda)$ and $D(\lambda)$, such that

$$R(\lambda)=C(\lambda)R_A+D(\lambda)R_h. \qquad (4)$$

This second formula will be shown to be accurate within the accuracy claimed for the catalog values of the glass manufacturers, i.e., ± 2 in the fifth decimal place, throughout the visible spectrum.

Now, let us take up these questions in detail. Optical glasses are usually identified by the index for the wave-length $d(0.5876\mu)$ and the Abbe number

$$\nu=\frac{n_d-1}{n_F-n_c}=\frac{\mu_d}{\mu_F-\mu_c}, \qquad (5)$$

from which two values we can find the dispersion

$$\mu_F-\mu_c=\frac{\mu_d}{\nu}. \qquad (6)$$

We can assume therefore that a glass is given by μ_d and $\mu_F-\mu_c$. According to our hypothesis, there are two functions $A(\lambda)$ and $B(\lambda)$ such that

$$\mu_\lambda-\mu_d=B(\lambda)\mu_d+A(\lambda)(\mu_F-\mu_c). \qquad (7)$$

This equation is not new: if it is divided by $\mu_F-\mu_c$, it states simply that the so-called θ-values (relative partial dispersions) are linear functions of the ν-values. F. E. Wright[3] published graphs

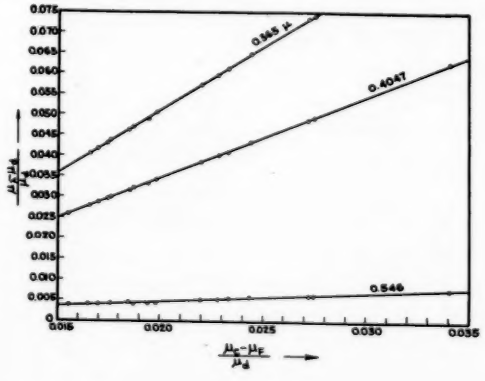

FIG 1

[3] Lt. Col. F. E. Wright, *The Manufacture of Optical Glass and of Optical Systems* (U.S.A. Ordnance Department Document No. 2037, 1921).

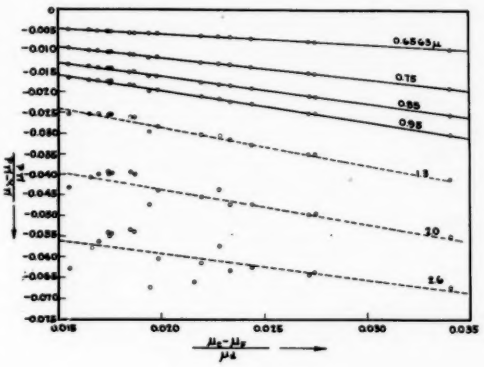

FIG. 2.

showing the straight lines which Eq. (7) implies. However, the quotient of two small numbers, $\mu_\lambda-\mu_d$ and $\mu_F-\mu_c$, is not very accurately determined, and so we suggest that A and B might better be found by plotting $(\mu_\lambda-\mu_d)/\mu_d$ against $(\mu_F-\mu_c)/\mu_d$. Figures 1 and 2 show these straight lines for several wave-lengths.

For our purposes, we have investigated the glass catalogs of Schott, Chance-Parsons, Parra-Mantois, and Bausch and Lomb. In addition, we have used the data published by Brauckhoff,[4] who measured ten Schott glasses at small intervals from 0.4047μ to 1.1404μ, and the measurements by Kingslake and Conrady on seventeen glasses from 0.365μ to 2.6μ. The data for eleven of these glasses have already been published by Kingslake and Conrady,[1*] and with their permission, I give here the data of the other six (Table I).

Figures 1 and 2 were made with the data from these seventeen glasses. We see that, from 0.365 to 1.0μ, the deviation from the straight line is slight for all the glasses, but that the rule becomes more and more doubtful as the wave-length increases. However, we can still compute by the method of least squares the best straight line through the points. Table II shows the two coefficients of the best straight line as functions of the wave-length, for the 17 Kingslake glasses,

[4] H. Brauckhoff, "Brechzahl und Dispersion optischer Glassorten im photographierbaren Ultrarot," Zeits. f. Instrumentenk. **59**, 154 (1939).

[*] It is suggested that, to make a smoother dispersion curve, the value of the index for glass 10, $\lambda=0.60$, be made 1.61995, and the index for glass 16, $\lambda=0.65$, be made 1.60874.

TABLE I. Refractive indices in the infra-red, measured by R. Kingslake and H. G. Conrady, (reproduced with authors' permission).

Glass No. Type	λ	12 LF	13 LBF	14 LBC	15 LF	16 DBC	17 DF
n_D		1.55838	1.56689	1.57262	1.58007	1.61163	1.61776
$n_F - n_C$		.01226	.01060	.01006	.01415	.01067	.01680
v		45.5	53.5	56.8	41.0	57.3	36.8
	0.3650	1.59044	1.59363	1.59769	1.61781	1.63818	1.66345
h	.4047	1.57994	1.58516	1.58983	1.60530	1.62984	1.64809
G'	.4340	1.57432	1.58048	1.58548	1.59862	1.62524	1.63997
g	.4358	1.57401	1.58021	1.58524	1.59828	1.62501	1.63955
F	.4861	1.56706	1.57437	1.57975	1.59016	1.61915	1.62977
e	.5461	1.56136	1.56945	1.57513	1.58357	1.61424	1.62186
D	.5893	1.55838	1.56689	1.57262	1.58007	1.61163	1.61776
C	.6563	1.55480	1.56377	1.56969	1.57601	1.60848	1.61297
	.60	1.55771	1.56632	(1.57212)	1.57928	1.61103	1.61686
	.65	1.55510	1.56402	1.56990	1.57626	1.60894(−20)	1.61329
	.70	1.55299	1.56213	1.56810	1.57392	1.60683	1.61057
	.75	1.55130	1.56064	1.56669	1.57201	1.60533	1.60829
	.80	1.54993	1.55947	1.56553	1.57048	1.60406	1.60650
	.85	1.54870	1.55836	1.56447	1.56906	1.60293	1.60490
	.90	1.54757	1.55738	1.56350	1.56783	1.60190	1.60349
	.95	1.54658	1.55650	1.56265	1.56675	1.60098	1.60222
	1.0	1.54571	1.55574	1.56187	1.56581	1.60014	1.60114
	1.1	1.54419	1.55435	1.56053	1.56407	1.59869	1.59929
	1.2	1.54283	1.55314	1.55925	(1.56262)	1.59737	1.59762
	1.3	1.54155	1.55200	1.55809	(1.56111)	1.59613	1.59616
	1.4	1.54035	1.55094	1.55695	1.56006	1.59491	1.59485
	1.5	1.53919	1.54987	1.55590	1.55880	1.59369	1.59357
	1.6	1.53801	1.54882	1.55478	1.55763	(1.59259)	1.59235
	1.7	1.53680	1.54777	1.55363	1.55645	1.59130	1.59110
	1.8	1.53557	1.54667	1.55251	1.55522	1.59009	1.58975
	1.9	1.53436	1.54549	1.55125	1.55402	1.58879	1.58854
	2.0	1.53305	1.54433	1.55000	1.55270	1.58746	1.58720
	2.1	1.53172	1.54312	1.54878	1.55139	1.58607	1.58580
	2.2	1.53032	1.54190	1.54742	1.55002	1.58464	(1.58442)
	2.3	1.52892	1.54057	1.54600	1.54855	1.58313	1.58291
	2.4	1.52742	1.53921	1.54458	1.54703	(1.58163)	1.58138
	2.5	(1.52574)	1.53786	1.54305	1.54541	1.57985	1.57981
	2.6	1.52409	1.53637	(1.54147)	1.54375	(1.57800)	1.57824

the 10 Brauckhoff glasses, and a series of 34 representative Schott glasses.

In order to find analytic expressions for these coefficients, we must now consider the dispersion theory. Figure 3 shows dispersion curves for some typical glasses. It is obvious that in all these cases there must be at least one absorption band in the ultraviolet; that is, there is at least one value of λ for which μ becomes infinite. The simplest form fulfilling this condition is

$$\mu = a + b/(\lambda - c), \tag{8}$$

which is known as the Hartmann formula. This is the equation for a hyperbola whose asymptotes are parallel to the coordinate axes. Some typical dispersion curves are shown in Fig. 3, and it is apparent that they do not fit these specifications. According to the dispersion theory of Helmholtz-Ketteler, the curve might be fitted with an equation of the form

$$\mu = \mu_0 + \frac{a_1}{\lambda^2 - \lambda_1^2} + \frac{a_2}{\lambda^2 - \lambda_2^2} + \frac{a_3}{\lambda^2 - \lambda_3^2} + \cdots. \tag{9}$$

As the investigations of Matossi[5] show, there are two distinct absorption bands in the infra-red for all silicate glasses. However, in computing refractive indices in the visible and near infra-red, we can replace these two terms by the first two members of their Taylor series. Thus, after trying, and failing, to use ordinary interpolation

[5] F. Matossi and H. Bluschke, "Das Ultrarote Reflexionsspektrum von Gläsern," Zeits. f. Physik **108**, 295 (1937–8); See also G. W. Morey, *The Properties of Glass* (Reinhold Publishing Company, New York, 1938).

TABLE II.

	A				B			
λ	Brauckhoff	Kingslake	Schott (34)	Formula	Brauckhoff	Kingslake	Schott	Formula
0.365		+3.107		+3.120		−0.01103		−0.01138
h	+2.021	+1.977	+1.959	+1.970	−0.00572	−0.00492	−0.00452	−0.00475
G′	+1.424	+1.402	+1.398	+1.403	−0.00279	−0.00239	−0.00229	−0.00237
g	+1.393	+1.373	+1.358	+1.374	−0.00266	−0.00219	−0.00198	−0.00227
F	+0.727	+0.725	+0.726	+0.724	−0.00054	−0.00051	−0.00053	−0.00048
e	+.234	+.235	+.245	+.234	−.00009	+.00004	+.00014	+.00006
d	0.0	0.0	0.0	0.0	0.0	0.0		0.0
D	−.008	−.008	−.008	−.008	−.00001	+.00001	−.00001	−.00001
0.5896	−.009			−.010	−.00024			−.00001
.6		−.057		−.059		−.00011		−.00006
.6103	−.102			−.104	−.00018			−.00012
.65		−.261		−.255		−.00033		−.00042
C	−.273	−.275	−.280	−.276	−.00054	−.00053	−.00039	−.00048
.6707	−.315			−.321	−.00073			−.00061
.7		−.401		−.402		−.00099		−.00091
.75		−.519		−.516		−.00148		−.00148
.7665	−.537			−.548	−.00190			−.00168
A′	−.541		−.550	−.551	−.00193		−.00171	−.00170
.7699	−.542			−.554	−.00199			−.00172
.78	−.558			−.572	−.00218			−.00185
.7947	−.582			−.596	−.00237			−.00203
.8		−.602		−.605		−.00218		−.00210
.8127	−.608			−.624	−.00262			−.00226
.85		−.665		−.675		−.00300		−.00276
.8521	−.661			−.678	−.00320			−.00279
.8943	−.707			−.726	−.00384			−.00338
.9		−.724		−.731		−.00365		−.00346
.9370	−.745			−.766	−.00449			−.00400
.95		−.770		−.776		−.00436		−.00419
.9610	−.763			−.785	−.00491			−.00433
1.0		−.805		−.813		−.00515		−.00495
1.0328	−.807			−.833	−.00601			−.00546
1.0915	−.833			−.861	−.00703			−.00641
1.1		−.863		−.865		−.00658		−.00655
1.1404	−.851			−.880	−.00785			−.00724
1.2		−.894		−.898		−.00836		−.00826
1.3		−.913		−.917		−.01018		−.01011
1.4		−.923		−.925		−.01206		−.01208
1.5		−.921		−.925		−.01413		−.01419
1.6		−.918		−.918		−.01623		−.01642
1.7		−.902		−.906		−.01863		−.01880
1.8		−.892		−.890		−.02092		−.02130
1.9		−.866		−.869		−.02365		−.02394
2.0		−.844		−.845		−.02640		−.02672
2.1		−.816		−.817		−.02931		−.02964
2.2		−.783		−.787		−.03242		−.03269
2.3		−.749		−.753		−.03566		−.03589
2.4		−.707		−.717		−.03923		−.03923
2.5		−.662		−.679		−.04294		−.04269
2.6		−.609		−.638		−.04702		−.04630

formulas based on a Taylor series for μ, we finally tried

$$\mu = a + b\lambda^2 + c/(\lambda^2 - \lambda_1^2), \qquad (10)$$

where λ_1 is an absorption band in the ultraviolet, the coefficient b replacing all the infra-red bands.

We obtained fairly good results in fitting individual glasses to this formula, but λ_1 changes from glass to glass, and we were not able to

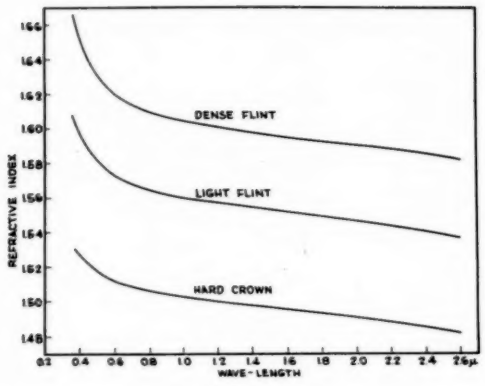

FIG. 3. Dispersion curves.

express the functions A and B in the same form. Therefore we added a term, representing a second ultraviolet band.

$$\mu=a+b\lambda^2+\frac{c}{\lambda^2-\lambda_1^2}+\frac{d}{\lambda^2-\lambda_2^2}, \qquad (11)$$

with λ_1 about 0.200μ and λ_2 about 0.160μ. This form seems to give a perfect fit. Since λ_1 and λ_2 are not very far from each other, Eq. (11) is not very good for the purpose of determining the coefficients a, b, c, and d by the method of least squares. We therefore transformed it to

$$\mu=a+b\lambda^2+\frac{c}{\lambda^2-0.035}+\frac{d}{(\lambda^2-0.035)^2}, \qquad (12)$$

which equation is equivalent to (11) for the interval of λ under investigation. (If wavelengths in the ultraviolet are to be considered, it might be better to return to the theoretical form (11).)

In order to make a critical test of the validity of (12), we asked Mr. Philip Scharf, of these Laboratories, to measure a number of glasses to an accuracy of a few units of the sixth decimal through the visible spectrum. We then determined the four coefficients of (12) by the method of least squares, and calculated the values of μ. Table III shows the deviations of these calculated values from the original measurements.

Having thus shown that formula (12) is quite adequate as a dispersion formula, we tried to fit A and B by expressions of the same form. We calculated the coefficients of A and B using data of all known glasses, with the exception of the special glasses enumerated above. These coefficients we found to be

$$A=-1.294878+0.088927\lambda^2+\frac{0.373490}{\lambda^2-0.035}+\frac{0.005799}{(\lambda^2-0.035)^2}.$$
$$B=+0.001255-0.007058\lambda^2+\frac{0.001071}{\lambda^2-0.035}-\frac{0.000218}{(\lambda^2-0.035)^2}. \qquad (13)$$

Figures 4 and 5 and Table II show the good agreement between these values and those obtained empirically. It is surprising that these functions, calculated from data for the visible spectrum only, give such a good approximation even out to 2.6μ, where at first the relation expressed in Eq. (7) seemed no longer to be valid.

Table IV shows a cross section of ordinary glasses, and their deviations, in the visible spectrum from formula (1), with constants computed from (13).

Table V is a complete list of those Schott glasses for which the remainder attains a value larger than one unit of the fourth place. Included here are also four other materials which show deviations, namely, quartz, lithium fluoride, fluorite, and sylvine. It is seen at once that all the glasses contain very little or no silicate, and when used in combination, they change the secondary spectrum, mostly for the worse.

To calculate the secondary spectrum from A and B for a system achromatized for any two wave-lengths λ_1 and λ_2, we proceed as follows: From (7) we find

$$\mu(\lambda_1)=(B_1+1)\mu_d+A_1(\mu_F-\mu_c),$$
$$\mu(\lambda_2)=(B_2+1)\mu_d+A_2(\mu_F-\mu_c),$$
$$[A_1=A(\lambda_1), \text{etc.}] \qquad (14)$$

TABLE III. Deviations in the *sixth* place from measurements made on six glasses by P. Scharf.

	BK 16	BK 8	K	KF	LLF	LF
C	0	0	+3	0	−1	+1
D	−1	−1	−5	0	+2	−3
e	+4	+1	−1	−1	−2	+1
F	−3	−1	+1	+1	−1	+4
g	0	+3	+1	0	+1	−3
G'	+1	−2	+2	−2	−3	0
h	0	0	−2	0	−1	+1
n_D	1.498974	1.515898	1.523666	1.522698	1.542571	1.574914
ν	67.4	64.6	58.9	49.8	47.4	43.0

or

$$\mu_F-\mu_c=\frac{B_1-B_2}{A_1-A_2}\mu_d+\frac{1}{A_1-A_2}[\mu(\lambda_1)-\mu(\lambda_2)]. \quad (15)$$

We substitute this in formula (7), and get

$$\mu_\lambda-\mu_d=\left\{B(\lambda)-\frac{B_1-B_2}{A_1-A_2}A(\lambda)\right\}\mu_d + \frac{A(\lambda)}{A_1-A_2}[\mu(\lambda_1)-\mu(\lambda_2)]. \quad (16)$$

From Eq. (16) and the well-known formulas for the power of thin lenses, we obtain finally

$$\phi(\lambda)=S(\lambda)\phi_d,$$

$$S(\lambda)=B(\lambda)+1-\frac{B_1-B_2}{A_1-A_2}A(\lambda). \quad (17)$$

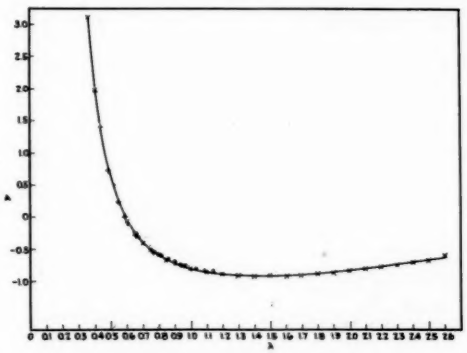

FIG. 4. A plotted against λ; ×—from Kingslake; ○—from Brauckhoff; +—from Schott catalog; solid line from formula.

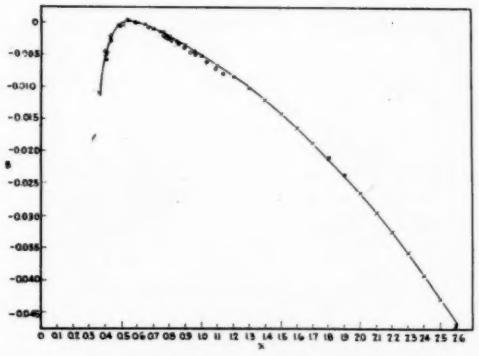

FIG. 5. B plotted against λ; ×—from Kingslake; ○—from Brauckhoff; +—from Schott catalog; solid line from formula.

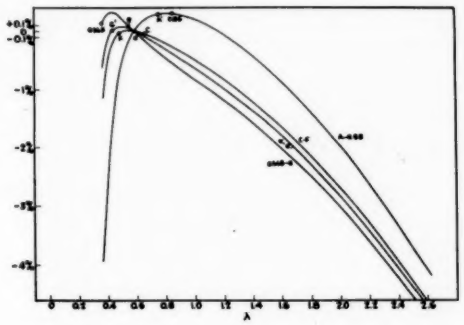

FIG. 6. Secondary spectrum for various chromatic corrections.

From this formula we can find the secondary spectrum for any system which does not contain extraordinary glasses, for any type of achromatism. We need know only two wave-lengths, λ_1 and λ_2, for which the system is achromatized. In Fig. 6 are plotted some examples of the secondary spectrum for different types of chromatic correction.

Let us now return to those glasses which give an unusual secondary spectrum. We want to determine the functions $C(\lambda)$ and $D(\lambda)$ which give the remainder in the original formula:

$$R(\lambda)=C(\lambda)R_A+D(\lambda)R_h. \quad (18)$$

We must keep in mind that R_A and R_h are very small values, and therefore $C(\lambda)$ and $D(\lambda)$ can vary considerably without affecting the accuracy of our approximations. An exact evaluation of C and D will be possible only when a sufficient number of temperature-controlled measurements of refractive indices, accurate to six places, is available, or when more measurements in the infra-red have been made, especially for some of the glasses with unusual partial dispersions. However, for present purposes, the results seem more than adequate.

C and D were determined from the list of special glasses shown in Table V. Figure 7 shows C and D plotted against λ, and Table VI shows that the remainders of these special glasses and minerals are now well within the usual accuracy of index measurements.

The values of the residuals R_A and R_h are not known accurately enough to extrapolate very far beyond the visible spectrum, but if one or more

TABLE IV. Residuals for ordinary glass. Catalog index minus calculated value.

	A'	C	D	e	G'	h
FK 1	−0.00003	0.00000	−0.00001	0.00000	+0.00003	+0.00009
BK 1	−.00002	−.00001	.00000	.00000	.00000	+.00003
K 1	.00000	−.00001	.00000	.00000	+.00001	+.00005
BaK 1	+.00002	−.00001	−.00001	.00000	.00000	+.00001
SK 1	+.00003	.00000	.00000	.00000	+.00001	.00000
LLF	−.00001	−.00001	−.00001	+.00001	−.00003	−.00003
F 1	−.00001	−.00002	−.00001	−.00001	−.00004	−.00004
BaF 1	+.00002	.00000	.00000	+.00001	−.00001	+.00001

TABLE V. Residuals for extraordinary glass. Catalog index minus calculated value.

	A'	C	D	e	G'	h
FK 4	0.00000	0.00000	−0.00001	0.00000	+0.00003	+0.00012
SF 1	+0.00005	0.00000	0.00000	+0.00001	+0.00003	+0.00016
3	+.00003	−.00002	−.00001	−.00002	+.00007	+.00025
4	+.00005	.00000	.00000	.00000	+.00011	+.00032
6	+.00009	+.00001	−.00002	−.00002	+.00023	+.00059
10	+.00001	.00000	−.00001	−.00001	+.00017	+.00051
11	+.00010	+.00005	.00000	.00000	+.00045	+.00113
13	+.00003	+.00002	.00000	−.00001	+.00027	+.00071
14	+.00008	+.00005	−.00001	+.00001	+.00039	+.00096
15	+.00004	+.00001	−.00001	.00000	+.00011	+.00032
KzF 1	−.00005	−.00003	−.00002	+.00001	−.00009	−.00013
2	−.00010	−.00003	.00000	.00000	−.00008	−.00014
3	−.00010	−.00003	−.00001	.00000	−.00010	−.00013
5	−.00010	−.00003	−.00001	.00000	−.00010	−.00017
6	−.00009	−.00003	−.00001	+.00001	−.00009	−.00018
PKS 1	+.00002	+.00001	.00000	+.00001	+.00008	+.00020
PSKS 1	+.00002	+.00001	.00000	+.00001	+.00005	+.00015
KzFS 1	−.00021	−.00006	.00000	.00000	−.00022	−.00040
2	−.00014	−.00003	.00000	+.00001	−.00013	−.00024
3	−.00016	−.00004	.00000	.00000	−.00013	−.00022
SFS 1	+.00036	+.00011	+.00001	−.00003	+.00095	+.00238
Quartz	−.00006	−.00004	.00000	+.00001	−.00007	−.00007
LiF	0	+2	0	+3	+15	+38
Fluorite	+27	+8	+2	−1	+33	+68
Sylvine	+23	+4	0	+2	−2	

values farther out are known, the formula can be adjusted to make interpolation more accurate.

This is done in the following way: We find by measurement the residuals for two wave-lengths at the opposite ends of the region in which we are interested, namely, R_1 and R_2 at wave-lengths λ_1 and λ_2. According to (18), these residuals would be given by

$$\begin{aligned} R_1 &= C_1 R_A + D_1 R_h, \\ R_2 &= C_2 R_A + D_2 R_h. \end{aligned} \tag{19}$$

Then, a residual at some other (intermediate) wave-length would be given in terms of R_1 and R_2 by

$$R(\lambda) = C^*(\lambda) R_1 + D^*(\lambda) R_2, \tag{20}$$

where

$$\begin{aligned} C^*(\lambda) &= \frac{D_2 C(\lambda) - C_2 D(\lambda)}{C_1 D_2 - C_2 D_1}, \\ D^*(\lambda) &= \frac{C_1 D(\lambda) - D_1 C(\lambda)}{C_1 D_2 - C_2 D_1}, \end{aligned} \tag{21}$$

$C(\lambda)$ and $D(\lambda)$ being the same functions shown in formula (18).

The values of the functions C and D will be given with greater accuracy as soon as sufficient data are available.

These investigations lead to the assumption that silicate glasses have two absorption bands in the near ultraviolet, probably around 2000A and 1600A. Since quartz is transparent far beyond these wave-lengths, silicate glasses must contain silica in a special form. This hypothesis is subject to experimental confirmation. In any case, the ability of the methods shown here to match all the data at present available seems to lead to the assumption that some unknown physical laws are responsible for the dispersion curve of a glass.

TABLE VI. Residuals for extraordinary glasses after applying final formula.

	C	D	e	G'
FK 4	0.00000	−1	0	−1
SF 1	−1	0	+1	−4
3	−3	−1	−2	−3
4	−1	0	0	−2
6	−2	−2	−2	−1
10	−1	−1	0	−1
11	+1	0	0	+2
13	0	0	0	+1
14	+2	−1	+1	+3
15	0	−1	0	−1
KzF 1	−2	−2	+1	−3
2	0	0	0	+1
3	−1	−1	0	−2
5	0	−1	0	−1
6	−1	−1	+1	+1
PKS 1	0	0	+1	0
PSKS 1	0	0	+1	−1
KzFS 1	−1	+1	−1	0
2	0	0	0	0
3	0	0	−1	+1
SFS 1	0	+1	0	−1
Quartz	−3	0	+1	−3
LiF	+1	+2	+4	+1
Fluorite	+1	0	−1	+2
Sylvine	0	−2	−1	−5

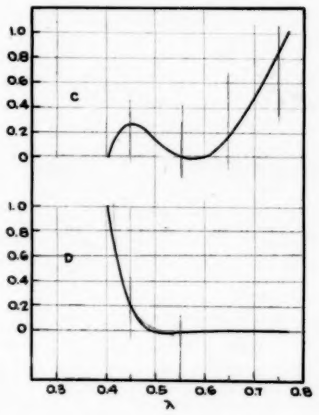

FIG. 7. Values of C and D for visible spectrum.

ACKNOWLEDGMENTS

I want to thank R. Kingslake and P. Scharf for the data on glass they furnished for this paper; and I also want to thank my assistants, especially H. Jenkins, for their help in carrying out the laborious calculations which were necessary.

Systems of Interferential Devices

B. P. RAMSAY AND F. B. PAULS
Department of Physics, University of Kentucky, Lexington, Kentucky
(Received November 1, 1941)

I. INTERFERENTIAL SYSTEMS

IN many cases it is important to use systems of optical devices, for many valuable optical instruments are ineffective when used alone. This is particularly true of high resolving power instruments. The echelon, the etalon, and the Lummer-Gehrcke plate are invariably used in combination with a spectrograph. In such cases, it is likely to be true that the properties of the combination have not been stated in any generalized way, although the theory of each element of the optical system may have been adequately developed. Because of this it seems important to discuss such combinations from the point of view of the interferential theory of optical instruments, and to formulate so far as possible rules for their design and use.

It is apparent from the outset that there are several kinds of questions which arise with regard to systems of interferential devices, and that each of these requires its own rule. For instance, the interferential theory yields an intensity function which describes the distribution of illumination in the focal plane of the observing mechanism. From this intensity function the optical properties of the system may be discovered. Thus the kinds of rules which are needed for systems of optical devices may be classified as (a) rules for the intensity function of the combination, (b) rules for the optical properties of the combination, and (c) rules for the arrangement of the optical elements which comprise the system.

Optical elements are frequently employed entrain. When this is done, however, there is often a choice as to whether the dispersions of the several elements shall have the same or opposite signs. The arrangement will be called a series arrangement when the dispersions of the elements are alike in sign, but will be called a tandem arrangement when the dispersions are unlike in sign. Thus the prisms of a multiple prism spectrograph are placed in series: but the prisms of a direct prism spectrograph are placed in tandem. In some cases it is wholly optional whether the optical elements shall be used in series or in tandem; as just mentioned, for example, prisms may be used either way. In other instances the signs of the dispersions are inherent properties of the devices, and cannot be changed at will. When two Fabry-Perot interferometers are used entrain, they are necessarily used in the series arrangement. This follows because the dispersion D of each interferometer has its maximum value at the center of the fringe system, and decreasing values in the intensity maxima of lower order away from the center. This may be seen from the equation for maxima,[1]

$$m\lambda = 2\mu t \cos\theta \tag{1}$$

in which m is the order of interference, λ is the wave-length, μ is the index of refraction, t is the linear separation of the reflecting surfaces, and θ is the angle of emergence for rays proceeding from the interferometer. Thus,

$$D = d\theta/d\lambda = -m/(2\mu t \sin\theta). \tag{2}$$

However, if a device for producing Newton's rings were used entrain with a Fabry-Perot interferometer, the combination would necessarily form a tandem arrangement. This is a consequence of the fact that the order of interference and dispersion of the Newton rings have values which vary inversely as the radius and have a minimum value at the center. Both the tandem and the series arrangements are used in the double crystal x-ray spectrometer.

A slight extension of the concept of the combination of optical instruments suggests taking note of the use of optical devices in parallel arrangements. Examples are the parallel arrangement of Fabry-Perot interferometers,[2] grating interferometers,[3] and compound gratings.[4,5]

[1] W. E. Williams, *Applications of Interferometry* (E. P. Dutton and Company, New York, 1930), p. 88.
[2] L. Sturkey, J. Opt. Soc. Am. **30**, 351–354 (1940).
[3] B. P. Ramsay, J. Opt. Soc. Am. **24**, 253–258 (1934).
[4] E. Gehrcke, *Die Anwendung der Interferenzen* (F. Vieweg und Sohn, Braunschweig, 1906), p. 62.
[5] N. Hilberry, J. Opt. Soc. Am. **26**, 1–11 (1936).

The reason for considering the parallel arrangement an extension of the concept of combination of optical elements is that interferential theory treats these combinations adequately as a single instrument. Pushed to the extreme, the concept of parallel arrangements presents a grating, for instance, not as a single optical device but as a parallel arrangement of optical elements. It appears from the theory of the compound grating that these optical elements may be single slits or groups of slits. There is therefore adequate excuse for calling the crossing of gratings with a Michelson interferometer "a grating interferometer," and for calling the parallel arrangement of two Fabry-Perot interferometers "a cofinesse interferometer"—as if these parallel combinations of optical devices constituted a single instrument in a more rigorous sense than is usually attributed to devices entrain.

In the use of combinations of optical elements in the parallel arrangement also, it is necessary to distinguish between two cases, depending upon whether the dispersions of the elements have the same or unlike signs. It has been previously suggested[6] that the parallel arrangements of optical elements be called complementary when the dispersions have the same direction in the focal plane of the system, and that the arrangements be called chromatic when the dispersions have opposite directions.

II. THE INTENSITY FUNCTION FOR THE SYSTEM

In the interferential method[7] an intensity function which is appropriate to a given optical system is called the *I* function. Actually, the *I* function is derived under conditions which assume a source of idealized simplicity. Nevertheless, the *I* function is characteristic of the device for which it was derived, and serves adequately as a basis for comparing instruments which may be applied to a given purpose. It is therefore an important consideration in the study of combinations of optical elements. Indeed, it seems desirable at the outset to investigate the nature of the intensity function which is characteristic of the system as a whole.

The derivation of an *I* function requires that the light traversing the system originate from a homogeneous point source. Thus, one of the purposes for using entrain combinations of collimators, prisms and gratings is to produce a beam which may be incident upon a single interferential element under conditions approaching those assumed in the derivation of the *I* function for that element. In this case, the *I* function for the system is not essentially different from that of the single element. The other purpose for which interferential elements are used entrain is to produce an intensity distribution which is different from that of any single interferential element. It may be seen from the mathematical discussion[7] that the *I* function for the latter case consists of several factors which may be so arranged that each may be displayed as the *I* function characteristic of one of the interferential devices which constitute the arrangement. This circumstance implies that it is possible to alter the order of elements in the arrangement without altering the characteristic intensity function. An example of this is presented by the several arrangements in which the prism-etalon system is employed. There are notable advantages and disadvantages in the use of each arrangement, but the basis of choosing one of the several possibilities for a given purpose cannot be found in the *I* function.[8]

It has been shown in the case of parallel arrangements that the intensity function consists of two factors. One factor is characteristic of the elements which comprise the system, and the other is characteristic of the arrangement of these elements. Since these factors follow quite naturally from the theory of interference, it is unnecessary to discuss further the *I* function for parallel arrangements. It may be noted, however, that the *I* function displays the distinction between the chromatic and complementary arrangements. The manner in which this is done has been shown in the discussion of the grating interferometer.

III. SPECTRAL RANGE AND OVERLAPPING

Overlapping of spectra is a phenomenon which may be either advantageous or disadvantageous

[6] J. H. Schroeder and B. P. Ramsay, J. Opt. Soc. Am. **30**, 355–361 (1940).

[7] L. Sturkey and B. P. Ramsay, Phil. Mag. **31**, 13–23 (1941).

[8] K. W. Meissner, J. Opt. Soc. Am. **31**, 405–427 (1941).

in spectroscopic studies. Its disadvantageous aspects may be readily illustrated by the consideration of diffraction spectra. The dispersion D of a grating is readily obtained from the formula for maxima,

$$a(\sin i+\sin\theta)=m\lambda, \tag{3}$$

where a is the grating space, i the angle of incidence, θ the angle of transmission, m the spectrum order, and λ the wave-length. The angular dispersion is

$$D=d\theta/d\lambda=m/(a\cos\theta). \tag{4}$$

It thus appears that the dispersion of the grating is directly proportional to the order of the spectrum. Because of this, the position of any line in the spectrum of the nth order will coincide in position with that of a line of wave-length $n\lambda$ in the first order, or of wave-length $n\lambda/2$ in the second order, or generally of wave-length $n\lambda/k$ in the kth order. This is one of the difficulties encountered in the use of large spectral orders with gratings.

On the other hand, the phenomenon of overlapping was the basis for measurements of wave-length with the Fizeau interferoscope, the Hamy extincteur, the Michelson method of visibilities, and the method of coincidences employed with the Fabry-Perot interferometer.

Spectral range is the optical property of a device which is defined as the maximum wave-length difference which may be employed in a given interferential arrangement without overlapping. Thus for a device for which the epoch angle is given by

$$\alpha=\pi d/\lambda=m\pi/2, \tag{5}$$

$$m=2d/\lambda, \tag{6}$$

$$dm/d\lambda=-2d/\lambda^2=-m/\lambda, \tag{7}$$

and

$$\Delta\lambda=-\lambda(\Delta m/m). \tag{8}$$

Overlapping cannot occur unless Δm is equal to, or greater than, unit difference in order. The value of $\Delta\lambda$ which results by placing $\Delta m=1$ is the spectral range as defined above. Thus it appears that for cases in which the epoch angle is given by Eq. (5) the spectral range is

$$|\Delta\lambda|=\lambda/m=\lambda^2/2d. \tag{9}$$

It may now be observed that one of the chief ends sought in the use of combinations of optical devices is the elimination of overlapping within the spectral region which is a matter of interest. In these cases, the spectral range is effectively increased in three ways which may be described as effecting collimation, auxiliary dispersion, and missing orders, respectively. In the collimator, the physical source is ideally restricted to a point source or to a line source when the interference effects are required in one direction only. This restriction prevents the overlapping of intensity patterns which would otherwise result from the geometrical distribution of the point sources constituting a physical source. Auxiliary dispersion prevents overlapping by isolating lines or spectral regions of a limited frequency range. Thus wave-lengths which might obscure measurements at a given point are eliminated. Some instruments require collimation although others do not; but those which do not require collimation sometimes acquire different properties when provided with it.[9]

The phenomenon of missing orders is characteristic of parallel arrangements. Lord Rayleigh was the first to suggest that spectral range could be effectively increased by designing optical instruments in such a way as to effect missing orders. Possibilities of this kind have been considered from time to time.[5,10] Missing orders can occur, however, in series arrangements. Houston,[11] Pauls[12] and others have made it clear that this is one of the significant possibilities arising from the use of Fabry-Perot interferometers in series.

IV. OPTICAL DISPERSION

The term dispersion is used to describe two different phenomena. For the purpose of distinction, the first of these may be called physical dispersion. This concept arises from the theory of groups of waves, and is defined as the rate of change of phase velocity with wave-length. Because of the several relations between phase velocity and group velocity, the relation between phase velocity and refractive index, and the

[9] W. E. Williams, reference 1, Chapter V.
[10] R. W. Wood, *Physical Optics* (The Macmillan Company, New York, 1911), pp. 227–230.
[11] W. V. Houston, Phys. Rev. **29**, 478–484 (1927).
[12] E. Pauls, Physik. Zeits. **33**, 405–410 (1932).

relation between wave-length and frequency, the definition of physical dispersion is expressed by a great number of formulas. The second use of the word dispersion refers to the relative separation of wave-lengths which is effected by an optical device. This meaning can be more specifically designated as optical dispersion. Optical dispersion may be produced in two independent ways. In prismatic devices, it results from physical dispersion; but in multiple beam devices, optical dispersion arises largely from the action of the principle of superposition.[13] In some devices of the latter kind, the only effect of physical dispersion results from the presence of air in the optical paths, and may be entirely eliminated by using the instrument in vacuum.

Optical dispersion also may be described by more than one formula. Usually, it is the angular dispersion D which is meant; this is defined as the rate of change with wave-length λ of the angle θ at which light emerges from an optical device. On the other hand, the wave-length rate of change of some function of this angle may also be called dispersion. Thus the dispersion of Fabry-Perot interferometers in series is sometimes[14] given as

$$d(\cos\theta)/d\lambda = \cos\theta/\lambda, \tag{10}$$

where the letters have the same significance as in Eq. (1). Another kind of optical dispersion is called linear dispersion. It is the product of angular dispersion by such a linear dimension that the product of linear dispersion by the difference in wave-length of two spectrum lines gives the separation of these lines on a screen, a photographic plate, or the focal plane of the optical system. Thus, if s is the distance along the screen, the linear dispersion is

$$ds/d\lambda = L(d\theta/d\lambda), \tag{11}$$

where L is the proper factor of proportionality.[15] For instance, the linear dispersion of a prism spectrograph is the product of the angular dispersion of the prism and the focal length of the camera lens.

Rules for the angular and linear dispersions of a combination of optical devices must be stated separately in spite of the close relation between them. When two or more optical elements are used entrain, the angular dispersion of the system is simply

$$d\theta/d\lambda = \sum_{j=1}^{j=N} (d\theta_j/d\lambda), \tag{12}$$

where $j = 1, 2, 3, \cdots, N$ is an index characteristic of the respective elements of the train, and $d\theta_j/d\lambda$ is the angular dispersion of the jth element of the system. The angular dispersion of any element may be taken as either positive or negative; but when a sign for the dispersion of one element has been chosen, that for every other element must be referred to this choice. It is the algebraic sum of these quantities which is indicated by the right-hand member of Eq. (12). The linear dispersion of the system is

$$ds/d\lambda = \sum_{j=1}^{j=N} L_j(d\theta_j/d\lambda), \tag{13}$$

where L_j is the appropriate linear factor of the jth element.

It may be seen from Eq. (12) and Eq. (13) that linear and angular dispersion are mathematically independent quantities. One may be positive when the other is negative, or one may be zero when the other is different from zero. However, it is an integral form of these relations which describes the phenomena of deviation without dispersion, and dispersion without deviation.

V. SPECTROSCOPIC RESOLVING POWER

On the single line theory,[16] spectroscopic resolving power has been expressed by the epoch-slope formula,

$$P = (\alpha/Y)(\Delta I/\Delta\alpha), \tag{14}$$

where α is the interferential epoch function, $\Delta I/\Delta\alpha$ is the intensity-epoch slope, and Y is a function which shows the dependence of resolving power upon the intensity employed. The relation of this epoch-slope resolving power to the Rayleigh resolving power ρ, as given by the relation

$$\rho = \lambda/\Delta\lambda, \tag{15}$$

[13] B. P. Ramsay, E. L. Cleveland, and O. T. Koppius, J. Opt. Soc. Am. **31**, 297–298 (1941).

[14] E.g., W. E. Williams, reference 1, p. 92.

[15] The reciprocal also of the quantity given in Eq. (11) is called linear dispersion. Cf. G. S. Monk, *Light* (McGraw-Hill, New York, 1937), p. 92.

[16] B. P. Ramsay, O. T. Koppius, and E. L. Cleveland, J. Opt. Soc. Am. **31**, 202–208 (1941).

has been considered; and it has been shown that P is proportional to ρ for any given intensity distribution. However, the ratio P/ρ is not a constant for P depends upon the form of the intensity distribution whereas ρ does not. For example, P/ρ for a transparent prism is not equal to that for an absorbing prism. Obviously, it is necessary to consider separately rules for the Rayleigh and the epoch-slope resolving power.

(a) Rayleigh Resolving Power

For the purpose of discussing the Rayleigh resolving power of systems of interferential devices, it is convenient to use the generalized Williams interpretation,

$$\rho = \Delta t/T. \tag{16}$$

Here ρ is numerically equal to the difference in time Δt required to propagate energy over the extreme optical paths, where the unit of time is the period T of the wave motion. Likewise convenient is the uncertainty formula,

$$\rho = \nu \Delta t. \tag{17}$$

According to this rule, ρ is the product of the frequency and the uncertainty in time specification introduced by the device. Both of these rules show that when optical devices are used entrain the Rayleigh resolving power of the system is

$$\rho = \sum_{j=1}^{j=N} \rho_j, \tag{18}$$

since

$$\Delta t = \sum_{j=1}^{j=N} (\Delta t)_j. \tag{19}$$

The proper sign for each ρ_j may be determined in the manner suggested for the corresponding terms in Eq. (12). Thus Eq. (18) suggests that the spectroscopic resolving power of a series of prisms can be increased indefinitely by increasing the number of prisms in the train. Because of prismatic absorption, laboratory experience is not in agreement with this conclusion, and the circumstance indicates a deficiency of the Rayleigh resolving power.[17]

[17] B. P. Ramsay, O. T. Koppius, and E. L. Cleveland, J. Opt. Soc. Am. **30**, 439–444 (1940).

(b) Epoch-Slope Resolving Power

In calculating the epoch-slope resolving power, it is only the difference in times of the extreme beams which are added algebraically. This additive property is always expressed in terms of the epoch function α. For zero-order instruments,

$$\alpha = \pi \rho, \tag{20}$$

but for multiple beam interferometers,

$$\alpha = \pi \nu d/u, \tag{21}$$

where ν is the frequency of the light, d is the path difference, and u is the group velocity. When the group velocity is equal to the phase velocity, Eq. (21) becomes

$$\alpha = \rho d/\lambda. \tag{22}$$

Thus P can be calculated for a system of interferential devices in terms of α when the intensity-epoch slope has been determined.

VI. ARRANGEMENTS OF INSTRUMENTS

There are several quantities which might affect the manner in which devices used entrain are to be placed. It is immediately obvious that algebraic quantities, such as the Rayleigh resolving power and the dispersion, cannot determine the order of arrangement. The Rayleigh resolving power of the interferometer can be increased indefinitely by using the instruments in high orders of interference. In this case, however, overlapping makes isolation of a single wavelength impossible and the use of a second instrument would not in this case prove the light to be much more monochromatic than that incident on the first. The dispersion of optical instruments used entrain is given by Eq. (12) or Eq. (13), which shows, that when due regard is given to the proper choice of signs, the final dispersion is the result of an algebraic summation. Thus Rayleigh resolving power and dispersion are not the kind of quantities that determine the order in which the instruments are to be used entrain.

Isolation is the process of preventing overlapping, with the spectral range available, by restricting the region of wave-lengths incident upon the ultimate high resolving power device. It is this consideration which prompts the use of prismatic dispersion before, rather than after, an interferometer. The problem is essentially one

of resolution rather than of resolving power; that is, it is a problem of interpreting the resulting J curve rather than the actual difference in separation of the wave-lengths affected by the train. If one were to examine a source of light which was strictly monochromatic with the most powerful spectroscope, the line would still have a finite width. This width, which it appeared to have, would not be its own real width, but the width due to the finite ability of the spectroscope. For a strictly monochromatic source the half-width of the intensity pattern would be small. If, however, the light became less monochromatic, the half-width of the line would increase accordingly. Now if the half-width for the monochromatic light is negligibly small as compared with the half-width of the actual line, the intensity pattern obtained is very closely the true intensity distribution. Hence, if this is unsymmetrical in any way, as seen with a microphotometer tracing, evidence of the existence of another line can be found.

If now a very narrow slit be placed over the spectral line with the larger half-width, and then this light be sent into a very powerful instrument, say a Michelson interferometer, one would get in the interferometer a path difference limited only by the narrowness of the slit. On the other hand, if the resolving power of the first instrument were unlimited, that is, if one placed the Michelson first, placing the narrow slit over a fringe would not prove the light more monochromatic than that incident upon the first instrument. The reason for this is that the slit would transmit the $\cos^2(\alpha/2)$ fringes for several wave-lengths. Thus the degree of isolation of different wave-lengths effected by an instrument will be a determining factor in the arrangement of instruments entrain.

Thus the final arrangement of the devices entrain will be independent of the Rayleigh resolving power and the dispersion of each device. The order chosen is sometimes one of convenience rather than of necessity. However, the final arrangement will not be independent of the intensity, the spectral range, and the isolation. The magnitude of the intensity transmitted is a matter of geometrical optics and is determined by a consideration of the numerical aperture and the absorption.

Eleventh Annual Meeting—Inter-Society Color Council

THE eleventh annual meeting of the Inter-Society Color Council will be held on February 26 and 27, 1942, at the Metropolitan Museum of Art in New York City. Members of member bodies are invited to this meeting and all persons interested in color in art education are cordially invited to attend any or all sessions.

February 26

10:00 A.M. Business Session
2:00 P.M. Technical Session: Color in Art Education
8:00 P.M. Popular Session on Lighting, Color and Design

February 27

10:00 A.M. School Exhibits Session
2:00 P.M. Discussion Session on Color in Art Education and Inter-Society Color Council Problems.

Reflection-Transmission Relationships in Sheet Materials

HERBERT F. LAUNER
National Bureau of Standards, Washington, D. C.

(Received September 24, 1941)

Reflectances of transmissive sheets, calculated from the transmissions of one and two sheets, are compared with reflectances obtained by using the General Electric recording spectrophotometer. The expression used as a basis for calculation, $R_a=(1-T_a^2/T_{2a})^{\frac{1}{2}}$, in which R_a is the reflectance, and T_a and T_{2a} are the transmissions of one and two sheets, respectively, of a, was derived by considering the infinite series of reflections undergone by light, or radiant energy in general, in passing through the two sheets. The expression was found to be valid and useful over a wide range of reflectances and wave-lengths, for materials such as paper, glass, and an organic plastic.

The method is an absolute one since it involves no reflectance standard. It involves no spherical or similar integrating device nor does it involve any reflecting surface other than that of the sample itself, as a fundamental part of the measurements. When transmission values for diffuse incidence are substituted into the expression, the reflectances thus calculated correspond to the conditions of diffuse incidence and diffuse viewing, and as such are somewhat higher than the usual directly measured reflectances for normal incidence and diffuse viewing (or diffuse incidence and normal viewing). For clear sheets, with normal incidence, specular reflectance may be calculated.

The method thus affords a means of determining, from two simple measurements, the specular-plus-diffuse reflectance of transmissive sheets for diffused light or radiant energy in general.

The expression as derived is theoretically inapplicable to diffusing sheets for light of normal incidence, but a compensation of errors allows close agreement over the visible range, at 365 millimicrons, and for "white" light, for all except tissue paper and other materials of like transmissivity. For diffuse incidence at 365, and to a certain extent, at 405 millimicrons, some papers show deviations from the simple theory because of fluorescence effects. This and other effects are discussed.

Reflectances in the infra-red region near 850 millimicrons are also calculated but no standard for comparison is available for these values. The sources of errors at the shorter wave-lengths, however, do not interfere in the infra-red region.

Transmissions of papers were found to be dependent upon the angle of incidence.

Reflectances throughout the visible region, measured at 45° from normal incidence were found to agree closely, for the type of papers studied, with those obtained using the General Electric recording spectrophotometer, which corresponds to the conditions of normal incidence and diffuse viewing.

I. INTRODUCTION

IN a current study of the photochemistry of paper it was necessary to determine the absolute total reflection and transmission factors of the sheets to permit calculation of the fractional light absorption. The measurement of transmission was relatively simple, but the determination of absolute reflectance, in, for example, the near infra-red, for which no reflectance standard is available, led to a consideration of absolute methods. Gibson[1] and Van den Akker[2] have recently reviewed various phases of spectrophotometry, particularly with respect to the problems of the reflectance standards and geometrical design of instruments which yield values in terms of a standard magnesium oxide, or similar, surface. Taylor[3] has described an absolute reflectometer in which magnesium oxide (or similar) surfaces play a fundamental part in the measurement but not in the calculation, of diffuse reflectance. No method, however, has been shown to yield absolute reflectance of diffusing materials, which does not involve, either explicitly or implicitly, the reflectance of either a standard or of the surface of an integrating sphere.

For transmissive materials in sheet form a method suggests itself for obtaining absolute reflectance without involving a standard or any other reflecting surface. Consider light, or radiant energy in general, passing through two sheets of any material, a, having the reflection and transmission factors R_a and T_a, corresponding to a definite kind of light. For unit incident flux, the light immediately after transmission by the first sheet has a flux equal to T_a. This light then undergoes an infinite series of reflections between the two sheets, so that the flux incident upon the

[1] Kasson S. Gibson, "Survey of spectrophotometers," Paper Trade J. **111** (Sept. 5, 1940).
[2] J. A. Van den Akker, "Survey of abridged spectrophotometers," Paper Trade J. **111** (Sept. 12, 1940).
[3] A. H. Taylor, "Measurement of reflection factors in the ultraviolet," J. Opt. Soc. Am. **21**, 776 (1931).

second sheet is $T_a/(1-R_a^2)$, which after transmission through the second sheet becomes $T_a^2/(1-R_a^2)$. Equating this to T_{2a}, the transmission of the two sheets, and transposing, the following expression is obtained:

$$R_a=(1-T_a^2/T_{2a})^{\frac{1}{2}}. \quad (1)$$

If the two sheets differ the expression becomes

$$R_aR_b=1-T_aT_b/T_{ab}. \quad (2)$$

Equation (1) was derived in its present form by Gurevich[4] and Smith,[5] and in other forms by Stokes,[6] Channon, Renwick, and Storr,[7] and Ryde and Cooper,[8] for diffusing materials, and by Benford[9] for sheets of glass. The expression, however, has apparently not been tested experimentally.

Gurevich assumed the expression to be valid and used it to calculate reflectances of some paper samples in heterogeneous light, but he presented no directly measured reflectances to allow a comparison. Also using heterogeneous light, Kubelka and Munk,[10] Steele,[11] and Judd[12] studied the relationships between reflectance, thickness and scattering for papers and other diffusing materials.

The experimental verification of Eq. (1) is of interest for various reasons. Aside from the value of an absolute method based upon principles entirely different from those of existing methods, it would permit the determination of the reflectance of transmissive sheets from relatively simple transmission measurements, using inexpensive equipment and weak sources of light, without amplification in the measuring system since practically all of the transmitted light is to be measured directly.

In the present paper, reflectance obtained by direct measurement, for a variety of materials, at various wave-lengths, are compared with reflectances calculated from transmission measurements of one and two sheets, using Eq. (1). Various factors causing deviations from the simple theory, such as changes in the values of R_a and T_a resulting from changes in spectral and geometric distribution of the light by the first sheet are discussed.

II. SAMPLES STUDIED

Six papers were selected for study which had been produced in the paper mill at the National Bureau of Standards from a wide variety of commercial materials to secure various representative types of papers. The data significant for the optical properties are listed in the tables; further details as to the papers may be obtained from the publication by Shaw and O'Leary.[13] Three widely differing commercial papers, namely, a tissue paper, a bluish-tint writing paper, and a heavily-filled cigarette paper, were also studied. All of the papers had a matt finish. A relatively thick sheet of an organic plastic, a urea-formaldehyde laminated with very thin paper, was included in the investigation, as was a sheet of photographic plate glass.

III. APPARATUS

1. Photoelectric Equipment

The photoelectric circuit used was that described by Brice.[14] Two General Electric "light-sensitive" cells were used, one of which measured the radiant energy transmitted by the sheets and the other of which compensated for lamp fluctuations. A galvanometer having a sensitivity of 0.5 microvolt per mm, and a calibrated potentiometer of 100 ohms total resistance, capable of being read to the nearest 0.1 percent transmission, completed the circuit. With this arrangement transmission values could be estimated to the nearest 0.05 percent transmission.

[4] M. Gurevich, "Ueber eine Rationelle Klassification der Lichtstreuenden Medien," Physik. Zeits. **31**, 753 (1930).
[5] T. Smith, "The hiding power of diffusing media," Trans. Opt. Soc. **33**, 150 (1931–1932).
[6] G. G. Stokes, "On the intensity of light reflected from or transmitted through a pile of plates," Proc. Roy. Soc. (London) **11**, 545 (1860–62).
[7] H. J. Channon, F. F. Renwick, and B. V. Storr, "The behavior of scattering media in fully diffused light," Proc. Roy. Soc. (London) **A94**, 222 (1918).
[8] J. W. Ryde and B. S. Cooper, "Scattering of light by turbid media," Proc. Roy. Soc. (London) **A131**, 451 (1931).
[9] Frank Benford, "Reflection and transmission by parallel plates," J. Opt. Soc. Am. **7**, 1017 (1923).
[10] P. Kubelka and F. Munk, "Ein Beitrag zur Optik der Farbanstriche," Zeits. f. tech. Physik **12**, 593 (1931).
[11] F. A. Steele, "Optical characteristics of paper," Paper Trade J. **100** (March 21, 1935).
[12] Deane B. Judd, "Optical specification of light scattering materials," J. Research Nat. Bur. Stand. **19**, 287 (1937), RP 1026.
[13] Merle B. Shaw and Martin J. O'Leary, "Effect of filling and sizing materials on stability of book papers," J. Research Nat. Bur. Stand. **21**, 671 (1938), RP 1149.
[14] B. A. Brice, "Potentiometer circuit for two barrier layer cells," Rev. Sci. Inst. **8**, 279 (1937).

The maximum flux density used corresponded to a photo-current of 5 microamperes or less, thus making for conditions of highest accuracy, as found by Brice. The apparatus was checked for accuracy by measuring the transmission of a polished glass, found by the Photometry and Colorimetry Section to transmit 16.0 percent at a certain wave-length, and by measuring the transmissions of two sectored disks transmitting 25.0 and 50.0 percent. The results showed that the probable error was less than 0.1 percent transmission.

The measuring cell was adapted for transmission measurements by removing the photo-sensitive selenium-covered steel plate from the hard-rubber case. The plate was mounted on a flat, hard-rubber surface, and the transmission samples were held under spring tension directly against the photo-sensitive surface by a flat metal frame, the opening of which was slightly larger than the photo-sensitive surface. Electrical contact with the plate was made on the back by two springs extending through holes drilled in the hard rubber. On the front surface contact was made by thin (0.0005″) silver foil, two strips of which covered the roughened borders and were held under tension against them by the frame. Thus, the spacing between the receiving surface and the transmission samples was actually 0.0005″ under the frame.

For the experiments with diffuse radiant energy, a sheet of paper, No. 198, 20×20 cm, which was mounted 38 mm in front of the cell, 19×41 mm, used for transmission measurements, served as a diffusing screen. Multiple reflections between this screen and the sample being studied can be shown to introduce negligible errors into the calculated reflectances. The light source was placed at distances of 35 to 60 cm from the diffusing screen. For experiments with normal (perpendicular) illumination this diffusing screen was removed.

2. Light Sources and Filters

Spectrally homogeneous radiant energy was obtained by isolating mercury lines from a 400-watt, "high-intensity" glass-enclosed commercial mercury vapor lamp. The infra-red and short ultraviolet regions were removed by a 15-mm thickness of 0.117 molar $CuCl_2 \cdot 2H_2O$ (2 percent) solution in a glass cell. Using this filter with the following glass filters, various Hg lines were isolated, respectively: Corning 986 (7 mm), 365 millimicrons; Corning Noviol O and 597, 405 millimicrons; Noviol A and 585, 436 millimicrons; Jena OG1, Corning 512, and Corning G584J, 546 millimicrons; Jena RG1, 623 millimicrons. The light thus isolated was not perfectly homogeneous in all cases. As an example, the bright 436 line was faintly contaminated with the 492 line, but not sufficiently so as to affect the results seriously. In no case, however, did the red and infra-red, also transmitted by the Corning filters, Nos. 986, 597 and 585, correspond to more than 0.05 percent of the cell response. For "white" light a 110-volt, 100-watt tungsten incandescent lamp, in combination with the cupric chloride filter was used. For the infra-red, a 110-volt, 1000-watt "Airway Beacon" incandescent lamp, in combination with a Corning 254 filter and a 15-mm layer of water was used. The effective wave-length of the infra-red thus isolated was approximately 850 millimicrons, calculated as the spectral centroid from the spectral distribution of the lamp, maximum at 900 millimicrons, the transmission of the filter, and the spectral sensitivity of the cell (manufacturers' data).

IV. EXPERIMENTAL RESULTS AND THEORETICAL DISCUSSION

1. Methods of Direct Measurement of Reflectance

The test of Eq. (1) consists in comparing reflectances calculated from transmission values with directly measured reflectances. The values obtained by using the General Electric recording spectrophotometer which employs the principle of normal incidence and diffuse viewing, were adopted as the basis for all of the directly measured reflectances. Not all of the reflectances were obtained in this manner, but the results obtained by an alternate method were found to be the same, within the limits of the experimental errors of both methods, for the papers included in this study.

The alternate method was the familiar one of normal incidence and 45° viewing. Light of the desired wave-length was focused on the paper or

standard MgO surface to give an image of 2×4 cm. A G.E. cell to receive reflected light was mounted at a distance of 15 cm from the light spot. Another cell, illuminated by reflection from a piece of clear glass placed at an angle in the incident beam, compensated for lamp fluctuations, as previously described. The MgO surface was freshly deposited to approximately $\frac{3}{4}$-mm thickness on a slab of Duralumin held in the smoke of burning magnesium ribbon.

TABLE I. Comparison between reflectances of papers obtained from curves using the General Electric recording spectrophotometer, and those obtained by measuring reflectances at 45° from normal incidence.

PAPER No.	405mμ G.E. %	405mμ 45° %	436mμ G.E. %	436mμ 45° %	546mμ G.E. %	546mμ 45° %	623mμ G.E. %	623mμ 45° %
1215	76.9	77.1	78.6	78.1	81.2	81.2	81.2	81.2
1214	66.5	65.6	69.5	69.9	73.6	74.2	73.8	73.1
1191	73.2	73.6	75.8	75.8	79.3	79.6	79.7	78.7
1170	63.0	62.4	67.9	67.3	73.2	73.2	73.6	72.2
1133	50.5	50.4	56.2	57.6	65.9	66.8	68.2	67.4
1136	54.6	55.6	61.4	62.5	71.9	72.9	74.1	73.7

The values obtained by using these two direct methods are compared in Table I for part of the papers included in this study. Parts of the same sheets, but not identical areas thereof, were measured in both cases. The agreement, however, is seen to be satisfactory, and independent of the wave-lengths studied. Since both methods yield values relative to MgO, the reflectances were converted to absolute ones by the use of Preston's[15] factors for MgO.

The spectrophotometer values at the wave-lengths 405, 436, 546, and 623 millimicrons were taken from curves obtained by H. J. Keegan of the Photometry and Colorimetry Section, for samples, Nos. 1215, 1214, 1191, 1170, 1133, 1136, and 200. The values were reduced in the manner described by Gibson and Keegan.[16] All other reflectances were determined by the alternate method, with the exception of that of the glass, which was calculated from the refractive index $n=1.5157$ obtained by C. A. Faick of the Glass Section for yellow light.

[15] J. S. Preston, "The reflection of magnesium oxide," Trans. Opt. Soc. **31**, 15 (1929–30).

[16] Kasson S. Gibson and Harry J. Keegan, "Calibration and operation of the General Electric recording spectrophotometer of the National Bureau of Standards," J. Opt. Soc. Am. **28**, 372 (1938).

2. Effect of Reflectance of the Measuring Cell

In measuring the transmission of sheets held very close to the photo-sensitive surface the small amount of radiant energy reflected by this surface must be taken into account. This may be done by considering separately the optical relationships involved for one and two sheets. By summing up the infinite series of reflections between one sheet and the cell surface, the following expression is obtained:

$$T_a=t_a(1-R_aR_c). \tag{3}$$

And similarly, for two sheets:

$$T_{2a}=t_{2a}(1-R_aR_c)/(1+t_{2a}R_aR_c), \tag{4}$$

where

T_a and T_{2a} = corrected transmissions of one and two sheets;

t_a and t_{2a} = measured transmissions of one and two sheets;

R_a and R_c = reflectances of the sheet and the cell.

Equations (3) and (4) are then substituted into Eq. (1) and the following complete expression is obtained:

$$R_a=\left(\left[\left(1-\frac{t_a^2}{t_{2a}}\right)\left(\frac{1}{1-t_a^2R_c^2}\right)\right]+\left[\frac{R_c}{2}\left(\frac{t_a^2}{t_{2a}}\right)\frac{1-t_{2a}}{1-t_a^2R_c^2}\right]^2\right)^{\frac{1}{2}}+\frac{R_c}{2}\left(\frac{t_a^2}{t_{2a}}\right)\frac{1-t_{2a}}{1-t_a^2R_c^2}. \tag{5}$$

For usual values of R_c (near 0.1) Eq. (5) may be simplified by omitting negligible terms:

$$R_a=\left(1-\frac{t_a^2}{t_{2a}}\right)^{\frac{1}{2}}+0.002+\tfrac{1}{2}R_c\left(\frac{t_a^2}{t_{2a}}\right)(1-t_{2a}). \tag{6}$$

The figure 0.002 applies for most papers but reaches a value of 0.004 for the more transmissive diffusing sheets.

For materials having low transmissions, as do some papers in the ultraviolet and violet, t_{2a} becomes very small, less than 0.01, and the errors correspondingly large. To avoid this, a more transmissive, auxiliary sheet may be used

TABLE II. Reflectances, calculated from the transmissions of one and two sheets, compared with the reflectances directly measured with a General Electric recording spectrophotometer[a] and other equipment.

NUMBER AND TYPE OF SHEET MATERIAL	623mμ			546mμ			436mμ			405mμ			365mμ			INFRA-RED[b]		HETEROGENEOUS ("WHITE") LIGHT[c]	
	DIRECT MEASUREMENT	CALCULATED FROM TRANSMISSIONS		DIRECT MEASUREMENT	CALCULATED FROM TRANSMISSIONS		DIRECT MEASUREMENT	CALCULATED FROM TRANSMISSIONS		DIRECT MEASUREMENT	CALCULATED FROM TRANSMISSIONS		DIRECT MEASUREMENT	CALCULATED FROM TRANSMISSIONS		CALCULATED FROM TRANSMISSIONS		DIRECT MEASUREMENT	CALCULATED FROM TRANSMISSIONS
	normal incidence %	normal incidence %	diffuse incidence %	normal incidence %	normal incidence %	diffuse incidence %	normal incidence %	normal incidence %	diffuse incidence %	normal incidence %	normal incidence %	diffuse incidence %	normal incidence %	normal incidence %	diffuse incidence %	normal incidence %	diffuse incidence %	normal incidence %	normal incidence %
1215[d]—rag paper; 14% $CaCO_3$ filler; 0.0036" thickness	81.2	80.7	81.8	81.2	81.4	82.4	78.6	78.3	80.5	76.9	77.3	79.9	73.2	73.9	78.2 (72.6)	76.7	76.9	80.6	81.4
1214—rag paper; no filler; 0.0038" thickness	73.8	72.6	74.7	73.6	73.1	74.7	69.5	68.1	69.8	66.5	65.6	67.1	60.8	61.0	66.3 (57.8)	69.7	69.9	73.9	73.3
1191—rag paper; 14% clay filler; 0.0036" thickness	79.3	78.8	80.2	79.3	79.5	80.9	75.8	75.2	77.6	73.2	73.7	75.8	68.2	69.8	75.8 (65.9)	76.0	73.9	79.2	79.7
1170—wood pulp paper; 14% clay filler; 0.0034" thickness	73.6	72.8	74.1	73.2	72.7	74.4	67.9	66.0	69.0	63.0	63.7	65.9	54.2	53.0	66.7 (48.9)	68.1	66.9	73.0	72.7
1133—yellowish wood pulp paper; no filler; 0.0035" thickness	68.2	66.6	70.3	65.9	63.9	68.1	56.2	52.1	56.7	50.5	51.5	53.4	41.6	38.0	54.8 (37.4)	66.0	67.2	66.5	65.8
1136—yellowish wood pulp paper; 9% clay filler; 0.0037" thickness	74.1	73.1	76.2	71.9	71.2	73.9	61.4	60.5	62.7	54.6	55.1	67.0	46.4	46.8	74.0 (58.6)	70.8	71.9	72.8	72.8
128—bluish tint rag bond paper; 0.004" thickness	66.7	66.6	69.8	67.7	67.6	69.8	67.6	64.9	68.6	64.4	62.9	66.6	61.2	60.1	64.0 (60.4)	61.9	63.3	67.9	66.4
1002—cigarette paper; 19% $CaCO_3$ filler; 0.0015" thickness	60.9	59.8	63.6	61.9	61.5	64.2	62.5	62.2	65.2	62.6	61.6	64.6	60.1	60.1	62.4 (62.0)	51.6	51.4	61.5	62.4
198—facing tissue; 0.001" thickness	37.7	32.1	40.3	39.4	34.9	40.9	40.2	33.0	40.9	38.6	29.0	37.6	35.2	16.7	33.7	24.3	29.5	39.0	32.2
200—"thick" organic plastic; 0.023" thickness	34.2	(u.v.)[e]	36.9	36.1	(u.v.)	37.9	35.1	(u.v.)	33.8	28.1	(u.v.)	30.4	—	—	—	(u.v.)	28.5	—	—
202—clear glass plate; 0.047" thickness	—	—	—	8.1[f]	7.8	11.5	—	—	—	—	—	—	—	—	—	—	—	—	—

[a] Used for values at 623, 546, 436 and 405 millimicrons for samples, Nos. 1215, 1214, 1191, 1170, 1133, 1136 and 200. See text for details.
[b] Wave-length approximately 850 millmicrons. See text for details.
[c] Heterogeneous light was that from a 100-watt, 110-volt tungsten lamp, after transmission through a 15-mm layer of 0.117 molar cupric chloride solution.
[d] The first six papers were made in the Bureau paper mill (reference 13 in text). Numbers 128 and 198 were standard samples of the same number from the Government Printing Office. The papers were near-white or neutral gray unless otherwise specified.
[e] "u.v." stands for "unreal value" since the expression $1-(t_a^2/t_{2a})$ had a negative value in these cases.
[f] Reflectance was calculated from the refractive index for yellow light, $n=1.5157$.

in combination with the sheet to be measured, instead of two sheets of the same material. For this case, Eq. (2) is used and becomes

$$R_b=\frac{1}{R_a}\left(1-\frac{T_a t_b}{t_{ab}}\right) \qquad (7)$$

where

R_a = reflectance of auxiliary sheet, as calculated from Eq. (6), or otherwise known;

T_a = corrected transmission of auxiliary sheet, calculated from Eq. (3);

t_b = measured transmission of sheet whose reflectance is being determined;

t_{ab} = measured transmission of the combination, with sheet b between a and the cell.

All of the calculated reflectances (reflectances calculated from transmissions) in Table II were obtained by substitution of the measured trans-

TABLE III. Transmission[a] data for the sheet materials.

NUMBER OF SHEET MATERIAL	WAVE-LENGTH IN MILLIMICRONS											
	INFRA-RED		623		546		436		405		365	
	t_a	t_{2a}	t_a	t_{2a}	t_a	t_{2a}	t_a	t_{ab} or t_{2a}	t_a	t_{ab} or t_{2a}	t_a	t_{ab} or t_{2a}
1215	0.244	0.136	0.167	0.078	0.153	0.067	0.114	0.0575	0.096	0.042	0.069	0.023
1214	.303	.170	.229	.111	.212	.095	.157	.068	.127	.047	.083	.024
1191	.257	.137	.173	.078	.158	.067	.111	.0535	.087	.036	.051	.0165
1170	.334	.192	.250	.130	.227	.109	.158	.0675	.118	.043	.062	.018
1133	.339	.199	.270	.136	.240	.101	.148	.0545	.107	.034	.0585	.015
1136	.283	.157	.213	.101	.187	.073	.104	.041	.065	.024	.0285	.009
128	.363	.210	.292	.158	.279	.143	.240	.104	.2185	.0815	.1765	.0504
1002	.488	.313	.370	.219	.347	.198	.304	.150	.277	.126	.2395	.090
198	.687	.510	.582	.394	.556	.364	.494	.287	.460	.241	.392	.170
200	.624	.418	.586	.390	.555	.352	.419	.195	.274	.081	.033	.009
202					.9260	.868						
					.9285[b]	.867[b]						

[a] Measured transmissions of diffusely incident radiant energy for one sheet are given as t_a, for two sheets of the same material as t_{2a}, and for the combination of the various materials with No. 128 as t_{ab}. This last combination was used for the first six papers at 436, 405 and 365 millimicrons. See text for further details.

[b] These values were obtained with light of perpendicular incidence.

missions, some of which are given in Table III, into Eqs. (6) or (7). These data will be analyzed in following sections as to significance and pertinent factors. Equation (7) was used for reflectances at 436, 405, and 365 millimicrons for papers Nos. 1215, 1214, 1191, 1170, 1133, and 1136, using paper No. 128 as sheet *a*. For all other cases t_{2a} was feasibly large (greater than 0.05) and the reflectances were calculated by means of Eq. (6). At 623 and 546 millimicrons the values calculated with both equations for the first six papers agreed well without any noticeable trend.

The reflectance, R_c, of the lacquered gold-selenium receiving surface of the G. E. cell was obtained as follows: Since the images reflected by the cell surface were fairly regular, R_c was determined relative to a piece of Corex-D glass. A beam was so focused, by means of a lens, that after 10° incidence upon the cell surface and reflection at 10°, the image was projected upon the center of another cell which measured the intensity of the reflected beam. A third cell was used to compensate for intensity fluctuations. By repeating the measurement with a piece of Corex-D glass at various wave-lengths, the following ratios of R_c to $R_{\text{Corex-D}}$ were obtained, for the indicated wave-lengths: 365 millimicrons, 0.85; 436 millimicrons, 0.92; 578 millimicrons, 0.96; 623 millimicrons, 1.0; infra-red, 1.27. Two other cells gave essentially the same reflectance ratios.

From the reflectance of the Corex-D glass, 0.085 (manufacturer's data), the reflectance of the cell-surface for normal incidence may be calculated. The use-conditions of the cell are such, however, that the reflectance for diffused incidence should be used for R_c. The values of R_c for normal incidence represent minimum values; maximum values may be obtained by weighting, from $\theta=0$ to $\theta=\pi/2$, the values of the reflectances of the cell for various angles of incidence.

The relationship between R_c and angle of incidence, θ, was found in the following way. A small spot of light of wave-length 578 millimicrons was focused on the surface of the cell which could be rotated through known angles. The cell-circuit was balanced against the compensating cell for normal incidence, and readings were then taken of cell-response at the various angles in terms of that for normal incidence. From this the variation in R_c with θ, angle of incidence, could be computed, based upon R_c at normal incidence, 0.082, for this wave-length. The values are recorded in Table IV.

From the data in Table IV, and from the

TABLE IV. Reflectance of receiving surface, R_c, of light sensitive cell as a function of the angle of incidence, θ, at 578 millimicrons.

θ(degrees)	0	10	20	30	40	50	60	70
R_c	0.082	0.082	0.083	0.084	0.088	0.097	0.118	0.146

reasonable assumption that $R_c=0.2$ at $\theta=80°$, which value is not heavily weighted in any case, the reflectance of the cell for completely diffused illumination may be computed using the method described by McNicholas,[17] and applied by Judd and Gibson[18] to a similar problem:

$$R_{c(\text{diffused})}=\sum_{0}^{\pi/2} R_\theta \sin 2\theta / \sum_{0}^{\pi/2} \sin 2\theta = 0.107. \qquad (8)$$

This value represents the upper limit corresponding to completely diffused illumination, which is, in general, not attained.

Great accuracy in the value for R_c is, however, not necessary, inasmuch as the correction factor, $\frac{1}{2}R_c(t_a^2/t_{2a})(1-t_{2a})$, usually contributes less than two percent in Eq. (6). For the present purposes, therefore, the value, 0.09, somewhat less than intermediate between the two extremes, was adopted for R_c at 578 millimicrons. This led to the following values for R_c at the other wavelengths: 365 millimicrons, 0.08; 436 millimicrons, 0.085; 623 millimicrons, 0.095; 850 millimicrons, 0.12. These values were used in Eq. (6) and in the calculations of T_a in Eq. (7).

3. Calculated Reflectances for Diffuse and Normal Incidence

The two sets of calculated reflectance values in Table II correspond to the two types of illumination used, namely diffuse and normal incidence, although it should be noted that even in the latter case the second sheet of a combination is illuminated diffusely to the extent that the first sheet acts as a diffuser. The transmission values for diffuse incidence are given in Table III; those for normal incidence were omitted for the sake of brevity.

As it was pointed out previously, the directly measured reflectances were intended to serve as a standard of comparison for the calculated reflectances. Such a comparison is strictly valid only if the geometrical conditions involved in both cases are identical. This is, however, not the case in the present work, inasmuch as the directly measured reflectances correspond to the condition of normal incidence and diffuse viewing (or, which is numerically the same for the papers, normal incidence and 45° viewing), whereas the calculated reflectances correspond to the condition of diffuse incidence and diffuse viewing. The latter condition obtains, to a varying extent, in the transmission measurements with normal incidence, but the reflectances calculated therefrom involve errors which will be discussed subsequently.

TABLE V. Transmission of papers as a function of angle of incident light at 578 millimicrons.

	Measured Transmissions (t_a)		
$\theta°$	Paper No. 198	Paper no. 1133	Paper No. 1215
0	0.607	0.268	0.160
10	.600	.264	.158
20	.589	.256	.154
30	.569	.243	.148
40	.547	.228	.141
50	.528	.213	.134
55	.518	.206	.131
60	.517[a]	.202[a]	.129[a]
70	.542	.203	.132
80	.680	.241	.156
Diffused	.569	.242	.150

[a] The increases in t_a with θ at angles greater than 60° are reproducible but probably do not represent real characteristics of papers. They are apparently the result of the particular method of measurement, which consisted in varying the angle of the measuring cell and balancing the circuit at each angle with no paper. Beyond 60° the specular reflectance of the bare cell surface appears to increase much more rapidly with θ than that of the paper, so that the cell-response per unit of radiant flux is greater with than without the paper. At angles below 60°, however, such an effect would be negligible since the reflectance of the cell changes only slightly with θ at the smaller angles.

It is not to be expected, however, that the values corresponding to the two sets of geometrical conditions should be greatly different. McNicholas,[17] using diffuse incidence (undispersed incandescent-lamp light) computed that the diffuse reflectances of a variety of matt materials were, in general, 1 to 3 percent reflectance higher than reflectance in the direction normal to the surface, which latter condition is equivalent to normal incidence and diffuse viewing, according to the Helmholtz reciprocity relation.

The samples studied by McNicholas were opaque or mounted on opaque backings, and had surface characteristics different from those of papers. It was found, however, that the materials of the present study behave similarly. This can be seen, although indirectly, from a comparison of the transmissions of various typical papers for normal and diffuse incidence,

[17] H. J. McNicholas, "Absolute methods in reflectometry," Bur. Stand. J. Research **1**, 50 (1928), RP 3.

[18] Deane B. Judd and Kasson S. Gibson, "Note on the effect of a cover glass in reflectance measurements," J. Research Nat. Bur. Stand. **16**, 261 (1936), RP 872.

given in Table V, in which the first and last values in each column are to be compared in the present connection.

The results in Table II show that the reflectances calculated from transmissions for diffuse incidence are higher than the directly measured reflectances by 1 to 3 percent reflectance, except in the extreme violet and ultraviolet, where the differences are, in general, much greater, and will be shown to be due to fluorescence effects. The values in parentheses for 365 millimicrons demonstrate the general result of correcting for fluorescence.

The reflectances, calculated from transmissions for normal incidence, are seen to be in good agreement with the directly measured reflectances, with the exception of the tissue paper, 198, and the organic plastic, 200, for which agreement is very poor, especially in the case of 200, for which no real values could be calculated. This is explained by the fact that the values for t_a for these sheets are much higher for normal than for diffuse incidence (as shown in Table V), and are raised to the second power, whereas the corresponding values for t_{2a}, which enter Eq. (1) to the first power, are more nearly equal, since the second sheet of the combination is illuminated diffusely, to a greater or less extent, by the first sheet. Thus, for normal incidence, the expression, $1-(t_a^2/t_{2a})$, assumes low or even negative values for very transmissive sheets, but for most papers yields values which are just sufficiently low to be in fortuitous agreement with directly measured reflectances.

The departure from the simple theory, when normal incidence is used, is thus seen to be due to a change in the value of T_a as a consequence of the change in geometrical distribution of the radiant energy in passing through the first sheet.

This effect occurred in all cases in normal incidence, except for the clear glass, but it was less pronounced for the thicker or more diffusing papers, since such sheets exhibited less difference in t_a for normal and diffuse incidence. Furthermore, the mathematical form of Eq. (1) is such that its value is much less sensitive to this type of effect for sheets of high or medium reflectance than for sheets of low reflectance.

Another effect of using normal incidence, tending to compensate the one just discussed, arises from the fact that the photo-sensitive surface of the measuring cell has a smaller response for diffused light, as transmitted by papers, than for an equal flux of normally incident light. Since the photoelectric circuit was balanced at 100 percent transmission with no paper the light was perpendicularly incident, but in a measurement with a diffusing material the light was at least partially diffused. Thus for normal incidence all values for t_a and t_{2a} were too low by the same fractional amount, leading to higher values for R_a.

Another effect which tended to give high values for R_a was that of fluorescence, as will be shown later in Section 5.

The fact that good agreement is obtained between the reflectances calculated from transmission values for normal incidence and the directly measured reflectances, is of practical rather than theoretical interest, inasmuch as this agreement is due to a compensation of errors.

TABLE VI. Fluorescence of papers caused by 365-millimicron ultraviolet.

Number of Paper	Fluorescent Light,[a] Expressed in Transmission Units[b]	
	1 Sheet	1 Sheet plus Paper No. 128
1215	0.002	0.003
1214	.004	.004
1191	.002	.003
1170	.006	.005
1133	.006	.004
1136	.005	.003
1002	.003	.003
128	.007	.007

[a] The ultraviolet incident upon the papers was excluded from the measurements by means of a 10-mm layer, contained in a glass cell, of 0.65 molar cupric chloride solution at 26°C, which has the following transmittances (unpublished data): at 365 mμ, 0.0005; at 405 mμ, 0.176; at 436 mμ, 0.738; at 546 mμ, 0.788; at 578 mμ, 0.447; at 623 mμ, 0.041; at 691 mμ, 0.005; at 750 to 1400 mμ, 0.000.

[b] The values in this table are expressed in the same units as those of Table III and thus may be subtracted directly from the values for t_a, t_{ab} or t_{2a} to obtain the corresponding transmission values for the incident ultraviolet.

The experiments with the glass sample, 202, aside from demonstrating the validity of Eq. (6) for very low reflectances, also show that valid results are obtainable for normally incident light as long as its geometric distribution is not altered in passing through the first sheet.

R_a for the glass for diffused light is higher than for normal incidence. This is in agreement with the theoretical conclusions of Judd and Gibson[18] who present data, obtained in another manner, from which it may be calculated that the glass

they used had a reflectance of 12.6 percent for diffused light. It should be pointed out, however, that the present method does not lend itself to precision at these low reflectances owing to the form of the expression.

4. Effect of Thickness of Sheets

In the case of the relatively thick organic plastic sheet, 0.023", an appreciable quantity of light may be lost edgewise. If x is the fraction of light *not* lost edgewise, in each sheet, then $x \cdot T_a$ will enter the numerator in Eq. (1), and $x^2 \cdot T_{2a}$ will enter the denominator. Since the former is then squared it is obvious that x cancels and that this type of loss does not invalidate Eq. (1).

Two other types of side losses are conceivable: one between the sheet or sheets and the cell, and the other between the two sheets. It can be shown that the former effect tends to raise the calculated reflectances and the latter tends to lower them. They thus tend to compensate and with the present experimental arrangement were probably negligible.

5. Effect of Fluorescence

The effect of fluorescence upon directly measured paper reflectance was studied at the Institute of Paper Chemistry,[19] where it was found that large amounts of near infra-red fluorescence arose from papers illuminated with incandescent-lamp light. In the present study, however, very little effect from infra-red fluorescence should be noted since this type of cell used is only about 1/30 to 1/50 as sensitive to infra-red as to visible energy.

The papers included in the present study, however, were found to fluoresce markedly in the visible region when illuminated with 365-millimicron ultraviolet. This was determined as follows: The circuit previously described for measuring transmissions was used. A filter which had a spectral transmission of practically zero at 365 millimicrons, but which transmitted rather freely at longer wave-lengths, was placed between the illuminated sheet or sheets and the measuring cell. Thus, only fluorescent energy was measured.

[19] Institute of Paper Chemistry, Report No. 8, "Adaptability of the G. E. reflection meter as color analyzer." Also in Paper Trade J. **104** (May 6, 1937); (May 13, 1937); (May 20, 1937).

Not all of the fluorescent energy was measured, however, since the filter, whose spectral characteristics are given in a footnote of Table VI, had an average energy transmission of about one-half in the visible region. Therefore, the measured values for fluorescent energy for each sheet of paper, and for the combinations of the various sheets with a sheet of paper No. 128 were multiplied by a factor of 2, since, furthermore, additional experiments (data not given) with other filters which cut off at various longer wavelengths, showed that the fluorescent energy was approximately equally distributed over the visible region. The corrected values are shown in Table VI.

The values for fluorescence thus obtained are obviously included in the values for t_a and t_{ab} or t_{2a} at 365 millimicrons in Table III. When the latter are corrected for fluorescence and when the corrected transmissions are substituted into Eq. (7) (or Eq. (6) for papers Nos. 128 and 1002) the values for calculated reflectance for diffuse incidence are in better agreement with the directly measured reflectances than when fluorescence is not considered. The recalculated reflectances are given in parentheses in Table II. The calculated reflectances for normal incidence were not corrected, since fluorescence is one of the compensating factors resulting in fortuitous but useful agreement with directly measured reflectances.

For papers of very low transmission, however, this method does not yield dependable values for reflectance in regions causing fluorescence, owing to the fact that inaccuracies in the values for fluorescence lead to magnified errors in reflectance if the values for t_{ab} or t_{2a} are very small. When t_{ab} or t_{2a} are 0.04 or larger, however, fluorescence has only small or negligible effects upon the calculated reflectances. Thus, Eqs. (6) or (7) may be used for calculating the reflectances of papers such as 128, 198, or 1002 in the 365-millimicron ultraviolet with only small errors caused by neglecting the fluorescence.

6. Results using Heterogeneous ("White") Light and Infra-Red

The spectral distribution of heterogeneous ("white") light is usually altered by selective

absorption in passing through a sheet of paper. This renders Eq. (1) theoretically inapplicable for such light, inasmuch as T_a and R_a may be changed by the first sheet. It was of interest from a practical standpoint, however, to determine the extent to which Eq. (1) could nevertheless be relied upon under these conditions. The reflectances in Table II for normally incident heterogeneous light were calculated using Eq. (6). A comparison with the directly measured reflectances shows that Eq. (1) is very useful for such measurements, except for very transmissive papers, such as 198, for which diffuse incidence must be used.

No comparison with directly measured reflectances was possible in the infra-red, inasmuch as no standard of diffuse reflectance for the infra-red is available, and inasmuch as the photoelectric responses in this region were too weak for unamplified measurement of reflectance, although they sufficed for measurement of transmission.

It should be noted, however, that the two principal causes for departure from the simple theory, namely fluorescence and change in geometric distribution during transmission, are not expected to be appreciable in the infra-red. Errors due to fluorescence would necessarily be very small in this region for a variety of reasons, and the slight effect of changing the geometric distribution is evident from the results in Table II.

The writer takes pleasure in acknowledging the advice and comments of Deane B. Judd of the Photometry and Colorimetry Section.

Zeeman Effects in the Arc Spectrum of Nickel

CHARLES H. LINDSLEY
Black Mountain College, Black Mountain, North Carolina

(Received October 9, 1941)

Zeeman data for 171 Ni I lines are given, based on measurements of Zeeman patterns photographed at M.I.T. in magnetic fields of 85,700 and 81,300 gauss. g values have been determined for the even energy levels arising from the $3d^84s^2$ and $3d^94s$ configurations, and for most of the odd levels arising from the $3d^84s4p$ and $3d^94p$ configurations.

THE spectum of neutral nickel has been classified by Russell,[1] but no data on the g values for the various levels have yet been presented. The experimental data here analyzed were obtained in the Spectroscopy Laboratories of the Massachusetts Institute of Technology and were made available to the author through the kindness of Professor George R. Harrison.

The spectrum was photographed from an arc of nickel and silver in the field of the large Bitter electromagnet,[2] using the F, G, and H gratings described elsewhere.[3] Two different exposures were made and two complete sets of plates were thus obtained. The lines on the plates were measured by means of the automatic comparator.[4] Those included in this paper lay in the range from about 2300A to nearly 7800A.

[1] H. N. Russell, Phys. Rev. **34**, 821 (1929).
[2] G. R. Harrison and F. Bitter, Phys. Rev. **57**, 15 (1940).
[3] G. R. Harrison and J. R. McNally, Jr., Phys. Rev. **58**, 703 (1940).
[4] G. R. Harrison, J. Opt. Soc. Am. **25**, 169 (1935); Rev. Sci. Inst. **9**, 15 (1938); G. R. Harrison and J. P. Molnar, J. Opt. Soc. Am. **30**, 343 (1940).

The intensity of the magnetic field for the two exposures was calculated from the Zeeman effects of these lines: Ca II 3933.666 and 3968.468, and Cu I 3247.540 and 3273.962. The field for the two cases was thus found to be 85,900 and 81,100 gauss. These values were then used to determine the two sets of g values for the Ni I lines. These latter were found to disagree consistently with one another by about 0.4 percent. Furthermore, when the g sums for the different configurations were compared with the corresponding sums of the Landé g values, the sums from the first set were found to be 0.2 percent lower than the Landé sums, and those from the second 0.2 percent higher. (The comparison was made using g sums for the even levels only, since these were better known.) It seemed justifiable, therefore, to increase all g values in the first set of determinations by 0.2 percent and to decrease those in the second set by a like amount. After these changes were made, the g values of the two sets were in complete agreement for the individual

TABLE I. Zeeman effects of Ni I lines.

Wave-Length	Wave No.	Int.	Classification	g Values		Wave-Length	Wave No.	Int.	Classification	g Values	
7788.95*U*	12,835.2	60	$a^3P_1 - w^3P^\circ_2$	1.495	(1.485)	3688.415	27,104.23	150	$a^3F_2 - w^3F^\circ_2$	0.667	1.084
7714.32	12,959.3	60	$a^3P_2 - w^3P^\circ_2$	1.356	(1.485)	3674.15	27,209.5	200	$b^1D_2 - w^3F^\circ_2$	1.014	0.743
6314.675*U*	15,831.76	300	$a^3P_2 - w^1D^\circ_2$	1.361	1.066	3670.427	27,237.06	150	$a^3F_2 - w^3P^\circ_2$	1.085	1.488
6256.365	15,979.31	600	$a^1D_2 - w^3P^\circ_1$	1.141	1.422	3669.241	27,245.86	150	$a^3F_3 - z^5G^\circ_3$	1.083	0.945
5892.878	16,964.94	6	$a^3P_0 - w^1P^\circ_1$	0/0	1.010	3664.095	27,284.13	300	$a^3F_2 - w^3P^\circ_1$	0.670	1.427
5476.906	18,253.42	400	$c^1S_0 - w^1P^\circ_1$	0/0	1.005	3661.951	27,300.10	50	$b^3D_1 - z^5G^\circ_2$	0.490	0.363
5137.075	19,460.92	150	$a^1D_2 - w^1P^\circ_1$	1.140	(1.005)	3634.941	27,502.95	50	$b^1D_2 - w^3D^\circ_1$	1.011	0.552
3973.562	25,159.25	800	$b^1D_2 - w^3P^\circ_2$	1.012	1.484	3624.733*U*	27,580.40	150	$a^3F_4 - z^5G^\circ_5$	(1.250)	1.276
3972.171*U*	25,168.06	100	$b^1D_2 - z^5G^\circ_3$	(1.014)	0.928	3619.392*U*	27,621.11	2000	$b^1D_2 - w^1F^\circ_3$	(1.014)	1.037
3858.301*U*	25,910.82	800	$b^1D_2 - w^3F^\circ_2$	(1.014)	1.080	3612.741	27,671.95	400	$a^3F_2 - w^3D^\circ_2$	0.669	1.042
3832.873	26,082.72	25	$a^3F_3 - z^5D^\circ_2$	(1.083)	1.494	3610.462	27,689.42	1000	$b^3D_2 - w^3P^\circ_2$	1.149	1.484
3831.690	26,090.77	300	$b^1D_2 - w^3P^\circ_1$	1.014	1.428	3609.314	27,698.22	200	$b^3D_2 - z^5G^\circ_3$	(1.149)	0.947
3807.144	26,258.98	800	$b^1D_2 - w^3D^\circ_2$	1.014	1.300	3602.281	27,752.30	150	$a^3F_3 - z^5F^\circ_4$	1.087	1.288
3793.608	26,352.68	50	$a^3F_2 - w^3P^\circ_2$	0.669	1.485	3597.705	27,787.60	1000	$b^3D_1 - w^3P^\circ_1$	0.502	1.428
3792.337	26,361.51	25	$a^3F_2 - z^5G^\circ_3$	(0.671)	0.946	3587.931	27,863.29	200	$b^3D_3 - z^5G^\circ_4$	1.330	1.168
3783.530	26,422.87	500	$b^1D_2 - z^5F^\circ_2$	1.016	1.209	3571.869*U*	27,988.59	1000	$a^3F_3 - w^3F^\circ_2$	1.086	1.086
3775.572*U*	26,478.56	500	$b^1D_2 - w^3D^\circ_2$	(1.014)	1.049	3566.372*U*	28,031.73	2000	$b^1D_2 - w^1D^\circ_2$	(1.014)	1.051
3772.530	26,499.91	15	$b^3D_1 - z^5D^\circ_0$	0.497	0/0	3561.751*U*	28,068.09	70	$a^3F_4 - z^5G^\circ_4$	(1.250)	1.177
3749.045	26,665.91	50	$a^3F_4 - z^5D^\circ_3$	1.255	1.495	3553.483	28,133.40	50	$b^3D_2 - z^5G^\circ_2$	1.149	0.365
3739.229*U*	26,735.91	100	$a^3F_3 - z^5G^\circ_4$	(1.083)	1.168	3551.534	28,148.84	50	$a^3F_3 - w^3F^\circ_4$	1.085	1.288
3736.813*U*	26,753.19	300	$b^1D_2 - z^5F^\circ_3$	(1.014)	0.988	3548.185	28,175.40	400	$a^3F_2 - z^5F^\circ_1$ $b^3D_1 - w^3D^\circ_2$	0.668 0.501	0.008 1.046
3722.484	26,856.17	200	$b^3D_1 - w^3P^\circ_2$	0.497	1.484	3527.982	28,336.75	200	$a^3F_3 - w^3D^\circ_3$	1.083	1.299
3693.932	27,063.75	50	$b^3D_2 - z^5D^\circ_1$	1.152	1.486						

TABLE I.—*Continued.*

Wave-Length	Wave No.	Int.	Classification	g Values	
3524.541	28,364.34	1000	$b^3D_3 - w^3P^\circ_2$	1.326	1.474
3523.444	28,373.24	100	$b^3D_3 - z^5G^\circ_3$	(1.332)	0.943
3519.766*U*	28,402.90	500	$a^3F_2 - w^3F^\circ_3$	0.669	0.736
3515.054*U*	28,440.96	1000	$b^3D_2 - w^3F^\circ_3$	(1.149)	1.083
3513.933	28,450.03	200	$b^3D_1 - z^5F^\circ_2$	0.502	0.989
3510.338	28,479.17	900	$b^3D_1 - w^3P^\circ_0$	0.495	0/0
3507.694	28,500.64	100	$a^3F_3 - z^5F^\circ_5$	1.088	1.207
3502.595	28,542.12	100	$a^3F_4 - z^5F^\circ_5$	(1.250)	1.377
3500.852*U*	28,556.33	500	$a^3F_3 - w^3D^\circ_2$	(1.083)	1.056
3492.956	28,620.89	1000	$b^3D_2 - w^3P^\circ_1$	1.148	1.423
3485.888	28,678.92	150	$b^3D_1 - z^5F^\circ_1$	0.494	0.005
3483.774*U*	28,696.32	500	$a^3F_2 - w^3D^\circ_1$	(0.671)	0.566
3472.545	28,789.11	800	$b^3D_2 - w^3D^\circ_2$	1.159	1.304
3469.486	28,814.49	300	$a^3F_2 - w^1F^\circ_3$	0.671	1.047
3467.502*U*	28,830.98	300	$a^3F_3 - z^5F^\circ_3$	1.085	0.995
3461.652*U*	28,879.70	800	$b^3D_3 - z^5F^\circ_4$	1.327	1.290
3458.474	28,906.23	800	$b^3D_1 - w^3F^\circ_2$	0.495	0.740
3452.890*U*	28,952.98	600	$b^3D_2 - z^5F^\circ_3$	(1.149)	1.197
3446.263*U*	29,008.66	1000	$b^3D_2 - w^3D^\circ_2$	(1.149)	1.046
3437.280*U*	29,084.47	600	$a^3F_4 - z^5F^\circ_4$	1.255	1.284
3433.558	29,115.99	800	$b^3D_3 - w^3F^\circ_3$	1.333	1.084
3423.711*U*	29,199.73	600	$b^3D_1 - w^3D^\circ_1$	0.495	0.550
3414.765*U*	29,277.08	1000	$b^3D_3 - w^3F^\circ_4$	(1.332)	1.300
3413.939	29 283.31	300	$b^3D_2 - z^5F^\circ_2$	1.148	0.982
3413.478	29,287.26	500	$a^3F_3 - w^3F^\circ_2$	1.080	0.739
3409.578	29,320.76	300	$a^3F_4 - w^3F^\circ_3$	1.254	1.093
3392.992*U*	29,464.08	600	$b^3D_3 - w^3D^\circ_3$	(1.332)	1.301
3391.050*U*	29,480.96	400	$a^3F_4 - w^3F^\circ_4$	(1.250)	1.288
3380.885*U*	29,569.60	200	$a^3F_2 - y^3G^\circ_3$	(0.671)	0.756
3380.574*U*	29,572.32	600	$b^1D_2 - w^1P^\circ_1$	(1.014)	1.014
3374.221	29,627.99	400	$b^3D_3 - z^5F^\circ_2$	1.331	1.206
3371.993*U*	29,647.57	400	$a^3F_3 - y^3G^\circ_4$	(1.083)	1.060
3369.573*U*	29,668.86	500	$a^5F_4 - w^3D^\circ_3$	(1.250)	1.282
3367.892	29,683.67	80	$b^3D_3 - w^3D^\circ_2$	(1.332)	1.043
3366.168*U*	29,698.87	400	$a^3F_2 - w^1F^\circ_3$	1.077	1.047
3365.766	29,702.42	400	$b^1D_2 - y^3F^\circ_3$	1.016	1.195
3362.806	29.728.56	100	$b^3D_1 - w^1D^\circ_2$	(0.497)	1.057
3361.556	29,739.62	500	$b^3D_2 - w^3F^\circ_2$	1.151	0.742
3328.714	30,033.02	15	$b^3D_2 - w^3D^\circ_1$	(1.149)	0.550
3322.310	30,090.91	400	$b^1D_2 - y^3D^\circ_3$	1.019	1.203
3320.257*U*	30,109.52	400	$a^3F_3 - w^1D^\circ_2$	(1.083)	1.068
3315.663*U*	30,151.23	400	$b^3D_2 - w^1F^\circ_3$	(1.149)	1.053
3310.202*U*	30,200.98	50	$b^1D_2 - y^3F^\circ_2$	1.012	0.970
3286.946	30,414.64	100	$b^3D_3 - w^3F^\circ_2$	1.333	0.737
3282.696	30,454.02	100	$a^3F_3 - y^3G^\circ_3$	(1.083)	0.755
3271.118*U*	30,561.81	125	$b^3D_2 - w^1D^\circ_2$	1.152	1.061
3250.743	30,753.36	125	$b^1D_2 - y^3D^\circ_2$	1.008	0.862
3249.440	30,765.69	30	$a^3F_2 - w^1P^\circ_1$	(0.671)	1.006
3248.457	30.775.00	150	$b^3D_3 - y^3G^\circ_4$	1.332	1.048
3243.058	30,826.23	400	$b^3D_2 - w^1F^\circ_3$	1.334	1.047
3234.649	30,906.36	300	$b^3D_2 - y^3G^\circ_3$	1.149	0.763
3232.963*U*	30,922.48	300	$a^3F_4 - y^3G^\circ_5$	(1.250)	1.214
3226.984	30,979.78	100	$a^3F_4 - y^3G^\circ_4$	1.244	1.056
3225.020	30,998 64	300	$b^1D_2 - y^3D^\circ_1$	1.014	0.508
3221.652	31,031.05	300	$a^3F_4 - w^1F^\circ_3$	1.253	1.050
3200.423	31,236.87	30	$b^3D_3 - w^1D^\circ_2$	1.337	1.060
3197.113	31,269.21	300	$b^3D_1 - w^1P^\circ_1$	0.498	1.002
3195.573	31,284.28	125	$a^3F_2 - y^3D^\circ_2$	0.671	1.198
3184.367	31,394.36	150	$a^3F_2 - y^3F^\circ_2$	0.667	0.974
3183.251	31,405.37	25	$a^3P_1 - y^3D^\circ_2$	1.498	1.211
3183.038	31,407.47	5	$a^3P_0 - y^3D^\circ_1$	0/0	0.727
3181.740*U*	31,420.29	50	$a^3P_2 - y^3D^\circ_3$	(1.356)	1.336
3145.719	31,780.06	200	$a^3F_3 - y^3F^\circ_3$	1.085	1.190
3134.108	31,897.79	1000	$b^3D_1 - y^3F^\circ_2$	0.494	0.970
3129.314	31,946.66	125	$a^3F_2 - y^3D^\circ_2$	0.673	0.856
3114.124*U*	32,102.48	300	$b^3D_2 - w^1P^\circ_1$	(1.149)	1.011
3105.469	32,191.94	200	$a^3F_3 - y^3D^\circ_3$	0.684	0.544
3101.879*U*	32,229.20	400	$b^1D_2 - y^1F^\circ_3$	(1.014)	0.98
3101.554*U*	32,232.58	1000	$b^3D_2 - y^3F^\circ_3$	(1.149)	1.18
3099.115*U*	32,257.94	200	$a^3F_3 - y^1G^\circ_4$	(1.083)	1.052
3097.118*U*	32,278.74	200	$a^3F_3 - y^3F^\circ_3$	(1.083)	0.986
3080.755	32,450.18	200	$b^3D_1 - y^3D^\circ_2$	0.501	0.858
3064.623*U*	32,620.99	200	$b^3D_2 - y^3D^\circ_3$	(1.149)	1.186
3057.638*U*	32,695.50	400	$b^3D_1 - y^3D^\circ_1$	(0.497)	0.471
3054.316	32,731.07	400	$b^3D_2 - y^3F^\circ_2$	1.141	0.972
3050.819*U*	32,768.58	1000	$b^3D_3 - y^3F^\circ_4$	(1.332)	1.218
3045.006	32,831.14	200	$a^3F_3 - y^3D^\circ_2$	1.087	0.865
3037.935*U*	32,907.55	800	$b^3D_3 - y^3F^\circ_3$	(1.332)	1.195
3031.870*U*	32,973.37	200	$a^3F_4 - y^3F^\circ_4$	(1.250)	1.223
3019.143*U*	33,112.36	200	$a^3F_4 - y^3F^\circ_5$	(1.250)	1.207
3012.004*U*	33,190.84	800	$b^1D_2 - y^1D^\circ_2$	(1.014)	1.001
3003 629	33.283.39	500	$b^3D_2 - y^3D^\circ_2$	1.150	0.855
3002.491*U*	33,296.00	1000	$b^3D_3 - y^3D^\circ_3$	(1.332)	1.197
2994.460	33,385.29	125	$b^3D_3 - y^1G^\circ_4$	1.328	1.035
2992.595	33,406.10	80	$b^3D_3 - y^3F^\circ_2$	1.337	0.977
2984.131*U*	33,500.85	50	$a^3F_4 - y^3D^\circ_3$	(1.250)	1.216
2983.422	33.508.81	10	$a^1D_2 - y^3D^\circ_2$	1.150	1.331
2981.651	33,528.71	80	$b^3D_2 - y^3D^\circ_1$	1.151	0.513
2958.29	33,793.5		$a^3P_2 - u^3P^\circ_1$	1.363	1.783
2949.22	33,897.4			1.667	2.001
2943.914	33,958.48	50	$b^3D_3 - y^3D^\circ_2$	1.336	0.860
2914.007*U*	34,306.99	20	$a^3F_3 - y^1F^\circ_3$	1.079	1.017
2907.459	34,384.25	40	$a^3F_2 - y^1D^\circ_2$	0.670	1.013
2865.502	34,887.68	5	$b^3D_1 - y^1D^\circ_2$	0.501	1.013
2834.553*U*	35,268.58	40	$a^3F_3 - y^1D^\circ_2$	(1.083)	1.030
2821.293	35,434.32	125	$b^3D_2 - y^1F^\circ_3$	1.331	1.014
2805.083	35,639.09	50	$a^3F_4 - y^1F^\circ_4$	1.244	1.012
2798.653*U*	35,720.97	125	$b^3D_2 - y^1D^\circ_2$	(1.149)	1.012
2746.746	36,395.97	125	$b^3D_3 - y^1D^\circ_2$	1.334	1.012
2540.020*U*	39,357.95	40	$b^1D_2 - z^3D^\circ_2$	(1.014)	1.195
2476.874	40,361.28	40	$a^3F_4 - 1^\circ_5$	(1.250)	1.627
2453.987*U*	40,737.67	40	$a^3F_2 - x^3D^\circ_2$	(0.671)	0.834
2434.415*U*	41,065.17	40	$b^1D_2 - z^3D^\circ_2$	(1.014)	1.155
2424.028	41,241.12	20	$b^3D_1 - x^3D^\circ_2$	(0.497)	0.829
2423.656	41,247.45	20	$a^3F_2 - x^1P^\circ_1$	(0.671)	1.393
2412.643*U*	41,435.71	20	$a^3F_3 - w^3D^\circ_2$	(1.083)	1.350
2401.841	41,622.05	40	$a^3F_3 - x^3D^\circ_3$	(1.083)	0.852
2392.96	41,776.5	10	$b^3D_2 - x^3P^\circ_1$	(1.149)	1.320
2386.58*U*	41,888.2	20	$b^3D_2 - z^3D^\circ_2$	(1.149)	1.192
2384.38*U*	41,926.8	15	$a^3F_3 - z^3F^\circ_4$	(1.083)	1.278
2360.63	42,348.6	10	$a^3F_2 - z^3F^\circ_3$	(0.671)	1.050
2347.52*U*	42,585.1	12	$a^3F_4 - x^3F^\circ_4$	(1.250)	1.346
2346.63	42,601.2	10	$a^3F_3 - x^1D^\circ_2$	1.082	1.476
2337.49*U*	42,767.8	8	$a^3F_4 - z^3D^\circ_3$	(1.250)	1.231
2337.09*U*	42,775.1	10	$b^3D_2 - x^3F^\circ_3$	(1.149)	1.243
2329.964*U*	42,905.93	12	$a^3F_3 - z^3D^\circ_1$	(0.671)	0.566
2325.79*U*	42,982.9	30	$a^3F_3 - z^3G^\circ_4$	(1.083)	1.182
2324.64	43,004.2	15	$a^3F_3 - 3^\circ_3$	1.075	1.329
2321.96*U*	43,053.8	5	$a^3D_3 - z^3F^\circ_4$	(1.332)	1.264
2321.38*U*	43,064.6	20	$a^3F_2 - z^3G^\circ_3$	(0.671)	0.779
2320.03*U*	43,089.6	30	$a^3F_4 - z^3G^\circ_5$	(1.250)	1.226
2313.982*U*	43,202.24	10	$a^3F_2 - z^3F^\circ_2$	0.677	0.677
2312.34*U*	43,232.9	30	$a^3F_3 - z^3F^\circ_3$	(1.083)	1.038
2310.965*U*	43,258.64	50	$a^3F_4 - z^3F^\circ_4$	(1.250)	1.230
2293.116*U*	43,595.32	10	$b^3D_2 - z^3D^\circ_2$	1.149	1.177

Notation: *a* denotes $3d^84s^2$; *b*, $3d^84s$; *c*, $3d^{10}$.
z denotes $3d^84s(^4F)4p$; *y*, $3d^84s(^2F)4p$; *x*, $3d^84s(^2D)4p$; *w*, $3d^84p$; *u*, $3d^95p$; *v*, $3d^84s(^4P)4p$.

lines, and the *g* sums agreed excellently with the Landé sums. The corresponding values for the field strength were 85,700 and 81,300 gauss.

The data for 171 Ni I lines are given in Table I. The wave-lengths and intensities (with two exceptions) were taken from the *M.I.T. Wavelength Tables*.[5] In general, Russell's classification was followed, though it is to be noted that the configurations for the various levels are those given by Bacher and Goudsmit.[6] In the cases of resolved patterns, the *J* values were confirmed. For unresolved patterns (indicated in the Table by *U* following the wave-length), the *J* values from the classification were assumed. Usually for unresolved patterns it was found desirable to use the average *g* value for one of the levels (in most cases the even level) in order to calculate the other *g* value. Also, occasionally only the differ-

[5] *M. I. T. Wavelength Tables* (John Wiley and Sons New York, 1939).

[6] R. F. Bacher and S. Goudsmit, *Atomic Energy States* (McGraw-Hill Book Company, Inc., New York, 1932).

TABLE II. Measured and Landé g values for even levels of Ni I.

Level		Term Value Wave No.	Meas. g Value	Landé g Value	No. Meas.	No. Lines
$3d^84s^2$	$^3F_4$	0.00	1.250	1.250	16	6
"a"	$^3F_3$	1332.15	1.083	1.083	34	11
	$^3F_2$	2216.55	0.671	0.667	40	13
	$^1D_2$	13,521.29	1.143	1.000	4	3
	$^3P_2$	15,609.81	1.356	1.500	3	3
	$^3P_1$	15,734.03	1.497	1.500	3	2
	$^3P_0$	16,017.30	0/0	0/0	3	2
	$^1G_4$	22,102.27	—	1.000	—	—
$3d^94s$	$^3D_3$	204.82	1.332	1.333	37	12
"b"	$^3D_2$	879.82	1.149	1.167	41	11
	$^3D_1$	1713.11	0.497	0.500	48	13
	$^1D_2$	3409.95	1.014	1.000	43	10
$3d^{10}$	$^1S_0$	14,728.92	0/0	0/0	3	1

ence of the g's could be determined from the pattern because of overlapping; in such cases the average value for the better known level was assumed. All g values which have thus been assumed are enclosed in parentheses in Table I.

Because of the two sets of plates and because of the overlapping of the ranges of the three gratings, from two to four determinations were possible for most of the lines. Also since for strong patterns there is frequently a well-defined σ-pattern appearing with the π, and a π with the σ, as many as seven measurements could be made for some lines. Except in the cases of very poor patterns, the agreement among these different measurements was good. Even in the cases of many unresolved patterns the agreement of several independent measurements was regarded as sufficient to warrant calculating the g values to three decimal places.

The g values for the various even and odd levels are given in Tables II and III. These values are weighted averages, the last two columns showing the number of separate lines and the total number of measurements actually used in determining the recorded values. Except in those cases where no better data were available, values from unresolved patterns were not used in calculating the average values. However, it is to be noted that the values for such patterns are often in excellent agreement with the averages.

TABLE III. Measured and Landé g values for odd levels of Ni I.

		Term Value Wave No.	Meas. g Value	Landé g Value	No. Lines	No. Meas.
$3d^84s(^4F)4p$ "z"	$^5D^\circ_4$	25,753.57	—	1.500	—	—
	$^5D^\circ_3$	26,665.97	1.49_5	1.500	1	2
	$^5D^\circ_2$	27,414.92	1.49_4	1.500	1	1
	$^5D^\circ_1$	27,943.58	1.486	1.500	1	4
	$^5D^\circ_0$	28,213.10	0/0	0/0	1	2
	$^5G^\circ_6$	27,260.96	—	1.333	—	—
	$^5G^\circ_5$	27,580.48	1.27_6	1.267	1	3
	$^5G^\circ_4$	28,068.18	1.171	1.150	3	11
	$^5G^\circ_3$	28,578.10	0.945	0.917	4	12
	$^5G^\circ_2$	29,013.28	0.364	0.333	2	5
	$^5F^\circ_5$	28,541.94	1.37_7	1.400	1	4
	$^5F^\circ_4$	29,084.47	1.288	1.350	1	4
	$^5F^\circ_3$	29,832.77	1.208	1.250	3	14
	$^5F^\circ_2$	30,163.16	0.985	1.000	2	7
	$^5F^\circ_1$	30,391.96	0.006	0.000	2	8
	$^3D^\circ_3$	42,767.72	1.21_8	1.333	2	4
	$^3D^\circ_2$	44,475.07	1.15_5	1.167	2	2
	$^3D^\circ_1$	45,122.29	0.56_6	0.500	1	2
	$^3G^\circ_5$	43,089.52	1.22_6	1.200	1	4
	$^3G^\circ_4$	44,314.85	1.18_2	1.050	1	2
	$^3G^\circ_3$	45,281.14	0.77_9	0.750	1	2
	$^3F^\circ_4$	43,258.67	1.24_7	1.250	2	4
	$^3F^\circ_3$	44,565.01	1.04_4	1.083	2	3
	$^3F^\circ_2$	45,418.81	0.67_7	0.667	1	2
$3d^84s(^2F)4p$ "y"	$^3G^\circ_5$	30,922.61	1.21_4	1.200	1	3
	$^3G^\circ_4$	30,979.70	1.052	1.050	2	6
	$^3G^\circ_3$	31,786.13	0.761	0.750	2	4
	$^3F^\circ_4$	32,973.33	1.22_7	1.250	2	8
	$^3F^\circ_3$	33,112.30	1.193	1.083	2	6
	$^3F^\circ_2$	33,610.88	0.973	0.667	4	14
	$^3D^\circ_3$	33,500.80	1.198	1.333	3	9
	$^3D^\circ_2$	34,163.24	0.859	1.167	6	19
	$^3D^\circ_1$	34,408.54	0.511	0.500	2	7
	$^1G^\circ_4$	33,590.12	1.035	1.000	1	3
	$^1F^\circ_3$	35,639.09	1.013	1.000	2	4
	$^1D^\circ_2$	36,600.78	1.013	1.000	3	7
$3d^94p$ "w"	$^3P^\circ_2$	28,569.30	1.485	1.500	5	20
	$^3P^\circ_1$	29,500.75	1.426	1.500	5	19
	$^3P^\circ_0$	30,192.30	0/0	0/0	1	4
	$^3F^\circ_3$	29,320.75	1.086	1.083	4	18
	$^3F^\circ_4$	29,480.96	1.287	1.250	1	4
	$^3F^\circ_2$	30,619.40	0.740	0.667	5	19
	$^3D^\circ_3$	29,668.89	1.300	1.333	3	13
	$^3D^\circ_2$	29,888.47	1.044	1.167	3	11
	$^3D^\circ_1$	30,912.87	0.552	0.500	1	4
	$^1F^\circ_3$	31,031.02	1.048	1.000	3	8
	$^1D^\circ_2$	31,441.64	1.060	1.000	3	8
	$^1P^\circ_1$	32,982.30	1.005	1.000	5	15
$3d^84s(^2D)4p$ "x"	$^3F^\circ_4$	42,585.04	1.34_6	1.250	1	2
	$^3F^\circ_3$	43,654.91	1.24_3	1.083	1	1
	$^3F^\circ_2$	—	—	0.667	—	—
	$^3D^\circ_3$	42,620.95	—	1.333	—	—
	$^3D^\circ_2$	42,954.17	0.840	1.167	3	5
	$^3D^\circ_1$	—	—	0.500	—	—
	$^3P^\circ_2$	42,653.65	—	1.500	—	—
	$^3P^\circ_1$	42,656.27	1.32_0	1.500	1	1
	$^3P^\circ_0$	—	—	0/0	—	—
	$^1P^\circ_1$	43,463.90	1.39_9	1.000	1	1
	$^1D^\circ_2$	43,933.37	1.47_6	1.000	1	2
	$^1F^\circ_3$	44,206.42	—	1.000	—	—
$3d^84s(^4P)4p$ "v"	$^5D^\circ_3$	47,029.98	1.331	1.333	2	4
	$^5D^\circ_2$	47,139.25	1.209	1.167	1	2
	$^5D^\circ_1$	47,424.93	0.726	0.500	1	2

TABLE IV. Comparison of measured and Landé g sums.

Configuration	J	g (meas.)	g (Landé)
$3d^84s^2$	4	(1.250)*	1.250
	3	1.083	1.083
	2	3.170	3.167
	1	1.497	1.500
$3d^94s$	3	1.332	1.333
	2	2.163	2.167
	1	0.497	0.500
$3d^84s(^4F)4p$	6	—	1.33
	5	3.88	3.87
	4	(4.89)*	4.80
	3	6.69	6.83
	2	4.68	4.67
	1	2.06	2.00
$3d^84s(^2F)4p$	5	1.21	1.20
	4	3.309	3.300
	3	4.165	4.167
	2	2.845	2.833
	1	0.511	0.500
$3d^94p$	4	1.287	1.250
	3	3.434	3.417
	2	4.329	4.333
	1	2.983	3.000

* g value for one level with this J value missing.

The g values in Table II for the even levels are probably correct to within ± 0.002 unit. This is borne out by the excellent agreement of the g sums with the Landé sums (see the first two configurations of Table IV). The g values for the odd levels in Table III are not so certain, since in general there are fewer lines involving each of them. When, however, the recorded value is not considered to be correct to within ± 0.003 unit, the last figure is indicated as being less reliable.

Table IV shows that for at least two groups of these odd levels the reliability is quite good. It should be observed that the agreement between the measured g sums and the Landé sums cannot be expected to be as close for these levels as for the even levels, since there are undoubtedly interactions between levels belonging to different configurations with term values not widely separated.

The plates contained many lines arising from transitions between the odd levels included here and higher even levels. However, in almost every case the Zeeman patterns of these lines were unresolved and irregular. Any g values obtained from such patterns would have been quite poor, and since the lines have already been classified, it did not seem worth while to analyze them.

The author wishes to thank Professor Harrison for supplying the experimental data. The work was aided by a grant from the North Carolina Academy of Sciences.

The Far Ultraviolet Reflectivities of Metallic Films

MARY BANNING
Johns Hopkins University, Baltimore, Maryland
(Received September 24, 1941)

The reflectivities of evaporated films of aluminum, copper, silver, and beryllium have been measured spectrographically in the region 1200–2200A before the films were exposed to air. Copper reflection was considerably higher before contamination by air than afterward; the other metals showed no effect. The pronounced minimum in beryllium reflectivity found by previous investigators did not occur here; it is believed that this minimum is due to a thin film of tungsten evaporated over the beryllium.

INTRODUCTION

DETERMINATION of the optical properties of metals yields important information about the electronic energies within the metals. Since a knowledge of these energies is necessary for the further development of metallic theory, the present investigation was made in an attempt to develop a method for obtaining accurate values of metallic reflection in the far ultraviolet.

Evaporated films, approximately 200A thick, were used throughout, because they seem to give the best mirror surfaces and the most consistent results. In all the previous work on metal films in the ultraviolet, the films were exposed to air before measurements were taken. In many cases they became so contaminated they could not be used at all; in others it was not clear how far the results were influenced by surface layers of oxides or other impurities. In 1936, O'Bryan[1] obtained the optical constants of several metals by measuring his films in the same vacuum in which they were evaporated. However, his results were only for the visible region; the present work extends this method to the ultraviolet.

Throughout this paper the values obtained for the reflecting power have been compared with those of Sabine,[2] because his work seems to be the most accurate and most closely approximates the methods used here. The only essential differences are that in Sabine's apparatus his metallic mirror was far removed from the source of light, he exposed his films to air before measurements, and his reference wave-lengths were over 200A apart as compared with 25A here. Also, Sabine used a different portion of his mirrors for each spectral region, which, if the mirrors were not perfect, may have affected his results.

APPARATUS

All reflection measurements were made with a normal incidence spectrograph in the apparatus shown in Figs. 1 and 2. An aluminized 3-inch grating gave a linear dispersion in the ultraviolet of 17.3A per millimeter on the photographic films. The films were wrapped around a cylinder[3] as shown in Fig. 2, which could be turned without opening the spectrograph to 15 different exposure positions; it was long enough so that the whole region 1000 to 2500A could be covered in one exposure. Eastman commercial films were used, sensitized with Cenco pump oil diluted with CCl_4.

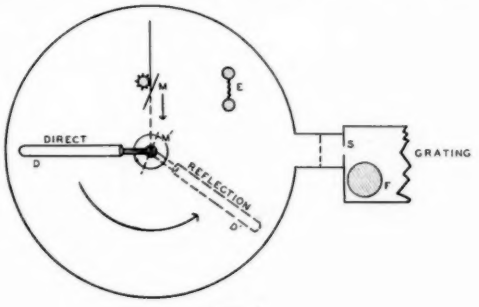

FIG. 1.

The other half of the apparatus was a large glass bell jar, 18 inches in diameter and 12 inches high; this had a two-inch hole in one side through which a connection was made to the spectrograph. Between the bell jar and spectrograph

[1] H. M. O'Bryan, J. Opt. Soc. Am. **26**, 122 (1936).
[2] G. B. Sabine, Phys. Rev. **55**, 1064 (1939).
[3] A. H. Pfund, Phys. Rev. **32**, 39 (1928).

there was a gate valve which allowed each side to be pumped down separately. With the valve closed a vacuum of 10^{-5} mm Hg was obtainable in the bell jar. Pressures were read with a McLeod gauge equipped with a two-way stopcock so that the pressure in either the bell jar or spectrograph could be read at any time. All the bell jar connections, to the base plate, the spectrograph and McLeod gauge were sealed only with Apiezon wax so that the bell jar could

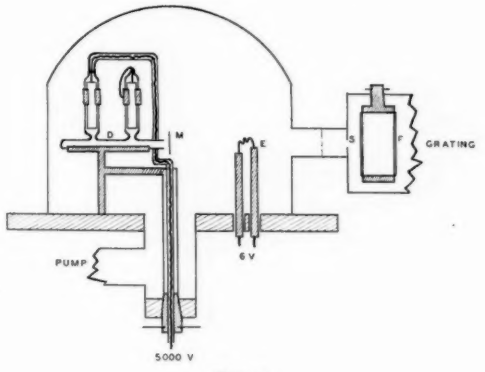

FIG. 2.

easily be removed. The slit of the spectrograph was made small enough for a vacuum of 5×10^{-2} to be obtained in the spectrograph with the gate valve open and a pressure of several millimeters in the bell jar. The evaporating apparatus, metal film, and the discharge tube were all inside the bell jar.

Two electrodes, one grounded to the base plate of the bell jar, the other connected to a variable transformer, were connected by a wire to form the evaporator. The shape and material of the wire depended on the metal to be evaporated and will be described later. As many as 20 amperes could be drawn from the transformer if necessary. Glass microscope slides, mounted on a rack so that they could be moved from a position in front of the evaporator into the reflection position, were coated with the metal to be investigated.

As the source of ultraviolet light, an open end alternating-current discharge tube was used at a potential of 4000 volts. Either hydrogen or carbon dioxide discharges were employed, H_2 for the 1000–1600A region and CO_2 for 1600–2200A. A pivot through the center of the base plate supported the discharge tube, allowing it either to light the spectrograph slit directly, or to reflect from the mirror onto the slit. The angle of reflection was approximately 20 degrees, giving nearly the same reflection as for normal incidence.

Both the pivot for the discharge tube and the rack for the mirror were moved from outside the vacuum system by ground joints; these joints were very carefully made and were practically vacuum tight.

The discharge electrode nearest the open end of the tube was grounded to the base plate, while the other lead passed through a glass tube down the middle of the pivot to the high voltage transformer. Hydrogen or carbon dioxide was admitted into the bell jar through the pump connection. A needle valve was used as a controllable leak; the gas was kept at atmospheric pressure on one side of the valve, and thus the pressure on the other side, in the bell jar, was constant. The gas was allowed to flow through the whole system and was pumped out continuously from the spectrograph.

PROCEDURE

Before each evaporation, the angle of the microscope slide and the position of the discharge tube were adjusted so that the central image of a light directly behind the discharge tube would appear in the position of the photographic film. When the central image appeared with maximum brightness for both direct and reflection positions, the adjustment was complete. Once the positions were established they could be repeated with negligible error.

With the valve to the spectrograph closed, a vacuum of 10^{-5} was obtained in the bell jar and the metal evaporated. In no case was evaporation continued if the pressure rose to greater than 10^{-4}. All films were nearly opaque, the thinnest transmitting less than 10 percent visible light. Measurements were made only on films with good mirror surfaces.

After evaporation, H_2 or CO_2 was admitted into the system until the pressure in the bell jar was a few millimeters. This pressure was kept as low as possible without the discharge jumping out of the tube. When an equilibrium pressure

was reached, the discharge tube was turned on and allowed to run about a half-hour to come to constant temperature and intensity.

The first exposure was taken in the reflection position, then a series of direct calibration exposures in steps of 5 or 10 percent were made, and finally another reflection. This procedure was repeated with the other gas, still without exposing the metal film to air. If the effect of air was to be investigated, the system was allowed

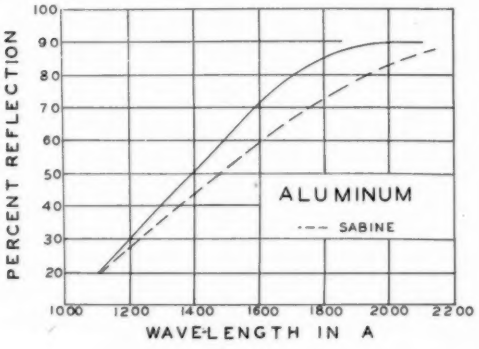

FIG. 3.

to stand overnight in air with no change in adjustment. Exposure times ranged from 3 to 40 minutes.

Each metal was evaporated on a fresh plate and with new settings at least four times for both parts of the spectrum. All films were measured on a microphotometer which had an accuracy of 2 percent. Spectral lines for reference were taken about 25A apart, using 48 lines in all. The final curves are the averages taken through all these points, which spread around the average approximately ten percent on each side.

POSSIBLE SOURCES OF ERROR

A persistent error in adjustment might make all values either too high or too low. Aluminum reflectivity however, reached the same maximum as Sabine found, and this is here assumed to be correct. The other metals were checked against aluminum by evaporating aluminum over them without changing the adjustment. Thus errors in adjustment can probably be neglected.

In order to make sure that the metal films acted like bulk metals, various thicknesses were used, from thin films transmitting 10 percent of visible light to those evaporated far beyond opacity. If no change in reflection was observed, the films were assumed to act like bulk metals. No error is expected here.

The discharge tube gives a constant intensity to within 5 percent over the range of time used here. Test exposures taken over a six-hour range of time showed that the pressure, and thus both the intensity of the discharge and amount of light absorbed in the spectrograph was sufficiently constant. McLeod gauge readings were taken every 20 minutes during exposures to make sure the pressure was constant.

Oiled films have been found to obey the reciprocity law to within 2 percent or better in the range of exposures used here.[4] And since lines at different wave-lengths which varied in intensity by a factor of 20 fell on a smooth curve in reflection measurements, the reciprocity law was assumed to hold here.

The first measurements of aluminum reflectivity in the hydrogen region were consistently much less than Sabine's. A series of four reflection exposures was then taken which showed that the

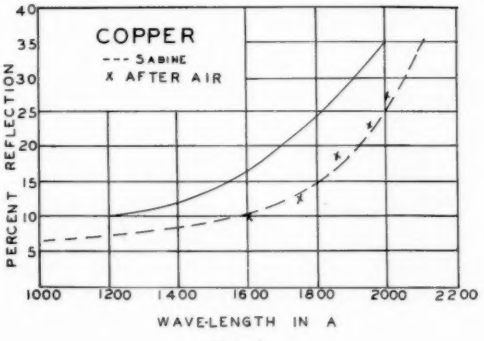

FIG. 4.

reflectivity decreased by about a half each time. This meant that the discharge itself was affecting the metal film. Neither direct current on the discharge tube nor electromagnets across the tube opening stopped the deterioration, thus eliminating the possibility that ions were the source of the trouble.

[4] G. R. Harrison, J. Opt. Soc. Am. **11**, 113, 341 (1925); G. R. Harrison and P. A. Leighton, J. Opt. Soc. Am. **20**, 313 (1930).

Finally it was suggested that perhaps atomic hydrogen, formed in the discharge, was recombining on the aluminum film and producing enough heat to melt it locally. Therefore, an aluminum foil, rolled into a cylinder, was placed inside the tube between the electrodes, and this almost completely stopped the deterioration. The foil was changed often and when care was taken this "hydrogen effect" was negligible.

Assuming there is no persistent error in adjustment the total error is estimated to be between 5 and 10 percent although it may be much less.

RESULTS

Aluminum

Aluminum wire was evaporated from an open tungsten filament of 20-mil wire. This metal showed by far the greatest "hydrogen effect"; the second exposure in the reflection position acted as a check in determining whether or not the hydrogen had attacked the film.

No change in reflectivity was observed when aluminum was exposed to air for 24 hours. Since it is known that aluminum oxide forms immediately when the pure metal is exposed to air, this probably means that the oxide is transparent to the ultraviolet.

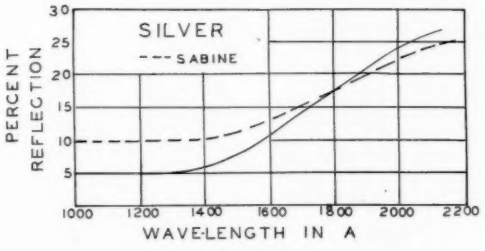

FIG. 5.

The curve for reflection from aluminum is compared with that of Sabine in Fig. 3. Both curves show 30 percent reflection at 1200A, and approach the same maximum of 90 percent at longer wave-lengths. The difference between the two curves may be due to a difference in evaporation technique and, if this is true, there is a strong possibility that the 90 percent reflectivity could be brought down to still shorter wave-lengths if greater care were taken.

Copper

Copper wire was evaporated from an open 20-mil molybdenum filament. It showed very little hydrogen effect. On the other hand, when the copper films were exposed to air a pronounced drop in reflectivity took place (Fig. 4). The difference between the results of the present work and Sabine's was practically removed after exposure to air.

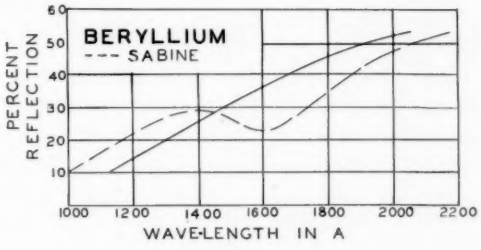

FIG. 6.

Silver

For the evaporation of silver, a molybdenum filament was used as with copper. The hydrogen effect necessitated the constant use of an aluminum foil in the discharge tube. Silver, like aluminum, showed no change in reflectivity when exposed overnight to air.

Above 1800A, as shown in Fig. 5, the curve obtained by Sabine and that of the present work are essentially the same. However, they differ by a factor of two in the short wave-lengths. It is not possible to say definitely which values are the right ones, although the present curve is identical with that recently obtained by Johnson.[5] Johnson's values for aluminum are much less (34 percent reflection at 2000A) than either those reported here or Sabine's.

Beryllium

Although beryllium dissolves tungsten when molten, it was possible to evaporate it from a conical helix of 20-mil tungsten wire, if the wires were pressed close together and the pieces of beryllium were very small. It showed neither an air nor a hydrogen effect.

[5] B. J. Johnson, Proc. Phys. Soc. **53**, 258 (1941).

The minimum in reflectivity near 1600A found by both Sabine and Gleason,[6] did not appear in these results (Fig. 6). Two different samples of beryllium were used, which showed less than 1 percent impurities when tested spectroscopically. Because the films had been evaporated from tungsten it was thought that perhaps a thin film of tungsten had also been evaporated and washed out the beryllium structure. To test this, two films were evaporated from tantalum; however, the same curve as that from tungsten was found to hold, with no minimum.

Upon examination of Sabine's curves it was noticed that all the high melting point metals either showed a minimum in this region or very low values. It seemed possible that Sabine had evaporated some tungsten over these metals, cutting down their reflectivity. To check this theory, a film of aluminum was evaporated and its reflectivity in the hydrogen region checked with the previous results. Then a piece of 20-mil tungsten wire was heated to as high a temperature as possible in front of the aluminum film. A second measurement showed that at 1600A the reflectivity had dropped from 70 to 20 percent and at 1436A from 40 to 20 percent. This great drop in reflectivity shows that even a very thin film of tungsten, not visible over the aluminum film, absorbs very highly in the 1600A region. The present curve, being the same for films evaporated from tungsten and tantalum, is assumed to be correct.

[6] P. R. Gleason, Proc. Nat. Acad. Sci. **15**, 555 (1929).

CONCLUSION

It is not claimed that these results are the accurate ones for pure metals; but it can be asserted that to within a ten percent error they are accurate for metallic surfaces prepared under the conditions described.

The results for copper show that although some metals appear to have oxides that are transparent to the far ultraviolet, a considerable error can arise in reflection measurements of others if the metallic films are exposed to air and allowed to oxidize.

The method of evaporation also has a considerable effect on the reflectivity, as beryllium shows. All metals that have a high melting point should be evaporated from filaments made of two different materials. A measurement of the reflectivity of tungsten would be very useful.

The author wishes to thank Dr. A. H. Pfund for suggesting this problem and supervising the work, and Dr. G. H. Dieke for the use of his microphotometer and his suggestion about the cause of the hydrogen effect. She is also grateful to Dr. J. A. Bearden for his kindly interest and to Dr. Nathan Ginsburg for his great help with experimental details.

Blank and Background Effect on Photographed Spectral Lines*

LESTER W. STROCK**
Spectrochemical Laboratory, Research Institute of the Saratoga Spa, Saratoga Springs, New York

THE quantitative spectrochemical determination of small amounts of Sr in some Rb-rich minerals has been undertaken at the invitation of several members of The Committee on the Measurement of Geologic Time of the National Research Council. This Committee is interested in determining the age of geologic formations from the isotope ratio Rb^{87}/Sr^{87}. The materials investigated to date are 15 samples of powdered lepidolite (lithium mica) provided by Dr. R. C. Wells, Chief Chemist of U. S. Geological Survey Laboratory. These samples represent portions of the same material used for his chemical and structural investigation on lepidolites by Rollin E. Stevens.[1]

It has been necessary to pay particular attention to the shape of the spectrochemical concentration calibration curve and to the preparation of synthetic standard mixtures; since the Sr content of these minerals is rather low and its value desired to the highest accuracy obtainable by spectrochemical methods. The actual Sr determinations will be published elsewhere, jointly with R. E. Stevens and R. C. Wells of the U. S. Geological Survey. The values found range from 0.03 to 0.0003 wt percent Sr.

The material presented in this paper is based on the experimental data obtained in the course of the above investigation. The value of these new data lies in the fortunate and the unusually high reproducibility obtained, so that it has been possible to attempt some quantitative treatment of these effects for the first time. This specific illustration of the blank and background effects on photographed faint spectral lines supports the more general observations emphasized in previous publications.[2–5]

STRONTIUM CONCENTRATION STANDARDS

The standard mixtures were prepared as dry powders, starting from a primary standard containing 0.1 percent Sr (as $SrCO_3$) in a $SiO_2+Al_2O_3+NaKCO_3$ base. This base will be referred to below as a "feldspar" mixture base, since its constituents are in the proper ratio (3.604+1.020 +1.906, respectively) to produce a Na-K-feldspar on sintering and reacting to liberate CO_3. The standard mixture base was prepared by combining the "feldspar" mixture with four parts of carbon powder and one part of a lepidolite (Stevens No. 9) whose spectrum showed only a faint trace of the Sr line 4607A. The series of Sr standards was then prepared by first diluting the 0.1 percent primary standard with one part of the same lepidolite and four parts of carbon powder to 0.05 percent which was further diluted with the standard mixture base in successive stages down to 0.00025 percent Sr. These Sr concentrations refer to the 1 : 1 feldspar : lepidolite content of the mixtures, each of which contains 1.238 percent Li derived from the lepidolite. This lithium provided the internal intensity standard in the spectra of the concentration standards.

The raw materials for synthesizing a feldspar (rather than an actual feldspar) were used in the mixture base and for diluting the samples, so that they could react directly in the arc. This enabled the $SrCO_3$ present to take part in the reaction, along with the alkali carbonate, and become distributed as an actual constituent of a feldspar-lepidolite melt before volatilized from

---

* Presented at the Ninth Summer Conference on Spectroscopy and Its Applications at Massachusetts Institute of Technology, Cambridge, Massachusetts, July 21–23, 1941.

** This work has been supported by a research grant from the American Philosophical Society, insofar as the experimental material presented in this paper has extended the application of the quantitative spectrochemical methods employed in my study on "The geochemistry of mineral waters."

[1] Rollin E. Stevens, Am. Mineral. **23**, 607–28 (1938).

[2] L. W. Strock, Bull. A. S. T. M. (March, 1941), pp. 37–40.

[3] L. W. Strock, *Proceedings of the Seventh Summer Conference on Spectroscopy* (Wiley & Sons, New York, 1939), pp. 134–41.

[4] L. W. Strock, Tidskrift f. Kjemi og Bergwesen (Oslo) No. 6 (1938).

[5] L. W. Strock, *Spectrum Analysis with the Carbon Arc Cathode Layer Method* (Adam Hilger, Ltd., London, 1936), p. 39.

TABLE I. Photometric data for Sr-standard mixtures. Lepidolite No. 9+"feldspar mixture"+carbon 1 : 1 : 4 (Sr-contaminated base).

% Sr IN 1 : 1 LEPIDOLITE + "FELDSPAR"	FILM	SPECTRUM	Δ LOG T (Li-Sr) Li 4603A Sr 4607A INDIV.	Δ LOG T (Li-Sr) Li 4603A Sr 4607A AV.	BACKGROUND Δ LOG T (Li-Bg)	Sr ABOVE BACKGROUND AS Δ LOG T (Bg-Sr) INDIV.	Sr ABOVE BACKGROUND AS Δ LOG T (Bg-Sr) AV.
0.05	61	3	−0.10		——	——	
"	61	4	−0.09		——	——	
"	100	2	−0.11	−0.08	−1.54	——	
"	"	3	−0.02		−1.41	——	
"	"	4	−0.07		−1.44	——	
"	"	5	−0.08		−1.32	——	
0.02	96	5	−0.34	(−0.34)	−1.62	+1.27	
0.007	96	4	−0.64	(−0.64)	−1.46	+0.86	
0.002	96	1	−0.97		−1.53	+0.63	
"	"	2	−0.96	−0.995	−1.38	+0.50	+0.555
"	"	3	−1.05		−1.58	+0.58	
"	98	3	−1.00		−1.51	+0.51	
0.001	98	1	−1.18		−1.58	+0.42	
"	"	2	−1.08	−1.146	−1.42	+0.41	+0.42
"	100	1	−1.18		−1.62	+0.44	
0.0005	99	2	−1.27	−1.27	−1.50	+0.24	+0.26
"	"	3	−1.27		−1.50	+0.28	
0.0004	106	4	−1.33	−1.31	−1.56	+0.23	+0.24
"	"	5	−1.29		−1.55	+0.25	
0.00025	106	1	−1.35		−1.52	+0.20	
"	"	2	−1.34	−1.36	−1.50	+0.15	+0.18
"	"	3	−1.39		−1.54	+0.19	

the arc. Under these conditions both Li and Sr were expected to have the best chance of volatilizing in a reproducible and nearly identical manner from standards and samples alike; since the standards are thus chemically and mineralogically identical with the samples when mixed with an equal weight of feldspar.

The presence of a faint trace of Sr in the lepidolite used in the standards was of course known, as well as a still fainter trace in the feldspar mixture. No other materials suitable for preparing chemically and mineralogically similar bases were found. It was felt that the concentration calibration curve could be corrected for the small residual amount of Sr in the standard mixture base, and that the slight contamination of the lepidolite samples by the Sr in the feldspar could be evaluated from the corrected curve and deducted from the analysis.

The attempt to obtain reproducible spectral line intensity ratios met with success beyond my expectation and experience with arc methods. On the other hand, the derivation of a *true* concentration calibration curve from an experimental one, based on standard mixtures with a Sr-contaminated base, has been more complicated than anticipated. However the necessary attempt to correct for the blank has revealed some features of the photographic photometry of faint spectral lines which are of general interest to spectrochemical analysts, especially in view of the frequency with which the background is claimed by others to limit the extension of spectrochemical methods at low concentrations.

The individual Δ log T values for the lines Sr 4607 and Li 4603, obtained from rotating stepped-time spectra of the standard mixtures, are shown in column 4 of Table I. These values are closely related *but not equal* to intensity ratios, as has been emphasized in previous papers.[3, 6] They were measured at a transparency

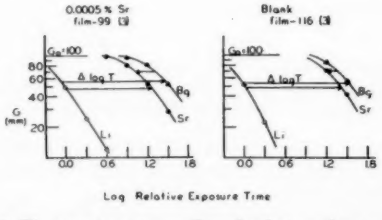

FIG. 1. Photometer curves. Standard strontium spectra.

[6] L. W. Strock, Spectrochimica Acta 1, 117–22 (1939).

TABLE II. Photometric data for standard mixture base. Lepidolite No. 9+"feldspar mixture"+carbon 1 : 1 : 4 (Sr-contaminated).

		Δ log T (Li-Sr) Li 4603A Sr 4607A		Background Δ log T (Li-Bg)		Sr-Background Δ log T (Bg-Sr)	
Film	Spectrum	Indiv.	Av.	Indiv.	Av.	Indiv.	Av.
98	4	−1.26	−1.245	−1.37	−1.36	+0.12	
99	4	−1.23		−1.35		+0.13	
99	5	−1.37		−1.47		+0.18	
101	2	−1.37		−1.60		+0.24	
116	1	−1.39	−1.375	−1.58	−1.54	+0.19	+0.19
"	2	−1.41		−1.62		+0.22	
"	3	−1.40		−1.56		+0.16	
"	4	−1.31		−1.48		+0.16	
Background (weighted average) = $\bar{1}.531$ 18 spectra up to 0.001 percent. (Two lowest for blank given 1/8 weight.)				*Blank* (weighted average) = $\bar{1}.385$* from 6 lower backgrounds. (Lowest given 1/6 weight.)			

* Rounded to $\bar{1}.39$ as Av. Bg is 0.01 lower.

value of 0.5 on a plot of log relative exposure time against galvanometer deflection (G), where $G_0 = 100$. This transparency of the photographed spectral line corresponds to a density level $D = 0.3$, and is a convenient range, as the photometer curves for both weaker Sr-lines and stronger Li-lines can be extrapolated easily to this level.

A typical set of photometer curves is shown in Fig. 1—one for the 0.0005 percent Sr standard, and the other for the standard mixture base. The manner of obtaining three different sets of experimental data from these curves is indicated in this figure, they are: (1) Δ log T measured from the Li line to the Sr line, (2) Δ log T from Li to the background, and (3) the height of Sr above the background as measured in Δ log T at $G = 70$. Such a set of curves was made for each spectrum in order to obtain the photometer data necessary for drawing the concentration calibration curve. It should be emphasized at this point that this procedure completely eliminates the necessity of making any separate plate calibration. Each line in a stepped spectrum serves as its own intensity calibration mark from which as many characteristic curves of the photographic emulsion can be constructed. The procedure was described in considerable detail in a previous publication.[5] It can be used as a routine for high speed control work and with an inherent greater accuracy, as it is a more straightforward procedure than methods involving separate plate calibration, in addition to eliminating errors due to single photometer readings.

DETERMINATION OF AVERAGE LIMITING VALUES OF Δ LOG T FROM LI TO BACKGROUND AND TO SR IN BLANK

It was necessary to determine the average limiting value of Δ log T for the blank and background as carefully as possible; since these two quantities determine the shape of the calibration curve at low concentrations. They also enter into all subsequent calculations in the attempt to correct the calibration curve for these disturbing quantities. Background readings were made at a constant position in the spectrum at a wave-length slightly greater than the Sr line. Individual values of Δ log T for Li to background usually varied about $\frac{1}{3}$ of a sector step (Δ log $T = 0.1$), but four of them were considerably heavier than the others. As is to be expected the background in two of the blank mixtures spectra, shown in upper group of Table II, have raised the Δ log T values of their Li to Sr lines considerably above the six others.

An average value of the background limit L_{bg} was determined from 18 spectra of the blank

and standard mixtures up to and including 0.001 percent added Sr. Spectral line intensities are most influenced at these lower Sr concentrations. An average of -1.53 was obtained by giving the group of 16 lower values eight times the weight given the two highest values. This weighted value of -1.531 is very close to -1.514, the arithmetical average of all these 18 spectra, and to -1.50 obtained for all standards and blank combined. The difference is on the practical limit of accu-

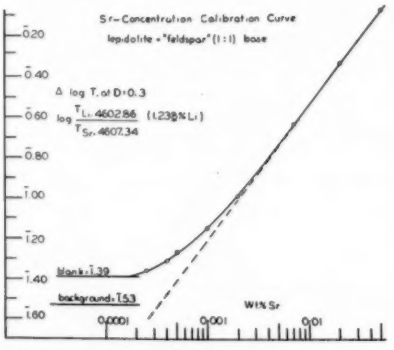

FIG. 2.

racy in drawing individual photometric curves which easily leads to differences of 0.01 in these values.

Comparison of the values for the low and high background groups in Table II shows that $\Delta \log T$ for Li to Sr rises from an average -1.375 to -1.245 as the background rises from -1.54 to -1.36 in the blank mixtures. This background effect would manifest itself in the photometer curves of Fig. 1 by a displacement of the background curve closer to the Li curve, pushing the Sr curve along in front of it, *but not by an identical amount.* This is the reason why a simple subtraction of the background intensity is a spurious correction for the background, or at best only a partial correction. The fact that the Sr line is not displaced by the same amount as the background, is clearly shown by the data in Table II. A background displacement of 0.18, measured as $\Delta \log T$, has shifted the Sr curve only 0.13 closer to the Li curve. The difference naturally brings the background closer to Sr whose separation is thereby decreased from 0.19 to 0.13. Obviously then, a photometrically determined intensity of the background does not provide a true value of the background intensity which can be applied as a correction factor. The background effect can be portrayed as a compression of the horizontal separation between the background and Sr curves of Fig. 1 as the background increases.

The present uncertainty of the quantitative effect of the high background on two of the base mixture spectra, makes it impossible to include their Li to Sr ratios in the average limiting value of $\Delta \log T$ for the blank. Accordingly the directly determined blank limit must be derived from the six spectra whose backgrounds are nearer the average. In this group the one with the highest background was given only $\frac{1}{6}$ the weight of the five others. The weighted average of $\Delta \log T$ for the blank so obtained is -1.385; a value actually identical with the average derived from the two spectra with backgrounds closest to the average.

The experimental concentration calibration curve drawn from the average $\Delta \log T$ values for the Li and Sr lines is shown in Fig. 2. This curve is extrapolated from the lowest added Sr content down to its lowest limit set by the residual Sr content of the mixture base. Had blank-free standards been used, this curve would have been

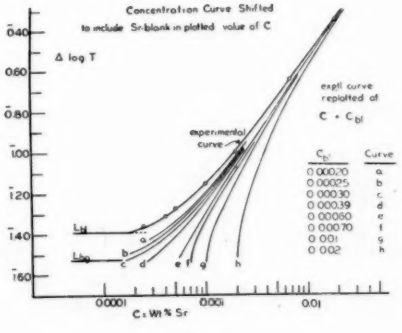

FIG. 3.

limited, instead, by the horizontal line at 0.14 lower on the $\Delta \log T$ axis. This lower line is the background limit.

It is obvious that the lower portion of this curve is displaced from its original linear form by two separate factors, namely: (1) The background effect, which deflects the otherwise linear curve out along the background limit (L_{bg}). (2) The blank effect, which raises the curved foot of the background-altered curve still higher to

the blank limit (L_{bl}). It is therefore necessary to determine the relation between this experimental curve and one which would be obtained from blank-free standards.

DERIVATION OF BLANK-FREE EXPERIMENTAL CALIBRATION CURVE

The experimental curve as drawn in Fig. 2 is obviously displaced on the concentration axis to the left of the blank-free curve. This displacement C_{bl} is equal to the Sr content of the blank, because a given $\Delta \log T$ on the blank-free curve will lie at $C+C_{bl}$ on the concentration axis; i.e., at a value of C which is the sum of Sr added plus Sr in the blank; rather than at a value of C representing percent Sr added only as was done in constructing the experimental curve of Fig. 2. If then, the position of the blank-free curve can be located, its horizontal displacement from the experimental curve is a measure of Sr in the blank; an evaluation of which was attempted with the above facts in mind.

The position of an experimental concentration calibration curve for which the abscissa values (C plotted on log scale) represent the Sr added, must alter in two distinct ways as the Sr content of the base mixture used to prepare the standards decreases. Its horizontal linear branch at low values of C will drop toward the background limit, accompanied by a lesser drop of the adjacent curved portion. This vertical drop of the experimental curve, caused by a decrease in the blank content, is accompanied by a simultaneous horizontal shift of the curve, which as mentioned above, is numerically equal to the Sr in the blank. Therefore it is only necessary to shift the experimental curve on the horizontal axis, by a given increment in C, in order to determine the accompanying vertical displacement over the range of C covered by both curves.

The correct position of the blank-free curve was sought by replotting the experimental $\Delta \log T$ values at $C+C_{bl}$ for several values of C_{bl}. The resulting curves, derived from the experimental curve in this manner, are shown in Fig. 3. Two features of this figure are important; namely, (1) the modified curves straighten out beyond a theoretical linear form and bow in the opposite direction for values of C_{bl} greater than 0.0006, and (2) the curve for $C_{bl}=0.0003$ can be extrapolated from the lowest experimental $\Delta \log T$ (-1.39) down to the background limit to produce a curve resembling a background-affected curve more closely than any others in this figure. The first feature demonstrates that the Sr content of the blank is much lower than 0.0006 percent since this value of C_{bl} is sufficiently high to shift the experimental curve by an amount equal to the combined blank and background

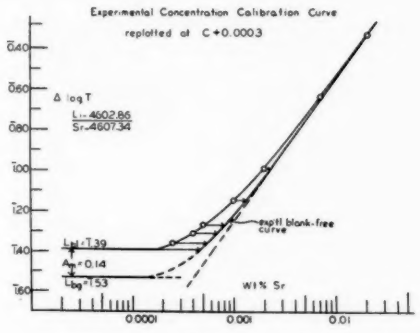

FIG. 4.

effects. The second feature fixes the Sr content of the blank at approximately 0.0003 percent.

The above approximate percentage of Sr in the standard mixture base was then used to determine the analytical features of the blank effect more exactly. The actual experimental curve is shown again in Fig. 4, and to its right another curve derived from the former merely by a horizontal displacement on the concentration axis amounting to the above derived Sr content of the blank as indicated by the arrows. The horizontal displacement of the two curves in Fig. 4 is accompanied by a vertical displacement which goes to practically zero at higher values of C on this logarithmic scale, but rises to a maximum value of 0.14 at lower concentrations. It is obvious that the vertical displacement between the two curves of Fig. 4 cannot be measured at values of C lower than 0.0005 as this is the value of C on the blank-free curve corresponding with the lowest $\Delta \log T$ reached by the experimental curve.

The measured vertical displacements, accompanying the horizontal displacement of $C=0.0003$ in Fig. 4, are shown as circles on the curve of Fig. 5. The displacement at a given value of C is

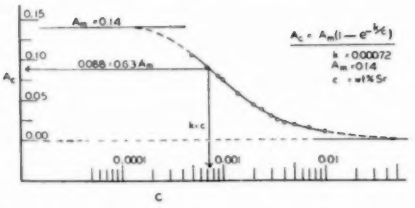

FIG. 5. Δ log T displacement of concentration curve by 0.0003 percent Sr in blank.

designated as A_e. These experimental values of A_e all fall (to well within the accuracy of the graphical measurements) on a portion of the A_e : log C curve of the equation $A_e = A_m(1-e^{-k/e})$, where A_m is the maximum value of A_e and equals $L_{b1} - L_{bg}$ (the limiting Δ log T values for the blank and background, respectively), and k is a constant which adjusts the calculated value of A_e to the experimental concentration range. The values in column 3 of Table III were calculated by the use of this equation, and are in excellent agreement with the experimental values over the entire range of C for which the latter could be obtained. The lower portion of the blank-free curve of Fig. 4 was then constructed down to the background limit by use of these calculated A_e values. The derivation of the entire curve from the experimental one is shown in Fig. 6, in which the arrows represent the values of A_e employed.

The position of the calculated A : log C curve on the log C axis, in Fig. 5, is determined by the value of k in its equation. The appropriate value of k is thus determined from the experimental A : log C curve as the value of C corresponding to $A_e = (1-1/e)A_m = 0.63A_m$ on this curve. In this work $A_m = 0.14$, so that $k = 0.00072$, i.e., the value of C corresponding to $A_e = 0.088$ on the curve of Fig. 5.

The Sr content of the blank can now be evaluated more exactly by means of the relationships derived above. The first step is to select the particular A_e : log C curve which reaches A_m for all practical purposes at the value of C representing the sensitivity limit of the experimental curve (Sr-contaminated base). Now it was shown above that the position on the concentration axis of the A_e : log C curve in Fig. 5 depends on the value of k in its equation, so that it is only necessary to determine the relation between k and its corresponding value of C_{b1} in order to select the proper A_e : log C curve for these experiments. The experimental curve was replotted at $C+0.0002$, and the vertical displacement A_e of this second curve from the original one was measured, in order to get additional data for determining the relation between k and C_{b1}. The resulting A_e values are shown as circles on the $k=0.00038$ curve of Fig. 7. The $k=0.00072$ curve, derived above where $C=0.0003$, is also shown with the measured values of A_e as circles. The other curves in Fig. 7 have been calculated by means of the equation derived for these experimental curves. The value of k used in each case is noted in the figure. Since the values of k are equal to the corresponding values of C at $A_e=0.088$, it is possible to draw portions of the curves for any other intermediate or adjacent values of k in this figure, as for example for $k=0.0010$. This particular value of k is noted in Fig. 7, because its corresponding value of C_{b1} (0.00038) was determined graphically by drawing a portion of a blank-free curve through the coordinates Δ log $T-0.088$ and $C=0.001$, and noting its horizontal separation from the original curve. This then provides the third set of k and C_{b1} values required to determine their relationship which is shown to be linear in Fig. 8. The equations, with appropriate constants for calculating either k or C_{b1} when one of them is known, are shown to the right of the curve.

The value of Sr in the blank is readily de-

TABLE III. Vertical separation of experimental curve from modified one plotted at $C+0.0003$.

C	A EXPERIMENTAL	A CALCULATED
0.0002	—	0.136
0.00025	—	0.132
0.0003	—	0.127
0.0004	—	0.117
0.0005	0.105	0.107
0.0007	0.090	0.090
0.0009	0.079	0.077
0.001	0.075	0.072
0.0014	0.058	0.056
0.002	0.043	0.043
0.0024	0.038	0.036
0.003	0.030	0.030
0.0035	0.025	0.026
0.004	0.022	0.023
0.005	0.019	0.019
0.007	0.015	0.014
0.01	0.01	0.0096

terminable from the experimental $\Delta \log T : \log C$ curve and the curves of Figs. 7 and 8, if the practical limit of A_c is set at $0.99A_m$, at the experimentally determined value of the sensitivity limit. This limit is reached when $k=4.6\cdot\Delta C$, since $0.99=(1-e^{-4.6})=(1-0.01)$. This means that the value of k is such that the calculated value of A_c just reaches zero for all practical purposes at a value of C where the experimental concentration curve reaches the blank limit. The value of k is therefore $4.6\cdot\Delta C$ to far within the limits of accuracy of the experimental data. The corresponding value of C_{bl} can then be read from the $k : C_{bl}$ curve of Fig. 8. For the experiments here described ΔC is 0.00018. The value of k is thus 0.00083 and C_{bl} is 0.00033. The more exactly determined Sr content of the blank is thus 0.00033 percent.

SENSITIVITY LOSS FACTOR

The above analysis of the relation between the experimental concentration curve and its blank-free equivalent have merely evolved a method of calculating the blank-free curve from the experimental curve. The problem was to lower the

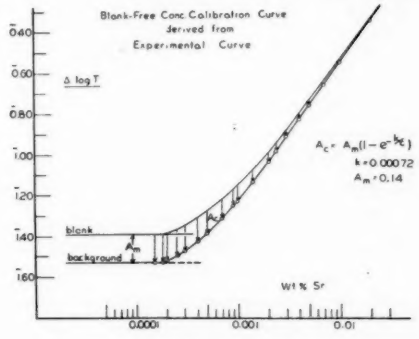

FIG. 6.

experimental curve down to the background limit without changing the sensitivity limit observed for the Sr-contaminated mixture base. Actually the lower portion of the *true concentration curve* is radically altered by the presence of a measurable residual Sr-content of the standard mixture base. The true curve (Sr-free base) and the above derived blank-free curve (Sr-contaminated base—see Fig. 6) differ by a factor designated below as the *sensitivity loss factor*. This work has specifically demonstrated the existence of this factor, and has shown the exact manner in which a true calibration curve is affected by it, when a contaminated standard base is used. The blank effect is thus composed of two separate factors. The first, an error in plotting the concentration curve at Sr-added rather than at total Sr-present, which is unavoidable as long as the blank content is unknown. The second is bound up with the photographic

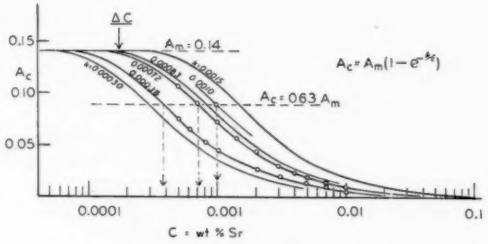

FIG. 7. Dependence of A_c on k and C_{bl}.

process, as some brief considerations will show. In the case of standards in a Sr-contaminated base, added increments of Sr had no opportunity of contributing to the photographic process *at and immediately above* the emulsion sensitivity threshold. The true and experimental blank-free curves are thus built up from different sensitivity levels. This may also be expressed another way as follows. The lower limit of the amount of an element added to a given mixture, which is detectable in a photographed spectrum, is only dependent on the threshold sensitivity of the photographic emulsion in the case of a blank-free mixture base—other things being equal. Whereas, if a detectable amount of that element is already present in the material used as a base to which a given amount of the element is added, the lower limit of the amount added which can be detected is no longer dependent on the emulsion threshold sensitivity; but on the necessity of raising an existing photographic density by a detectable increment.

Since the amount of Sr already present in the base mixture used in this investigation was sufficient to produce a line of measurable density none of the radiation from the Sr-added, need be used to overcome the emulsion threshold. This might at first be expected to lead to an increase in

the photographic sensitivity of detection of a spectral line and of the amount of an element added. However, the arc cannot distinguish added Sr from the residual Sr in the mixture base; so that a calibration curve, based on a contaminated mixture base, must exhibit the resultant of these two additive sensitivity losses. The net loss in sensitivity in these experiments, as measured in percent Sr, is 0.00018—the sensitivity limit of detection of Sr added as shown by the $\Delta \log T : \log C$ curve of Fig. 2. This is the sum of the emulsion threshold loss and the loss due to the residual Sr in the blank. The presence of this sensitivity loss in the blank-free curve of Fig. 6, compared with a true curve based on blank-free standards, is apparent by attempting

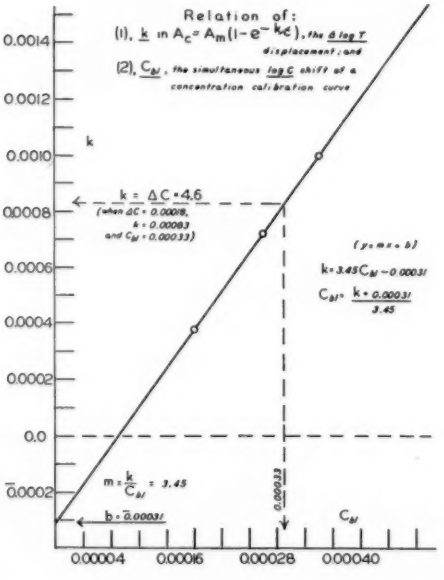

FIG. 8.

to use the former to determine Sr in the lepidolite +feldspar mixture used as the standard base. The blank-free curve of Fig. 6, based on a blank content of 0.0003 percent Sr, will be used to demonstrate the effect of the sensitivity loss in order to avoid introducing an extra figure. On this curve, $\Delta \log T$ for the blank corresponds with 0.00048 percent Sr in spite of the fact that the curve was derived from an assumed blank content of 0.0003 percent. (Using the more exact value of 0.00033 percent and the corresponding

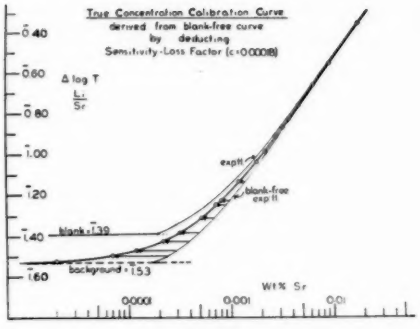

FIG. 9.

curve, gives 0.00051 percent.) This proves that the blank-free curve prepared from contaminated mixture is displaced to higher values of C for a given value of $\Delta \log T$; or in other words that $\Delta \log T$ is greater on the true curve, than on the blank-free one, at any given value of C. Obviously then the true concentration curve can be constructed from the blank-free experimental one by replotting each $\Delta \log T$ value at a lower value of C, i.e., by an amount equal to the sensitivity loss factor (ΔC) which is 0.00018 percent in these experiments. The relative positions of the three curves discussed in this paper are shown in Fig. 9. The true concentration calibration curve is shown in the center and to its right the blank-free experimental curve, from which it is derived by a displacement equal to the sensitivity loss indicated by the arrows. At the left is the original experimental curve obtained from the standards prepared with a Sr-contaminated base.

It should be especially noted that this true concentration calibration curve now exhibits the two prominent features of background-affected curves emphasized in previous publications. These features are the slow asymptotic approach of such curves to the background limit and their rather sharp departure from their initial linear form at $\Delta \log T$ values in the neighborhood of 0.3 above the background. The blank-affected curves, on the other hand, reach the background much more quickly as concentration is decreased, because their lower portion is destroyed by the sensitivity loss factor. The slow fading of spectral lines of regularly decreasing intensity into a background is exhibited by the photometric curves (density : log relative exposure time)

shown as Fig. 1 in a previous paper.[3] This feature of the background effect is always obvious by mere qualitative inspection of a series of photographed concentration standards where faint lines are superimposed on a background of measurable density. It will be observed that spectral lines remain faintly visible above the background with scarcely a perceptible dependence on concentration, at concentrations far below the normal sensitivity limit.

The final stage of this investigation involves the derivation of an equation representing the vertical displacement of the true curve above its extended linear branch by the background. This will enable the spectrochemical analyst to correct experimental $\Delta \log T$ values to a zero background, or to the background for which his concentration curve was constructed.

It seems superfluous, but perhaps advisable, to point out that most actual spectrochemical concentration curves are not complicated by a sensitivity loss due to a measurable residual trace of the analysis element in the standard's base. This is so, because considerable effect is usually expended to avoid such standards. The difficulty of obtaining blank-free standards has undoubtedly prevented many applications of spectrochemical methods to specific industrial problems, or has seriously limited their use and accuracy. It is also well to add that coincidences of spectral lines, and in special cases variation of the intensity of lines with sample composition are comparable with the blank effect. Mixture bases contaminated with undetectable traces of the element to be added as a standard, will also produce a blank effect in varying degrees.

The general analytical features of the blank effect on concentration calibration curves as presented in this paper will be supplemented shortly by a final practical solution of the background effect; while a practical application of the combined work on these effects will be contained in a separate paper on the analysis of Sr in lepidolites.

Application of a Calculating Board to Quantitative Spectro-Analysis*

CARL KING
Harry W. Dietert Company, Detroit, Michigan

BEFORE the application of the calculating board to quantitative spectrographic analysis can be described the fundamental steps of the internal standard procedure should be reviewed. The procedure of reduction depends upon the measuring of the ratio of the intensities of a pair of spectral lines which belong to the two elements whose relative concentration we wish to determine. In most cases, one of the elements used for the ratio is the major constituent, such as iron in steel. This major constituent is referred to as the matrix element or internal standard.

The medium by which the spectral lines are usually measured simultaneously is the photographic emulsion. The spectral lines are recorded upon it as lines having different transparencies, depending upon the intensity of radiation that was focused within the spectrograph at the respective points. These transparencies are measured by means of the densitometer. Transparency is defined as the ratio of the transmitted light to the incident light,

$$T = I_t / I_i. \tag{1}$$

Under conditions of constant incident light, transparency can be determined from a single measurement of I_t. A suitable adjustment of the densitometer will make I_i equal to unity, so that the instrument reads directly in transparency.[1]

An important step in the procedure is that of calibrating the photographic emulsion. This is done by making a graded exposure, the steps of which have a known relationship to one another. The calibration curve plotted from the data thus obtained may be referred to as the gamma-curve.[2]

* Presented at the Ninth Summer Conference on Spectroscopy and Its Applications, at Massachusetts Institute of Technology, Cambridge, Massachusetts, July 21–23, 1941.

[1] See G. R. Harrison, J. Opt. Soc. Am. and Rev. Sci. Inst. **19**, 305 (1929).

[2] This terminology is used with all due apologies to the original experimenters who gave the name gamma-curve

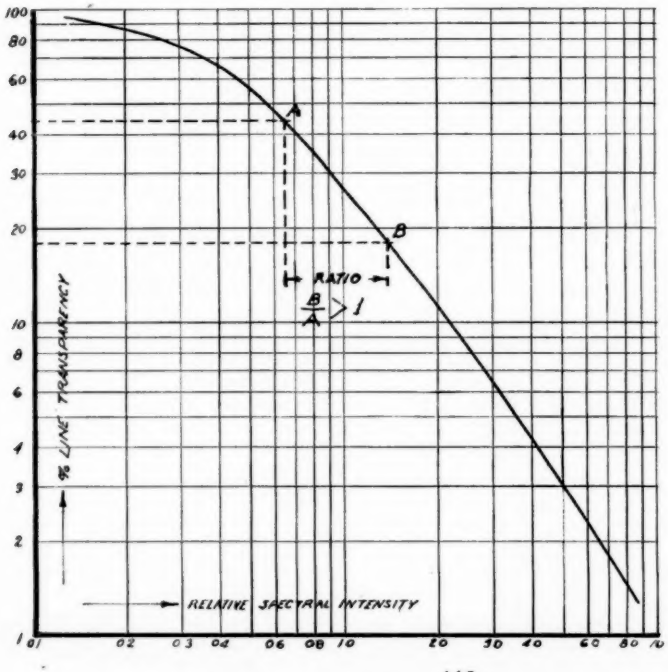

FIG. 1. Gamma-curve plotted on log axes. A typical sheet from the calculating board.

The gamma-curve can conveniently be plotted on a calculating board using the log scales provided (as shown in Fig. 1). The vertical coordinate, which is stationary, is used to represent film transparency. The horizontal scale is used to represent relative exposure or spectral line intensity. Due to the use of log scales, we are now in a position to read off ratios between spectral lines directly from the calculating board, just as one can do with a slide-rule. The horizontal scale is mounted on an arm like a tee-square, and is also free to slide longitudinally in a groove in the arm. To measure the intensity ratio of a pair of lines, we index the unity point of the horizontal scale to the point on the gamma-curve corresponding to the densitometer reading of the line we have chosen for the denominator of our ratio. Next, move the tee-square until the cross-line on the vertical scale finds the densitometer reading of our other chosen line. Then the reading on the horizontal scale where the gamma-curve intersects it gives us the desired intensity ratio.

Before we can interpret this ratio in terms of chemical concentrations, we must run a set of standard determinations for each element in each type of sample that we expect to encounter. From each set of standards, we plot a standardization curve which expresses the relationship between the known chemical concentrations and the measured ratios.

At this point, we will be able actually to run quantitative analyses, for the calculating board will interpret the densitometer readings in terms of intensity ratios and the standardization curves will interpret the ratios in terms of chemical concentrations. However, it is possible to simplify the manipulations even further, for our calculating board with its log scales can introduce multiplying factors and even expand to powers if the proper scales are provided.

Let us examine the type of standardization curve we are likely to obtain. Obviously, when the concentration of an element is zero, its intensity ratio should be zero. Hence, all standardization curves should pass through (0, 0) when plotted on linear coordinates. Also, experience has shown that we cannot expect them always to be linear functions.

To a very good degree of approximation, we may assign analytical expressions to them that will be valid over useful ranges of concentration. In general, the expressions for the standardization curves will have the following form (see Fig. 2):

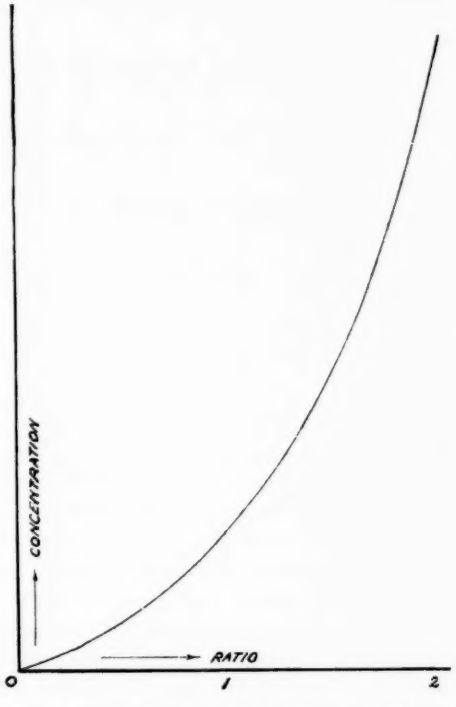

FIG. 2. Standardization curve on linear coordinates.

$$(\text{Conc.}) = (\text{ratio})^n. \tag{2}$$

This same function expressed in logarithms would be as follows (see Fig. 3):

$$\log (\text{Conc.}) = n \log (\text{ratio}) + \log m. \tag{3}$$

Plotted on log-paper, our curve would appear as a straight line, from which we could find the value of n as its measured slope and m as the value of concentration corresponding to a ratio of unity.

to the curve plotted with log O as the ordinate and log E as the abscissa. The author feels justified in taking this step since his curve is plotted even more directly from the same data, the step of computing O as $1/T$ or log O as $(-\log T)$ being omitted. We have but turned the curve upside down, and do not choose to give it a new name for so doing.

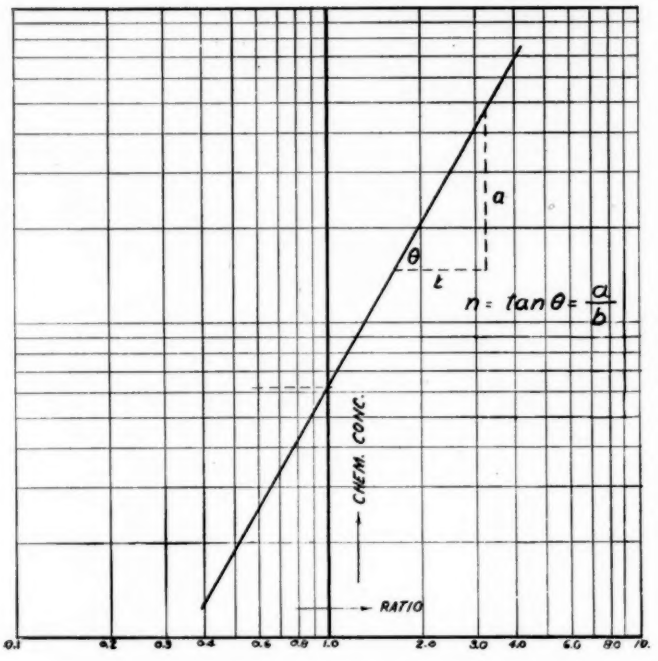

FIG. 3. Standardization curve on log coordinates.

Suppose we had plotted Fig. 3 on a surface elastic in its vertical dimension, then by permitting it to contract the proper amount, the plotted line could be made to assume a slope of unity. In the process the scale to which the concentration axis was plotted would become contracted in actual linear dimension by the factor b/a. Hence, to transpose directly from intensity ratio to concentration readings on the calculating board (Fig. 4), we need only prepare such a contracted log scale.

Another alternative to the preparation of contracted or altered concentrations scales for the horizontal member of the calculating board, is to use the same horizontal scale but plot expanded gamma-curves for the concentration readings. Thus, the original gamma-curve would be obtained in the usual fashion using the horizontal scale to read intensity ratios or relative exposure. Then for each standardization curve having a different value of "n," we shall derive a new gamma-curve from the original one by merely expanding its horizontal axis linearly by the factor "n" or a/b.

The use of the calculating board with the expanded gamma-curve is identical to that when special contracted concentration scales are used. In any event, to introduce the factor "m" as indicated in Eq. (3) or Eq. (4), we index the horizontal concentration scale to the value of "m" for the particular element involved. Other-

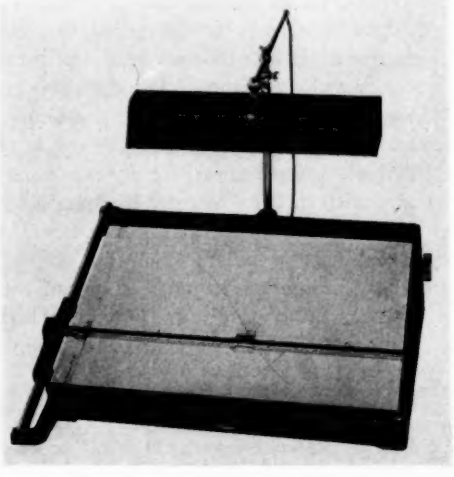

FIG. 4. Calculating board.

wise the reading of a concentration is identical to the reading of an intensity ratio as previously described.

It has been our experience that this procedure using the calculating board is the fastest and most accurate procedure for quantitative spectrographic analysis that has been devised. The reason for this is the elimination from the routine of all steps demanding the exercise of the operator's judgment. Also allowance is automatically made for the obviously non-linear response characteristic of the photographic emulsion. These two comprise the major sources of error in all spectrographic analyses, and it is toward the minimizing of the errors that we continually bend our efforts.

Film and Plate Processing Equipment*

JOHN SCHUCH
Harry W. Dietert Company, Detroit, Michigan

ONE of the more important factors that requires consideration in order to secure precise spectrochemical analysis is the proper development of emulsions.

Wide variations in development from spectrogram to spectrogram are normally corrected by determining the characteristic curve of each negative. This procedure can be simplified to a large extent through the use of equipment that allows close control, so that nearly the same development will be secured at all times, thus relieving the operator of the necessity of determining the characteristic curve of each spectrogram.

To attain the same degree of development of all spectrograms for a considerable period of time, it is rather obvious that one must consider the main factors that contribute to the development of the photographic images; namely, (1) emulsion, (2) type and concentration of developer, (3) time of development, (4) agitation of developing solutions, and (5) temperature of the solutions.

Most of these factors can be standardized quite easily. Uniformity of emulsion can be secured by simply specifying, when a quantity of film or plates are purchased, that the complete order be of the same emulsion number. Developers of uniform characteristics can be obtained by using care in compounding the solutions and also by mixing several weeks supply at a time and storing in air tight containers. The control of the duration that the spectrograms are immersed in the developer involves nothing more than the observance of a timer or stop watch. This leaves only the agitation and temperature of the solutions to be considered. Agitation of the developer is perhaps most easily accomplished by rocking the solution trays. The use of an electric motor will assure a constant speed of oscillation and if the volume of solution used is a definite measured amount, uniformity of agitation will be obtained. The need for close control of temperature is apparent when one considers that the speed of development roughly doubles for every 10° rise in temperature. The maintenance of constant temperature is perhaps the most difficult of the factors to maintain except by the use of suitable thermo-switches.

To provide the spectrographer with equipment for maintaining uniform agitation and temperature of the processing solutions, a developing machine was designed. The plate developing machine, shown in Fig. 1, contains 3 trays of a size suitable for the development of 4×10 inch plates. A similar model with 4 trays is available for the development of films.

The developing machine illustrated provides the spectrographer with controlled agitation and temperature so that nearly identical development can be obtained. The machine consists of cast metal base and water tank mounted on trunnions. Within the base is located an electric motor which oscillates the tank by means of a simple cam arrangement at a rate of 20 cycles per minute. At this rate of oscillation no standing waves are obtained in the trays. Constant temperature is maintained through the use of a water bath which circulates about the trays as

FIG. 1. Plate developing machine.

* Presented at Ninth Summer Conference on Spectroscopy and Its Applications held at the Massachusetts Institute of Technology, Cambridge, Massachusetts, July 21–23, 1941.

directed by baffles within the tank. The circulating water temperature is regulated by a thermo-switch and water valve. As the temperature of the bath rises, the thermo-switch actuates the water valve through a relay and permits cold water to enter the oscillating tank. In this way temperature regulation to within a few tenths of a degree C is obtained. Since in most localities the temperature of tap water is often warmer than the temperature at which the solutions are to be kept, the use of a water cooler to supply cold water to the machine is usually required.

WASHING OF SPECTROGRAMS

The rate of washing of plates or films depends almost entirely on the rate of diffusion of the hypo out of the emulsion into the water. While the rate is largely independent of the temperature of the water[1] and the presence of hardeners in the fixing bath, it is closely allied to the rate of flow of water over the emulsion. For instance, with tank washing, about one-half of the hypo will be removed from the average emulsion in about 30 seconds. The process will then stop unless the water in the tray is changed. On the other hand, if the emulsion is exposed to a continuous flow of fresh water the amount of hypo remaining in the gelatin is halved every fifteen seconds. Thus, at the end of 60 seconds only 1/16 of the original amount of hypo remains and at the end of two minutes only 1/256 of the fixer remains and at the end of 3 minutes only 1/4096 of hypo remains.

The film and plate washers were designed to conform to the principles as outlined above. The plate washer is depicted in Fig. 2.

Water enters the front basin and as it rises in the basin it spills over the plate that lies on a horizontal position on the washer as shown in illustration. The waste water spills into the large overflow basin at the rear of the washer and is drained away.

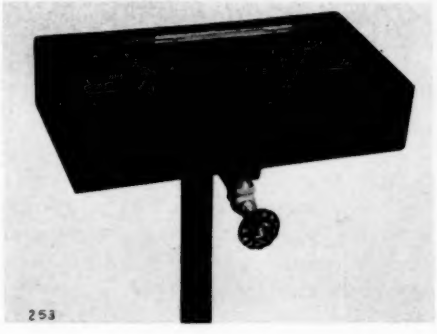

FIG. 2. Plate washer.

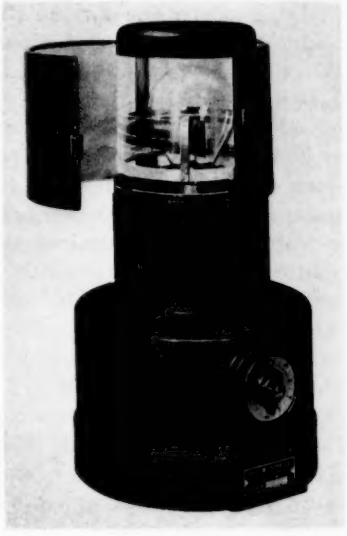

FIG. 3. Film dryer.

The film washer is somewhat similar to the plate washer except that the inlet water is sprayed in a continuous sheet along the upper longitudinal edge of the film and flows across the width of the film. The waste water collects in the integral catch-basin of the washer and from there, either spills directly into a sink or is piped to a drain.

Washing spectrograms in either of the two washers for 30 to 60 seconds suffices to dilute the residual hypo to about 1/4 to 1/16 the original amount. Film washed to this extent will keep several days or weeks which is usually enough for most routine spectrochemical laboratories.

[1] *Elementary photographic chemistry* (Eastman Kodak Company), pp. 32–33.

DRYING OF SPECTROGRAMS

Emulsions will dry faster if the heat is applied on the film or glass side of the spectrograms. If the heat is applied directly on the emulsion side, the surface of the emulsion dries first and retards the egress of the moisture in the lower depths of the gelatin.

The film dryer, Fig. 3, employs an infra-red lamp as a source of heat for drying the spectrograms. The film is wrapped around the Pyrex glass cylinder, emulsion side out and clipped in position with the two phosphor bronze clips shown. When the timer-switch is turned on, the infra-red ray lamp within the Pyrex cylinder glows and a blower mounted within the base of the dryer blows warmed, dust-filtered air over the emulsion side of the film to carry away the water vapor liberated by the infra-red rays. After the elapse of a predetermined time, the timer mounted in the front face of the dryer shuts off the lamp and the air blast heater located in the blower. The blower, however, will continue to run so as quickly to cool the film to room temperature. Normal drying time is from 45 seconds to about 2 minutes, depending on type of emulsion and the time that the films were soaking in developing and washing baths.

The plate dryer is somewhat similar to the film dryer except that a large nichrome wire heating element is used to supply the infra-red rays. After the plate has been washed and sponged it is placed in a horizontal position, emulsion side up on the dryer. When the timer switch has been set the nichrome grid which is located about 4 inches below the plate becomes incandescent. At the same time a blower mounted in the base of the dryer blows warmed air over the top surface of the plate and sweeps away the water vapor from the emulsioned surface of the plate. After the elapse of the predetermined time the timer switches off the main nichrome heating element and also the air blast heating element. However, the blower will continue to function for the purpose of cooling the plate so that it may be handled as soon as possible. The blower is turned off by means of the left-hand toggle switch.

As in the case of the film dryer, the air blast is filtered through a 500-mesh monel wire cloth to prevent the deposition of dust particles on the emulsion.

Because of the rapid drying that takes place in the dryers it is necessary that most of the free water be wiped from the surface of the emulsion with a viscose sponge. Otherwise the heat generated by the drying elements will tend to melt the gelatin.

The "Purple Ring" Illusion

RONALD L. IVES
Fort Worth, Texas
(Received November 5, 1941)

A brilliant purple ring, concentrically surrounding a rapidly receding brilliant red light, is here attributed to after-image effects, and the factors influencing this spectacular and transitory illusion are briefly outlined.

OBSERVED PHENOMENA

WHILE witnessing a number of rapid night take-offs of commercial aircraft, it was noted that, in some instances, the port wing-tip light[1] was momentarily surrounded by a brilliant purple ring, which grew rapidly in width from zero to a maximum, and as rapidly shrank. Arrangement of light and purple ring are shown schematically in Fig. 1, *A*.

In a few instances, as the purple ring approached maximum width, it was separated from the red light by a narrow ring of blackness. This condition is shown schematically in Fig. 1, *B*.

If, as soon as the ring was noted, the observer's eyes were closed, the red inner light vanished, but the ring remained. The circular inner area, formerly occupied by the red light, was filled with an indefinite network of dull red lines, which were rapidly obliterated as the ring grew inward, becoming, in a fraction of a second, a purple circle. This rapidly decreased in diameter, and vanished about $\frac{3}{4}$ of a second after the eyes were closed. A similar effect can be produced by interposing a piece of opaque paper between the observer's eyes and the red light. In this case, the ring will appear, slightly out of focus, on the paper; and will become, in a fraction of a second, a shrinking purple circle.

NECESSARY CONDITIONS

Numerous careful observations disclose that the purple ring can only be seen at night, by an observer whose eyes are on "night" vision, and when the intensity of the red light, at the observer's eye, is very great. Necessarily rough observations indicate that the ring will not be perceived if the general sky light has an intensity exceeding 0.05 foot-candle.

[1] Civil Air Regulations (1940) 60.610*a*. . . . . (this light) shall be visible at least two miles.

Mathematical consideration of relationships during the presence of the ring illusion showed that a rapid decrease in the intensity of the red light, as measured at the observer's eye, was necessary for its occurrence. Preliminary computations indicate that the purple ring was visible only when the intensity of the receding light, as calculated for the observer's position, was decreasing at a rate in excess of 30 percent per second; and that the black ring between the red light and the purple ring (Fig. 1, *B*) was present only when the intensity decreased more than 50 percent per second. These rates of decrease must apparently continue for a finite time interval, probably greater than $\frac{1}{3}$ second, before the illusion will be perceived.

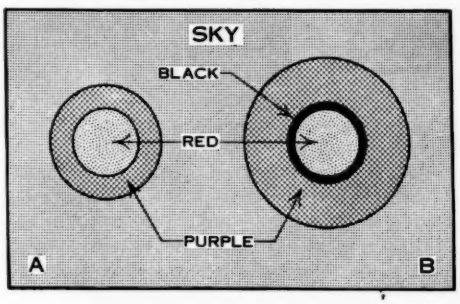

FIG. 1. Relations of the purple ring to the red light within it. *A*, most common form of illusion; *B*, rare form.

At all times when the illusion was noted, the apparent diameter of the receding red light was far greater than its true angular diameter. The apparent angular diameter of the red light, in many instances, was fifteen times its true diameter. Although atmospheric and ocular diffusion are present, they are of negligible importance, and this diametric increase must be attributed to irradiation.

Repeated observations of receding red lights of moderate intensities (the tail-lights of automobiles), which had similar apparent and angular diameters, failed to produce any purple ring illusion, even when the loss of intensity, due to recession, was identical to that noted during the presence of the illusion when brighter lights were observed. Thus, it appears that a great diametric increment, due to irradiation, is a necessary condition for the occurrence of the purple ring illusion.

From the foregoing discussion, it appears that this illusion will be noted only by an observer whose eyes are on night vision; when there is great contrast between skylight and the light observed; when the apparent image of the observed light is very much larger than its true image, due to irradiation; when the loss of intensity of the light, due to recession, exceeds certain values (30 percent per second is here suggested); and when this loss of intensity continues for a definite time (probably more than $\frac{1}{3}$ second).

TENTATIVE EXPLANATION

That this illusion is in large part an after-image phenomenon is plainly shown by the persistence of the purple ring after the stimulus is withdrawn. A similar illusion can be produced by gazing intently at a brilliant red light in a dark room for a few moments and then turning the light off. The illusion will be heightened (and also followed by a headache) if the light is blinked rapidly ten or twelve times.

Those parts of the visual field in which the purple ring normally appears are those considerably outside the area directly stimulated by the red light. Thus, the purple ring illusion, when produced by a receding red light, may be described as an after-image produced by a decrease in irradiation; and the changes in the width and outer diameter of the ring explained as functions of the rate of decrease in the diameter of the perceived image (a function, but probably not a simple function, of the intensity of the stimulus); the rate of growth of the after-image; and its rate of decay. According to this analysis, a black ring will be present between the inner red circle and the purple ring whenever the rate of shrinkage of the perceived image exceeds the rate of growth of the after-image. This requires a greater rate of change than is necessary for the mere presence of the illusion, a condition in exact accord with observations.

It will be noted that this explanation appears substantially valid whether irradiation occurs in the retina, and is analogous to photographic halation; or in the optic nerve, and is analogous to telephonic crosstalk.

Ultraviolet Irradiation by Means of Linear High Pressure Mercury Lamps

WM. T. ANDERSON, JR.*
Research Laboratory, Hanovia Chemical and Mfg. Company, Newark, New Jersey

INDUSTRIAL production depends upon working drawings. Since approximately 150,000 reproductions of drawings are required for the construction of a small bombing plane or tank, photo-reproduction has become an important factor in our national defense.

The newer photo-reproduction processes employ diazo- or similar compound-impregnated papers which are mostly photo-responsive to radiations in the ultraviolet spectrum bordering the visible. Since tracing cloths and papers are very transparent to these radiations, it is entirely practical to use ultraviolet light sources for contact printing. The high pressure mercury arc with its high emission at wave-length 3660A was found to be an excellent source, but in its initial forms was not easily adaptable to a printing optical system.

The popular size for working drawings specifies a width of 42 inches. Irradiation of a field 42 inches in width may be accomplished with sufficient uniformity by an arrangement of a number of conventional mercury arc lamps, each about 7 inches in length. However, the economies of the installation and operation suggested the need for the development of single linear light sources with an arc length of about 48 inches. These have been developed[1] and have been found very satisfactory for operation at arc wattages between 40 and 85 watts per linear inch of arc length. Their employment has resulted in the production of photocopying machines with printing rates of 1 to 25 feet per minute, the paper being exposed to the ultraviolet for 6 or more seconds.

With the development of linear fluorescent light sources, it became evident that the familiar rules established for illumination by tungsten filament incandescent lamps, which are essentially point sources, no longer applied. A mathematical discussion of the propagation of light from linear sources has been presented by Halbertsma and Ittmann[2] which agrees closely with experimentally determined results.

The problems involved in the utilization of linear mercury arc lamps were in many respects similar. The economics of the process required a very efficient arrangement of lamp and printing surface. This requirement is fulfilled when the lamp becomes the axis about which the glass printing cylinder revolves. Since the photosensitive paper and the tracing must pass on and off this cylinder, the ideal arrangement of 360° of circumference is not obtainable. In practice only about 315° of circumference may be used and receives direct irradiation by the coaxial mercury arc lamp. The light lost in the remaining 45° of circumference is partially reclaimed by the employment of a suitable reflector.

For any given light source, the velocity of the photoprinting reactions are determined by the

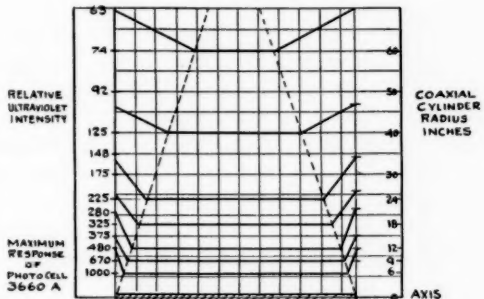

FIG. 1.

time of exposure and the intensity of the light. With a constant light intensity, such reactions normally vary with time (t) in accordance with the first-order equation, namely, $dx/dt=k(a-x)$. The diazo-papers for a practical range of times and intensities follow a simplified form of the equation, namely, $x/t=k$. This is a very convenient result, because if time (t) and light in-

* Presented at the Twenty-Sixth Annual Meeting, Optical Society of America, New York, October 25, 1941.

[1] J. H. Laub, Elect. Eng. **60**, 384 (1941).

[2] N. A. Halbertsma and G. P. Ittmann, Philips Tech. Rev. **4**, 181 (1939).

tensity (E) are varied so that their product $Et=c$, where c is a constant, the degree of printing is constant, $x=kc'$.

Figure 1 gives the experimentally measured intensities on the surface of coaxial cylinders about a linear quartz high pressure mercury arc with 47-inch arc length operated with an electrical input of 75 watts per inch of arc. It will be noted that the light intensity on the cylinders coaxial with the arc decreases near the ends of the arc. This is a factor in the selection of the diameter of the printing cylinder because the arc lamp must be sufficiently longer than the printing surface to permit the production of a uniform intensity on the cylinder. Practical considerations such as cost and dimensions of equipment limit the radius of the printing cylinder to $\frac{1}{5}$ or less of the arc length. Under these conditions, the arc may be considered to be an infinitely long luminous line, excepting for a few inches at each end.

The light intensity E upon a coaxial cylinder varies as the radius r. If I_0 be the intensity per unit of length of the linear arc,

$$E=bI_0/r.$$

It can be shown that $b=\pi/2$, and that therefore $E=1.57I_0/r$. It follows that the intensity of the light field on a cylinder of 6-inch radius will be just half that on a cylinder of three-inch radius. This is in agreement with the experimentally determined results (see Fig. 1).

If the same angles of circumference of a 3- and 6-inch cylinder are covered by the printing paper and irradiated, and if the angular velocities of the two cylinders are equal, the exposure times are equal. However, since the light intensities are in the ratio of 2 : 1, the intensity on the smaller cylinder being the greater, the reaction on the paper is entirely dissimilar.

If the angular velocity of the larger cylinder be reduced to half that of the smaller cylinder, the exposure time of the paper on the larger cylinder will be doubled. Since $Et=c$, the degree of photochemical reaction resulting in the two instances are now comparable. The speed at which the paper moves is determined by the peripheral velocity. If the angular velocities of the cylinders are varied inversely as the radii, the peripheral velocities become equal. The paper speed is then constant.

These results indicate that, provided that effective length of the linear arc is ten or more times the radius of the coaxial printing cylinder, the radius of the coaxial cylinder is not a factor in the printing speed of the paper in feet per minute.

Linear light sources comprising a large ultraviolet component are useful in many photochemical processes other than photoprinting. When used for the irradiation of liquids and gases a coaxial arrangement is entirely practical and provides a most economical utilization of the light energy. While in such reactions the uniformity of irrandiation field required for photoprinting is usually not required, the manner in which the light intensity varies with distance and along the arc is highly important.